



Numerical Simulation of a Stratified Gas ICF Cavity

Tim Bartel, R.R. Peterson, G.A. Moses

April 1986

UWFDM-679

FUSION TECHNOLOGY INSTITUTE
UNIVERSITY OF WISCONSIN
MADISON WISCONSIN

DISCLAIMER

This report was prepared as an account of work sponsored by an agency of the United States Government. Neither the United States Government, nor any agency thereof, nor any of their employees, makes any warranty, express or implied, or assumes any legal liability or responsibility for the accuracy, completeness, or usefulness of any information, apparatus, product, or process disclosed, or represents that its use would not infringe privately owned rights. Reference herein to any specific commercial product, process, or service by trade name, trademark, manufacturer, or otherwise, does not necessarily constitute or imply its endorsement, recommendation, or favoring by the United States Government or any agency thereof. The views and opinions of authors expressed herein do not necessarily state or reflect those of the United States Government or any agency thereof.

Numerical Simulation of a Stratified Gas ICF Cavity

Tim Bartel, R.R. Peterson, G.A. Moses

Fusion Technology Institute
University of Wisconsin
1500 Engineering Drive
Madison, WI 53706

<http://fti.neep.wisc.edu>

April 1986

UWFDM-679

**NUMERICAL SIMULATIONS OF A STRATIFIED GAS
ICF CAVITY**

**T. J. Bartel
R. R. Peterson
G. A. Moses**

April 1986

**Nuclear Engineering Department
University of Wisconsin-Madison
1500 Johnson Drive
Madison, Wisconsin 53706**

A B S T R A C T

One and two dimensional radiation hydrodynamic simulations of a light ion fusion target generated microfireball in a stratified gas atmosphere have been performed. Three scenarios were investigated: the target in nitrogen gas with a layer of helium above it, the target in helium with a layer of nitrogen below it, and the target in a sphere of helium surrounded by nitrogen. The gases were of equal pressure (15 torr). The distance from the target to the gas interface was varied from 10 to 100 cm. Target micro-explosions of 200, 400, and 800 MJ were investigated. The intent of these configurations was to determine if stratified gases (with different opacities) could be used to reduce the overpressure on the diodes placed at the walls of the target chamber and also the diagnostic equipment placed below the target explosion. Nonspherical fireball propagation caused by "venting" of the fireball once its radiation front reached the gas interface was investigated. The interface was within the distance from the target where the fireball shock breaks away from the radiation diffusion wave.

The configuration with the target in the nitrogen resulted in an overpressure reduction of only 20%. The blast wave was formed very early and the venting process was insufficient to greatly modify its magnitude. The configurations with the target in the helium gas, in either gas layers or spherical shells, resulted in a reduction of at least 50%. This is because a fireball was created at the gas interface and was free to expand in either direction. However, the wall heat flux in the helium gas layer was very high due to the low X-ray stopping power of helium. A target in a central cell of helium, surrounded by nitrogen, is the best compromise configuration for both pressure load and heat flux reduction.

T A B L E O F C O N T E N T S

1. Introduction	1
2. Target in N ₂ Region	4
2.1 200 MJ Target Yield	4
2.1.1 100 cm	6
2.1.2 40 cm	11
2.1.3 10 cm	11
2.2 800 MJ Target Yield	15
2.2.1 20 cm	18
3. Target in He Region	25
3.1 400 MJ Target Yield	25
3.2 800 MJ Target Yield	28
4. Analysis	30
4.1 Target in N ₂ Region	30
4.2 Target in He Region	30
5. Conclusions	33
6. References	35
7. Appendix A	36
7.1 GAS2DRFD Overview	36
7.2 Governing Equations	37
7.3 Equation-of-State	38
7.4 Special Features	39
7.4.1 Ion Deposition	39
7.4.2 Time Step	39
7.4.3 Radiation Diffusion Stencil	40
7.5 Code Listing	43

1. Introduction

The design of a cavity vessel for a light ion beam inertial confinement fusion (ICF) reactor must consider effects from intense pressure loading on the cavity wall¹. This is because most of the target X-ray and ionic debris energy is absorbed in the cavity gas which is converted to the mechanical and radiant energy of a blast wave. This blast wave exhibits mechanical shock and thermal radiation wave behavior. The vessel must both be able to withstand the high peak overpressure which is experienced from a single event and, since this is a cyclic process, the effect of cavity wall fatigue. Therefore, there is an important advantage to reducing the mechanical impulse on the cavity wall and several approaches have been suggested². The present investigation explores the possibility of reducing the pressure impulse by using multiple layered cavity gases with different abilities to stop both thermal and X-ray photons. Strong shock theory^{3,4} states that the overpressure is proportional to the energy behind the shock. It is hoped that the expanding radiation field can be directed such that the resulting nonspherical fireball expansion would decrease the mechanical impulse on the diodes or on diagnostic equipment placed below the target. Also, the absorption of target generated X-rays can be controlled by using a non-uniform gas which can be optimized to reduce damage of the facility. This approach would help avoid excessive structural material in the instrumentation module that affects the measured X-ray and neutron spectra.

Figure 1 illustrates the geometry under consideration. The diagnostics package is depicted by the module beneath the target. The target chamber was taken as a right circular cylinder for the simulation. This study considered the cavity gases segregated into the two regions as illustrated; the top region would contain an optically transparent gas, helium, and the bottom region contained a gas with a much higher opacity, nitrogen. Three scenarios were investigated. Two were with the geometry of fig 1: the target location was either in the helium or in the nitrogen region. The target in figure 1 is shown for example in the lower or nitrogen gas region. The last scenario was to enclose the target in a spherical region of helium which was surrounded by nitrogen. This configuration is shown in fig. 2.

The hypothesis for the target in the nitrogen region is that once the radiation front of the expanding fireball has reached the gas interface, "vent-

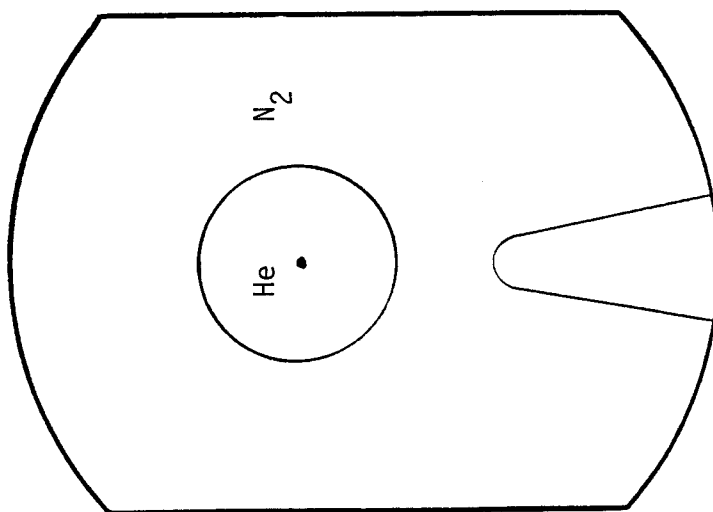


Fig. 2 Target in He 'Bag'

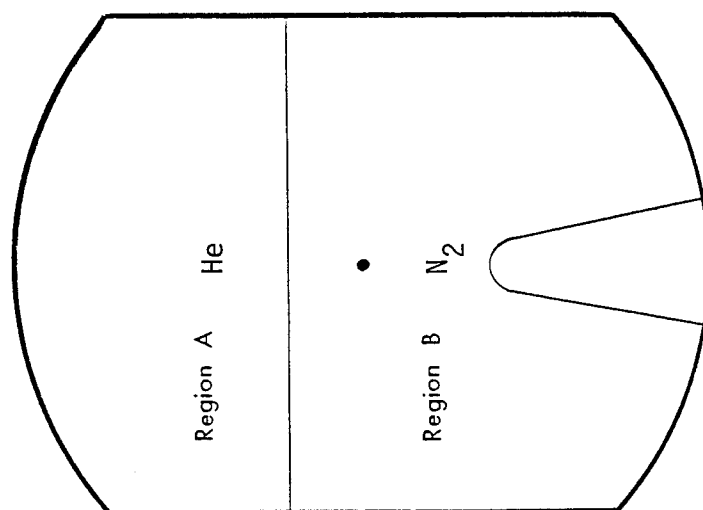


Fig. 1 Stratified Gas Cavity Geometry
(target shown in N₂ region)

ing" of the radiation upward into the He gas would result in a nonspherical hydrodynamic pressure expansion in the nitrogen gas region and thus reduce the pressure loading in the radial (diodes) and downward axial (instrumentation) directions⁵. These effects are not unlike an explosion of a depth charge near the surface of the water; the opacity differences take the role of the density ratio.

To examine the viability of this approach, a 2-D Eulerian radiation fluid dynamics computer code was written. A short description and a complete listing of the code is presented in Appendix A. The diffusion approximation⁶ was used for modelling the radiation field, where the radiation is assumed to act as a fluid with a single well defined temperature. This assumption is valid for the lower cavity gas but is incorrect for the upper gas, where because of its low opacity, the photons are not diffusing but are free-streaming. However, since we were not interested in modelling the behavior of the fireball in this region, the diffusion model was sufficient to obtain realistic boundary conditions for the lower gas region. The ramifications of this approximation will be discussed later. A tabular equation of state was used for the lower gas⁷; the upper gas was modelled as optically transparent.

A different effect was important for the case of the target in the He region. Since He is not truly optically transparent, some of the initial X-ray energy will be absorbed in He. However, a larger effect is that the X-ray absorption will be very high in the N_2 , at the gas interface. Now the fireball will be free to expand back into the helium as well as into the nitrogen. Also, the peak energy density in the nitrogen will be reduced, compared to an explosion in nitrogen, due to the isotropic spreading of the X-rays before they are absorbed. The pressure impulse on the instrumentation package and the diodes would then be reduced. This scenario is predicated on the assumption that plasma channels can be formed in the helium region for the ion beam to propagate through. We do not intend to investigate this, but merely assume it.

A 1-D Lagrangian radiation fluid dynamics computer code⁸ was used to simulate this problem. This code has the ability to model radiation, fluid dynamics, and X-ray deposition in multiple materials. It was used to determine if a full multidimensional treatment of this situation was warranted; a spherical coordinate system was used for the present study.

2. Target in N₂ Region

The present analysis used helium as the transparent gas in region A and nitrogen as the target cavity gas in region B as shown in fig. 1. The calculations were done in a cylindrical geometry using 5 cm square computational meshes. The radius was taken as 250 cm with a no-flow right boundary. The axial "top" and "bottom" were modelled as free-flow boundaries. Typically the region below the target was 250 cm and the He region 200 cm. This was done to prevent boundary contamination from phenomena such as artificial shock reflections from affecting the regions of interest. Figure 3 shows the computational domain for the 100 cm calculation.

The initial cavity gas number density was taken as that which would have a pressure at 0° C of 15 torr; both gas regions were at the same initial pressure. The shot energy was either 200 MJ (the standard TDF base case) or 800 MJ (for high yield targets). The present code does not model X-ray attenuation; therefore, MF-FIRE⁸ was used to obtain the initial gas temperature profile. Figure 4 shows this profile for the 200 MJ case.

The present investigation was not concerned with detailed modelling of the nitrogen-helium interface. Thus, the computer code considered only a single species; the helium region was just modelled as a nitrogen gas with negligible opacity. Essentially, the helium region served as a pseudo-boundary condition for the nitrogen region. Only the fireball loading in the nitrogen region, both radially outward and axially downward from the target, were of interest. The pure hydrodynamic analogy for this situation is an underwater depth charge blast near the water surface; when the pressure pulse 'breaks' the surface, the explosion energy is directed upward.

2.1 200 MJ Target Yield

Indicated on Fig 4, the initial temperature profile for the 200 MJ case, is the region where the shock is "launched"; that is where the fireball hydrodynamic speed is greater than the diffusion speed. For the present test conditions, this value was found to be approximately 130 cm⁹. The distance between the He region and the target was varied in this study; fig. 4 indicates the three values used: 10, 40, and 100 cm. These were chosen for one to be inside the initial high energy deposition region, just beyond it, and prior to launching the shock.

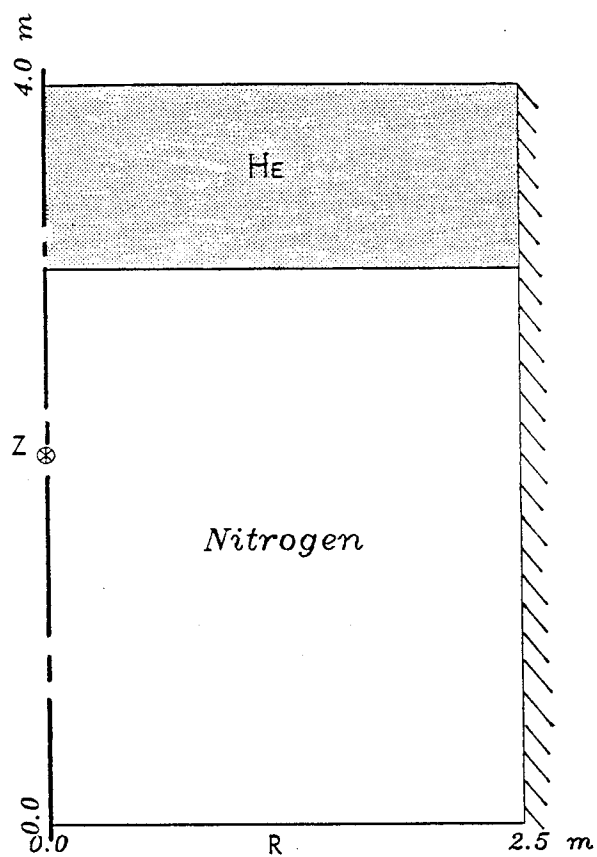


Fig. 3 Typical Computational Domain
(100 cm case)

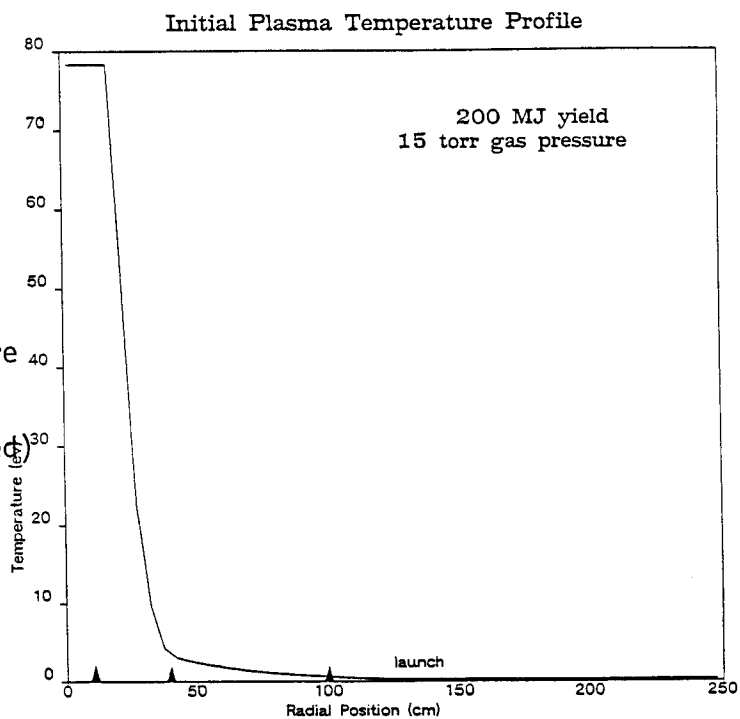


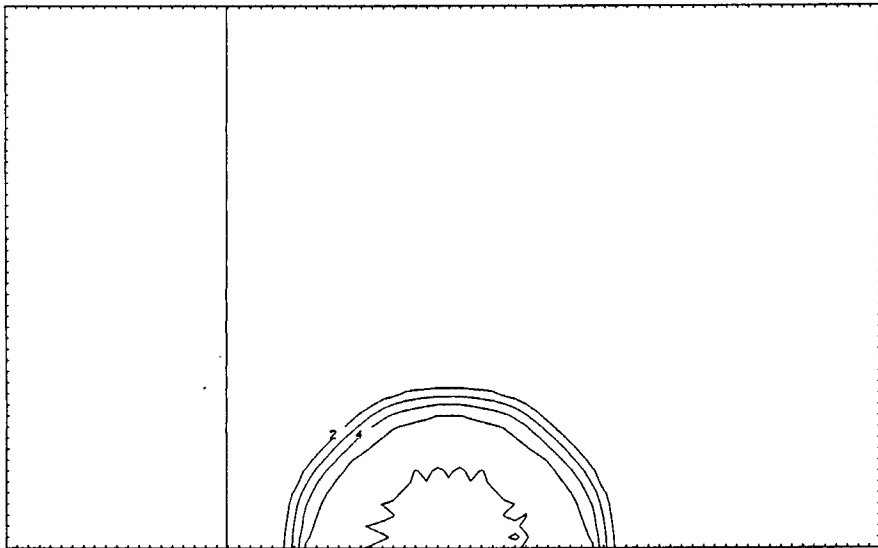
Fig. 4 Initial Gas Temperature
Profile (target
locations are indicated)

2.1.1 100 cm.

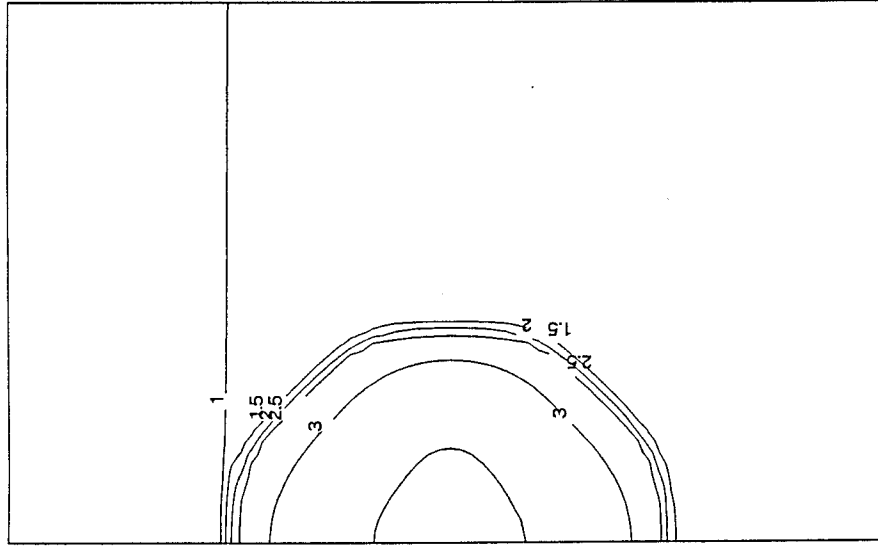
The first calculation positioned the interface 100 cm above the target. This allowed sufficient time for the fireball to develop before it encountered the He region. Figure 5 shows the development of the fireball from contours of gas temperature. One can note that the fireball has just begun to interact with the He at 17 microseconds. Prior to this time, it has essentially undergone a spherical expansion in the nitrogen. At about 32 microseconds, the gas temperature contours have become nonspherical due to the change in gas properties at the interface; the helium was optically transparent to the radiation while the nitrogen was not. Thus, a radiation enhanced thermal wave propagated into the nitrogen but since the radiation free-streamed in the helium, only a thermal conduction wave propagated in this region. The nitrogen thermal wave was enhanced due to the tight coupling of the radiation and gas fields; its propagation speed is dominated by the energy exchange between these fields. The propagation speed of a thermal conduction wave is due solely to its thermal conductivity; therefore, on the time scales under consideration, the thermal wave does not propagate as far into the helium as into the nitrogen region. Figure 6 illustrates an interesting effect due to the opacity difference at the interface: the gas temperature in the first helium zone becomes very high. Compression heating of the helium from the essentially stationary pressure gradient at the interface rapidly increased its temperature. Since the region was modelled as optically transparent, the gas could not lose energy by radiating.

Finally figure 7 illustrates the spatial distribution of the radiation temperature after the fireball has reached the interface. Here we can see that the radiation field had "burst" into the He gas and the fireball vented energy "upward" into the cavity. One will note that the radiation temperature is approximately 2.5 eV at this point. This will be a crucial value in determining the effectiveness of this pressure reduction scheme.

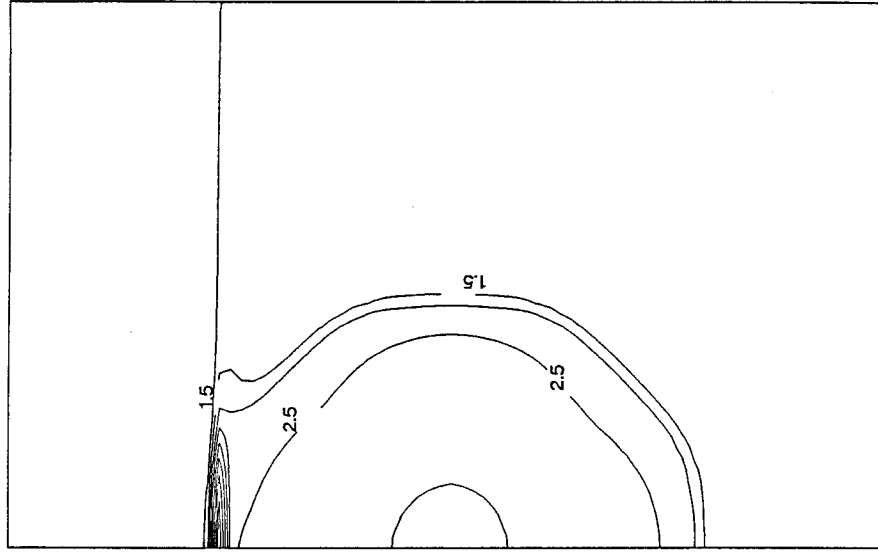
Figure 8 shows the comparison between the vented 100 cm case and a single region nitrogen case. Essentially there are only minor differences. This is due to the relatively low radiation interface temperature when the fireball reached the He. Since the radiation energy density is proportional to the fourth power of temperature, the actual energy flux being "vented" out of the fireball is comparatively small; the overpressure reduction would be negligible.



Plasma Temperature $t = 2.e-06$ s

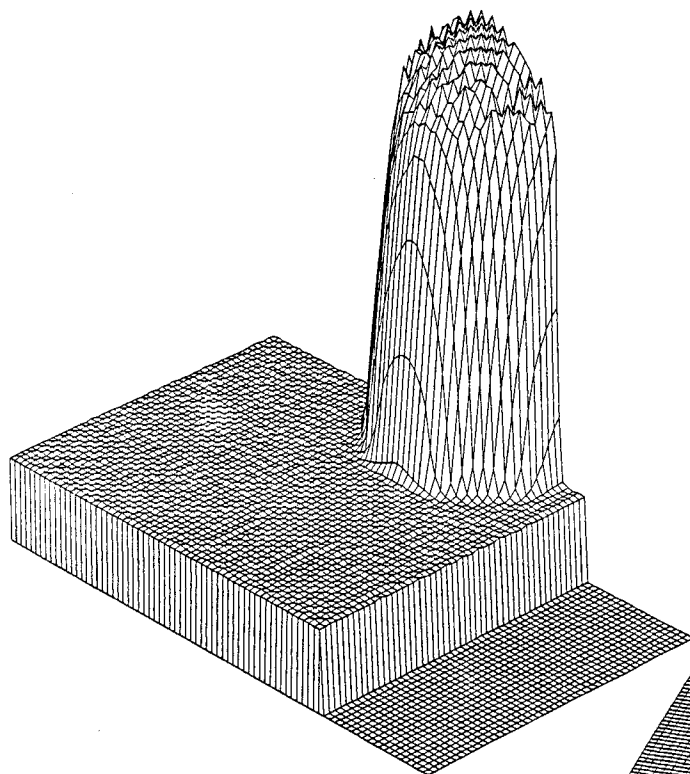


Plasma Temperature $t = 1.7e-05$

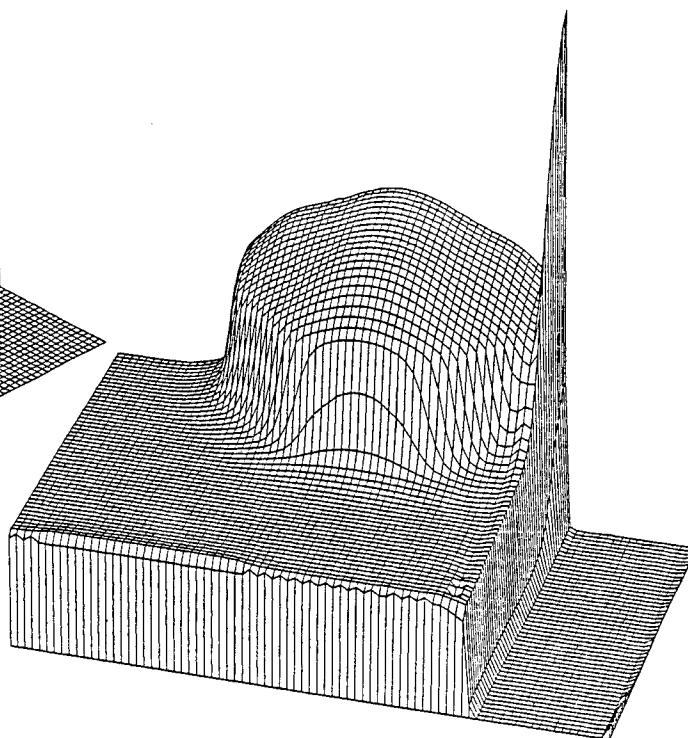


Plasma Temperature $3.17 e-5$ s

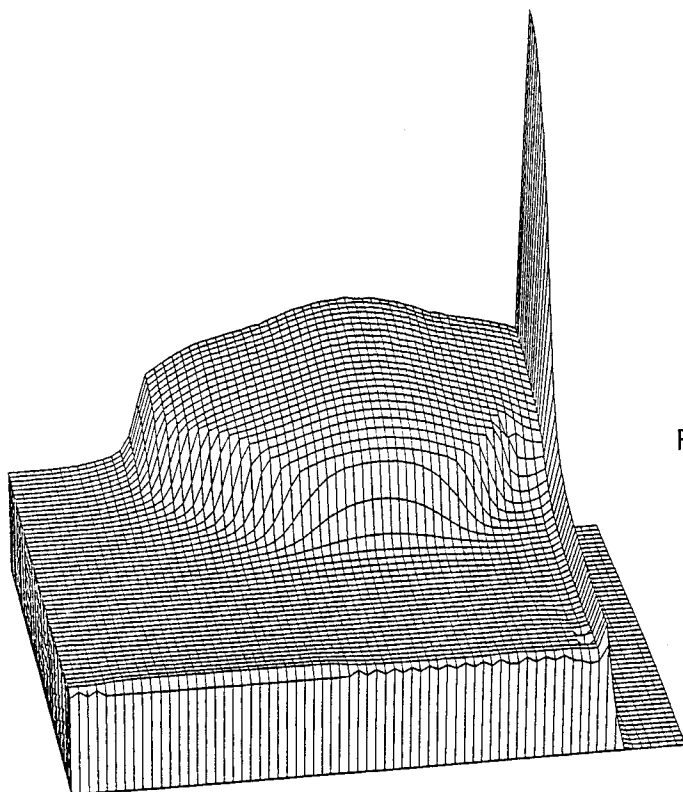
Fig. 5 Gas Temperature Contours for the 100 cm case.



Plasma Temperature $t = 2 \text{ e-}06 \text{ s}$

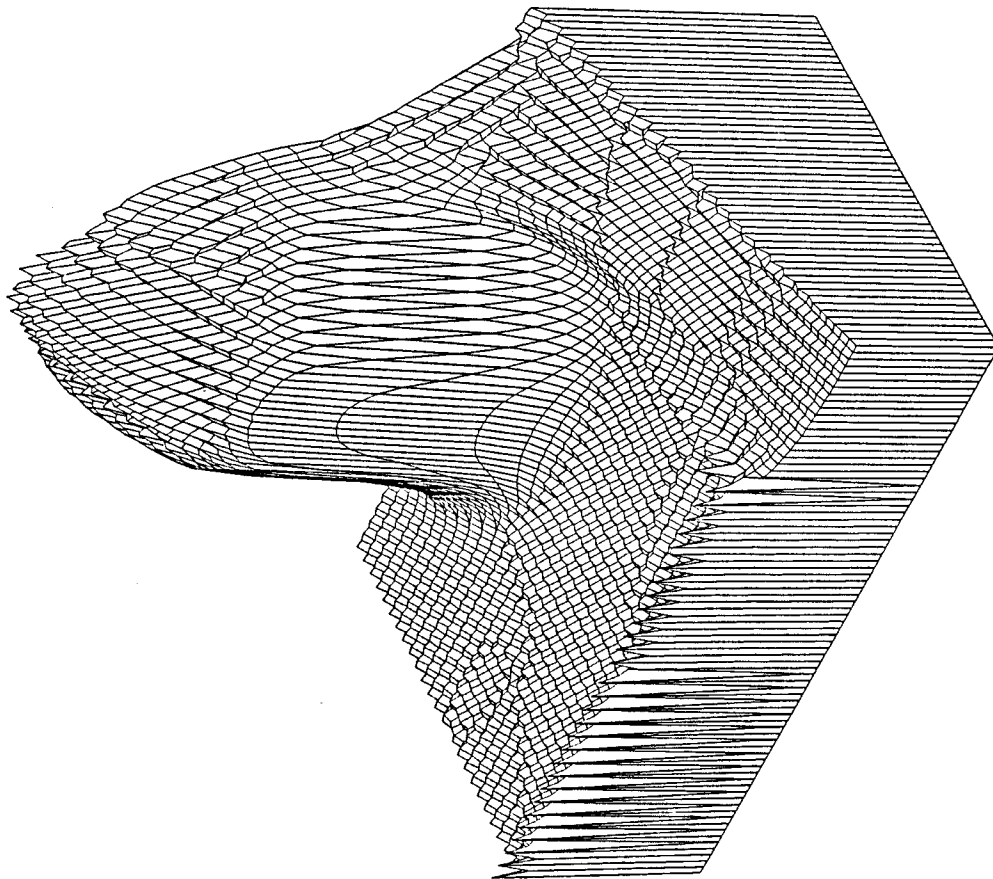


Plasma Temperature $3.17\text{e-}5 \text{ s}$

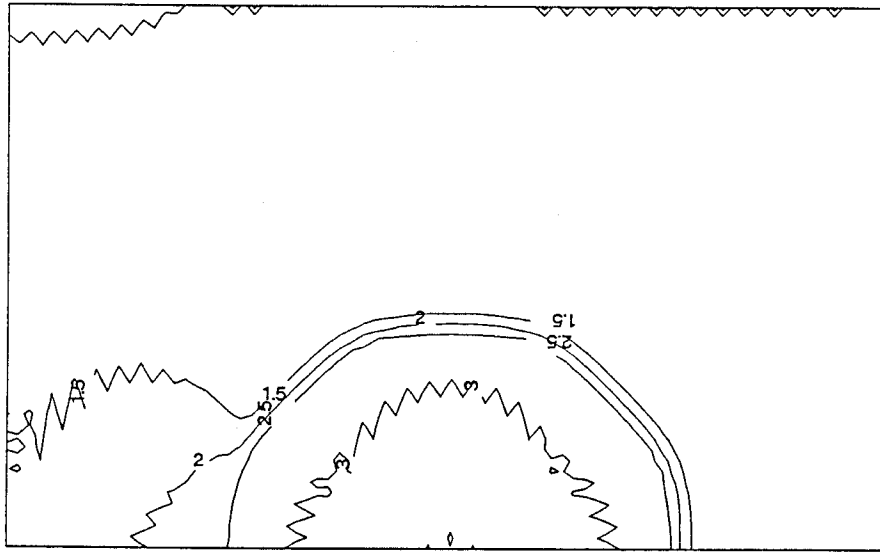


Plasma Temperature (100cm) $44.5\text{e-}6\text{s}$

Fig. 6 Gas Temperature for
100 cm case.



Radiation Temperature $2.16e-5$ s



Radiation Temperature $2.16e-5$ s

Fig. 7 Radiation Temperature for 100 cm case

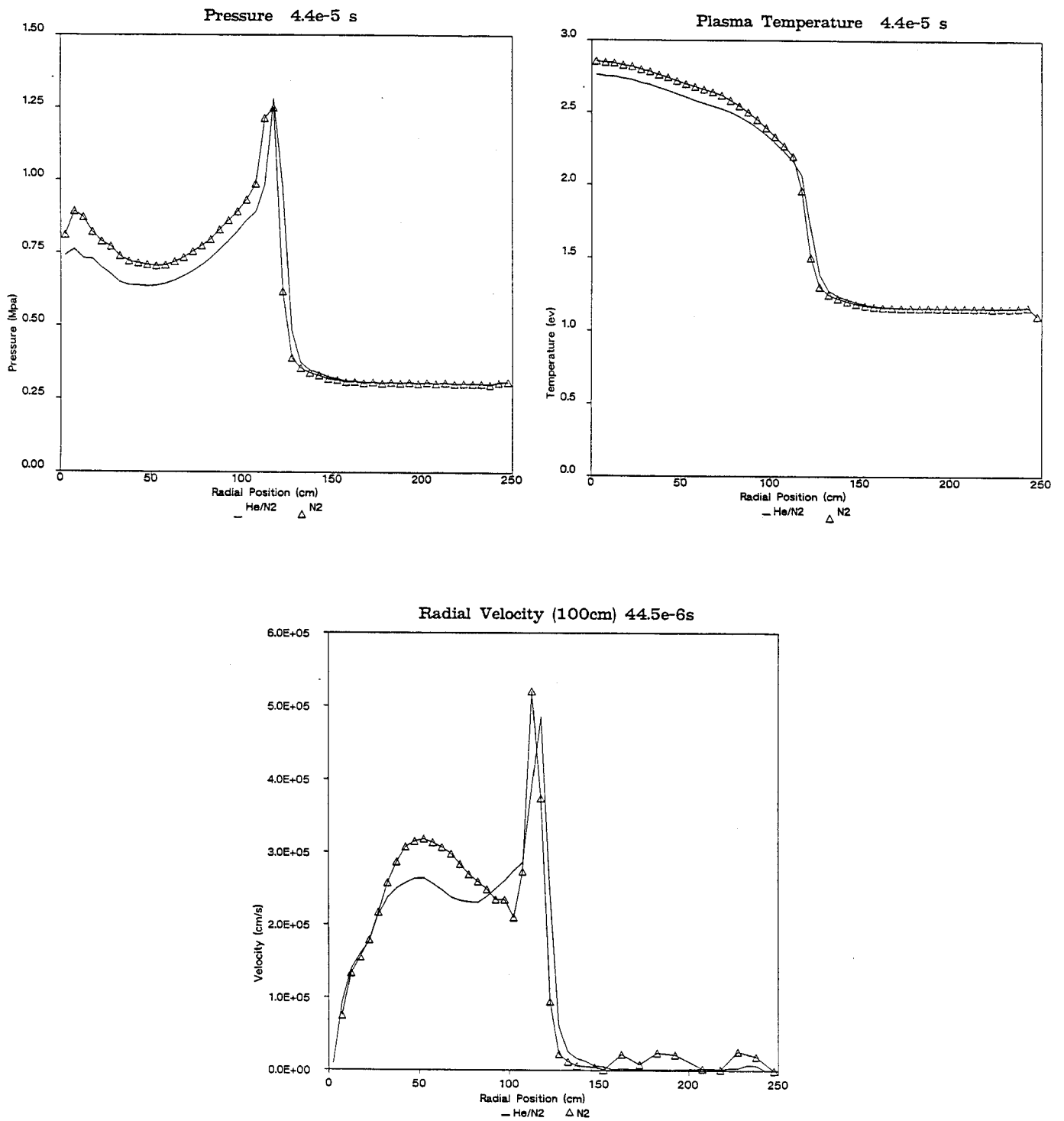


Fig. 8 Comparison of Pressure, Gas Temperature and Velocity between the Vented 100 cm case and Pure N₂ solution (plotted along the radial direction from the target)

2.1.2 40 cm.

In an effort to increase the interface radiation temperature when the fireball reached the He region, the separation distance was reduced from 100 cm to 40 cm. Figure 9 shows the gas and radiation temperatures along the vertical axis for two early times. The target was at 200 cm and the interface located at 240 cm. Here we see that the interface radiation temperature was much higher than the 100 cm case when the fireball reaches the helium. A temperature of 16 eV resulted in approximately 1700 times the vented energy flux than the 100 cm case. The spatial and temporal behavior of the fireball was otherwise similar to the 100 cm case.

Figure 10 shows the comparison between the 40 cm vented case and a one dimensional simulation of a 200 MJ explosion in pure nitrogen. One interesting point is that the location of the fireball edge, using the point of the maximum velocity, is the same for both calculations. This will simplify the later analysis. One can easily see that the vented fireball contains less energy due to the reduced core gas temperature and velocity. However, the peak velocities are similar because they are essentially determined from the pressure gradient at the edge of the fireball, which are also similar for both calculations. It is speculated that the pressure gradient, or equivalently the temperature gradient in the diffusion dominated region, is determined by the temperature dependence of the cavity gas opacity at the thermal front. If true, one would expect the gradients to be similar irrespective of the venting process, as the present calculations show.

2.1.3 10 cm.

The final calculation for the 200 MJ simulations reduced the distance between the target and the He region to 10 cm. This was done to determine the maximum realistic effect of energy venting. Figure 11 shows the gas and radiation temperatures along the vertical axis during the initial stages of the fireball evolution. Here, one can easily see the interaction of the He region with the formation of the fireball. One interesting point is that the radiation temperature quickly reached a steady value of about 7 eV while the gas temperature remained somewhat higher, 12 eV; the energy loss by venting was then balanced at these temperatures by the radiation emission from the gas. These values are determined by the opacity differences for the temperatures and number densities of interest. This equilibrium radiation temperature placed

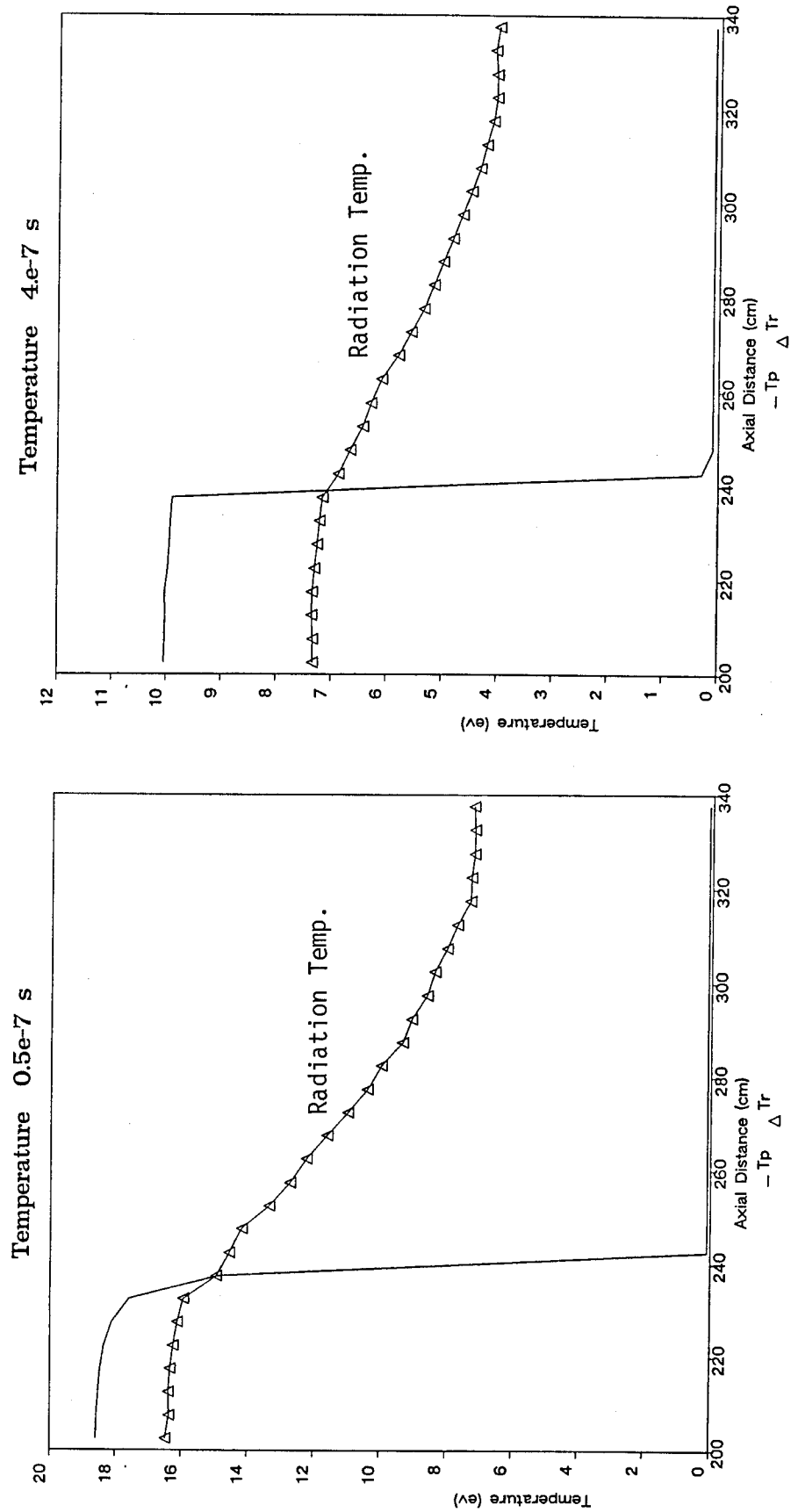


Fig. 9 Gas and Radiation Temperatures in the Axial Direction (upward from the target) for the 40 cm case (target located at 200 cm and gas interface at 240 cm)

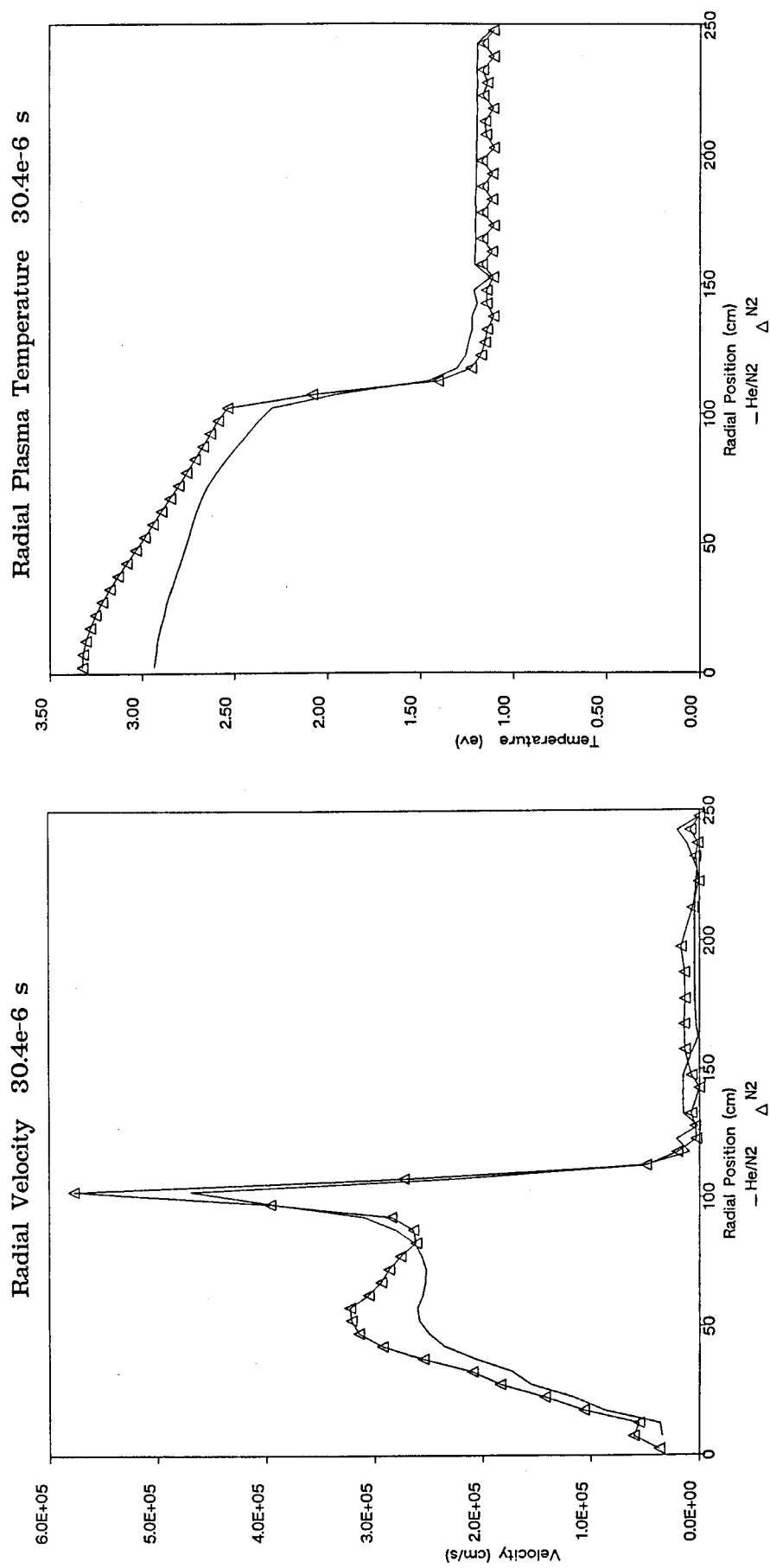


Fig. 10 Comparison of Velocity and Gas Temperatures between the Vented 40 cm case and pure N₂ solution (plotted along the radial direction from the target)

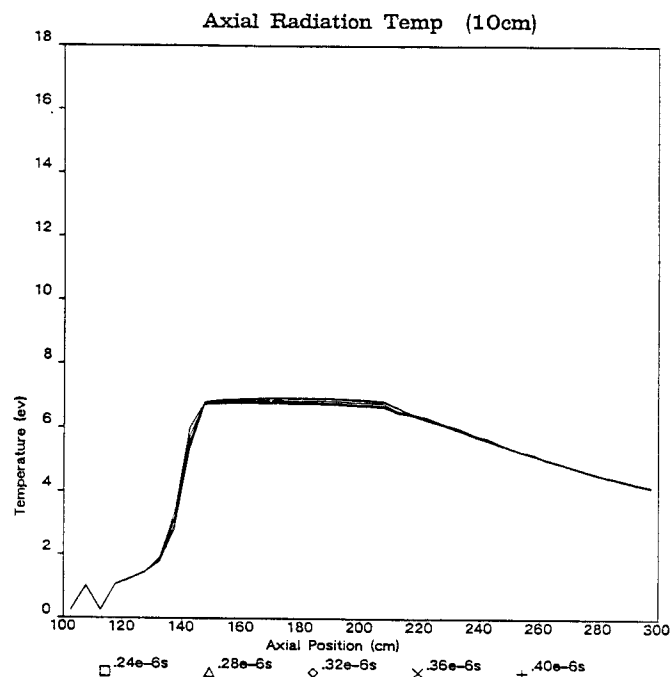
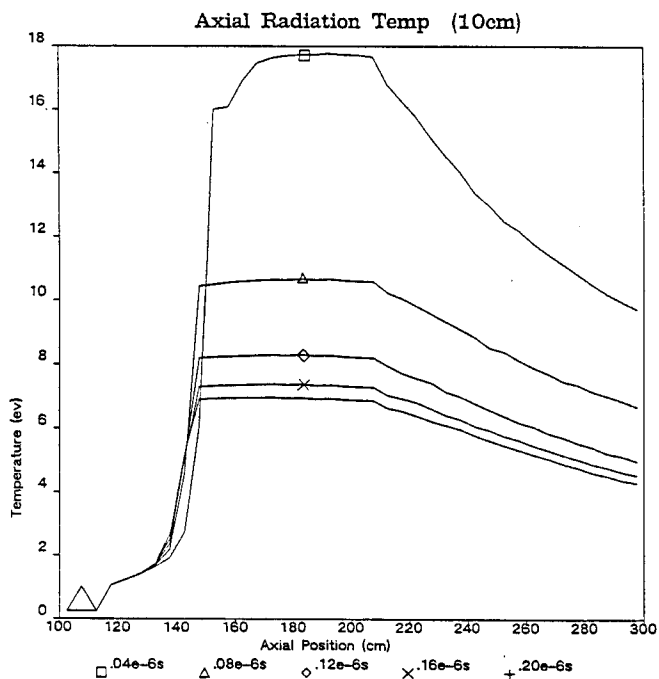
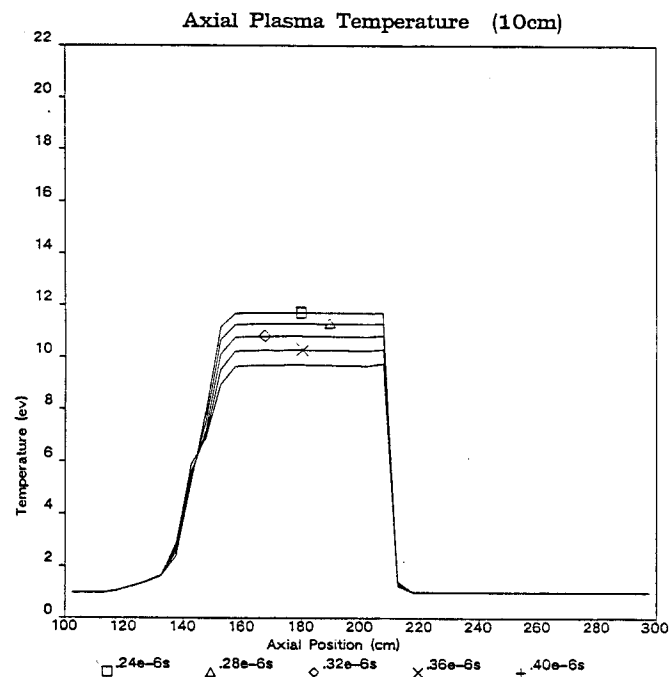
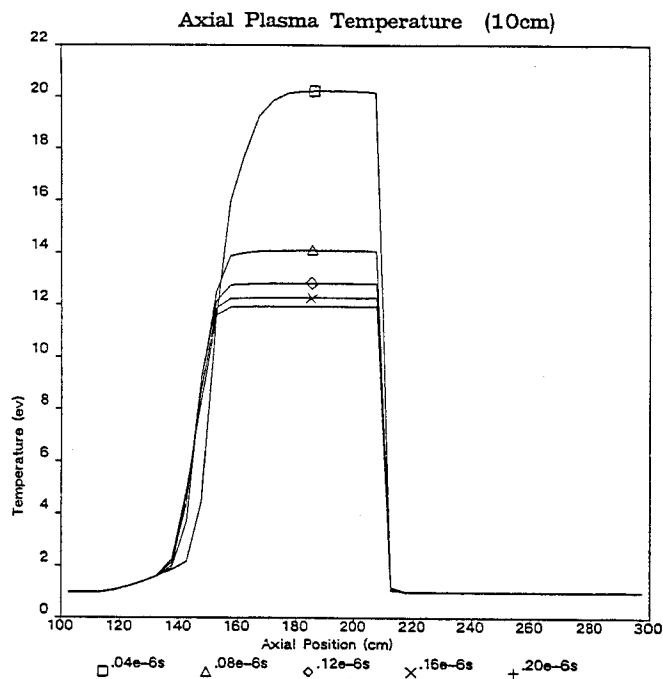


Fig. 11 Axial Gas and Radiation Temperatures for 10 cm case
(target located at 200 cm and gas interface at 210 cm).

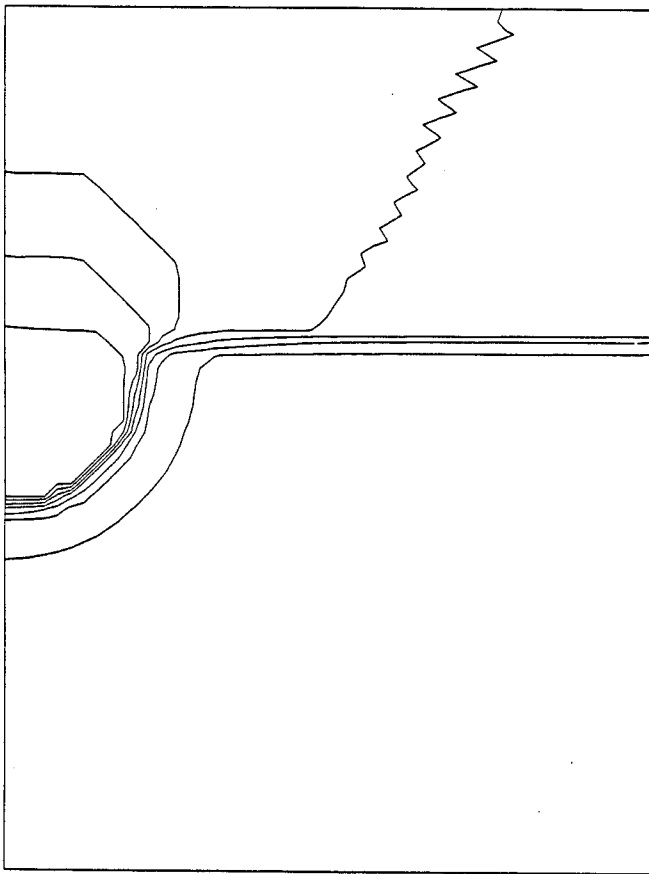
a limit on the vented energy loss. Different gas or fluid conditions might yield a more favorable equilibrium temperature.

As mentioned earlier, the diffusion approximation was used to model the radiation transport. This assumption is not valid in the helium region with the assumption of the optically transparent gas. Figure 13 vividly shows a consequence of this. The contour plot radiation temperature shows the non-physical propagation of the radiation wave in the He region. One would expect little radial diffusion as the radiation energy was transported into the helium from the interface; it would have the characteristics of a columnar beam. However, the diffusion approximation with its scalar effective diffusivity predicted large radial spreading. For this simulation, the radiation energy then reentered the nitrogen region and was subsequently attenuated, increasing its temperature. This resulted in a diffuse region near the interface and is illustrated in fig. 12, the perspective plot of the gas temperature. In this figure, one can contrast the sharp temperature gradient along the downward axial direction with the gentle slope in the radial direction. This is entirely an artifact of the computational models used for radiation diffusion. This effect was only observed for the situations where the target was very close to the gas interface.

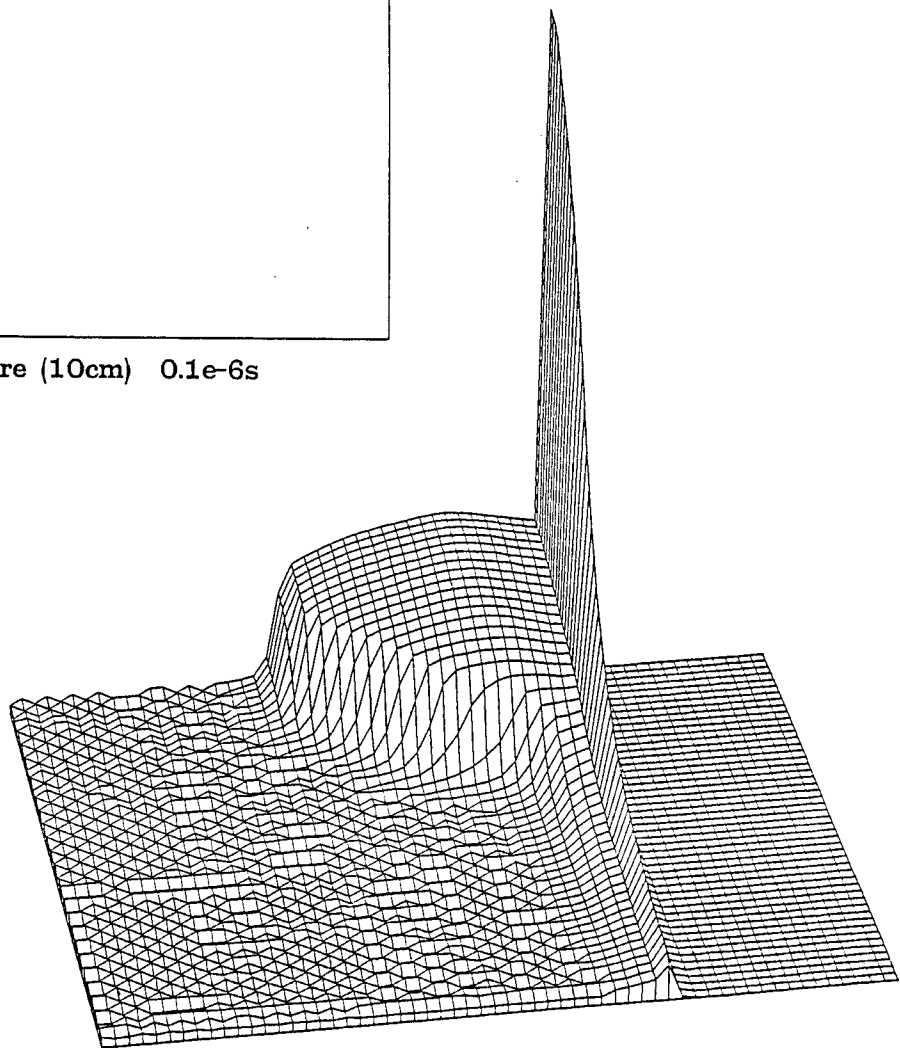
For this reason, comparisons between the pure nitrogen calculation were done using the fluid values along the downward axial direction from the target, that would be unaffected by this interface problem. Figure 13 shows this comparison. One can observe that although the peak stagnation pressure was essentially the same for both cases, the core values were noticeably reduced for the vented case. The same trends are also seen in the plot of total energy density. However, since the total fireball energy is a volume integral of this quantity and the majority of the volume of a sphere is in its outer radius, the differences are not as great as the plots would tend to indicate.

2.2 800 MJ Target Yield

Although a target yield of 200 MJ was the design base value for the TDF cavity, high gain targets will be periodically tested. For this reason, a stratified cavity gas simulation was performed with a target yield of 800 MJ; the separation distance was taken as 20 cm. Figure 14 shows the initial gas temperature profile for the 800 MJ case as calculated by MF-FIRE⁸. Its peak temperature is much higher than that for the 200 MJ case as shown in figure



Radiation Temperature (10cm) 0.1e-6s



Plasma Temperature (10cm) 16.9e-5s

Fig. 12 Gas and Radiation Temperatures for the 10 cm vented case.

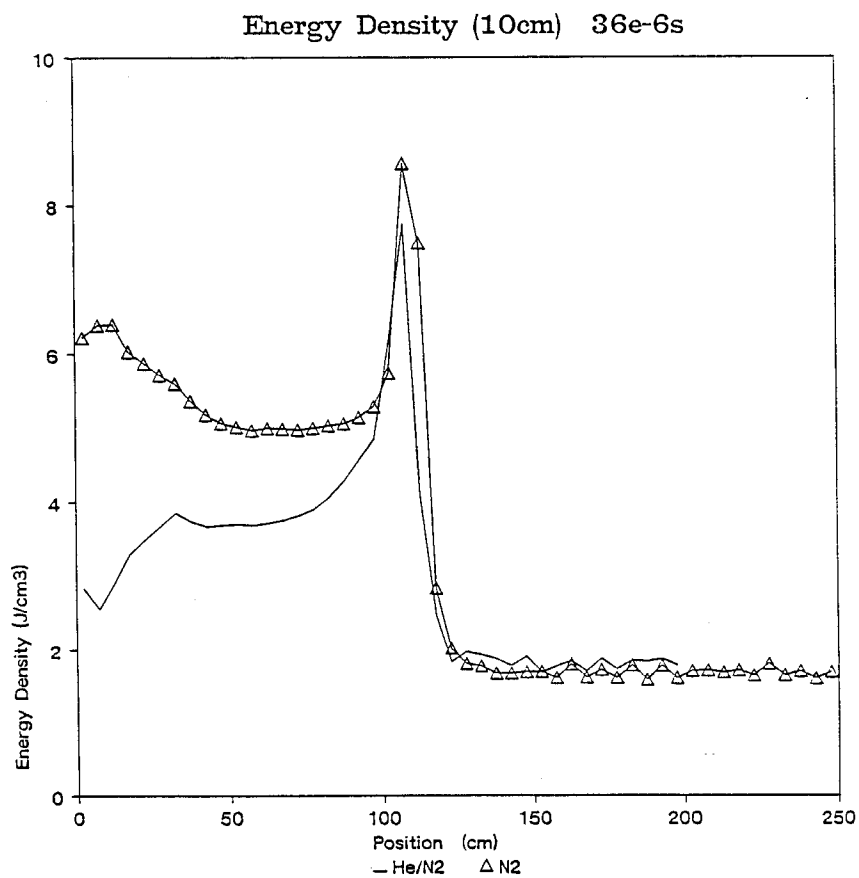
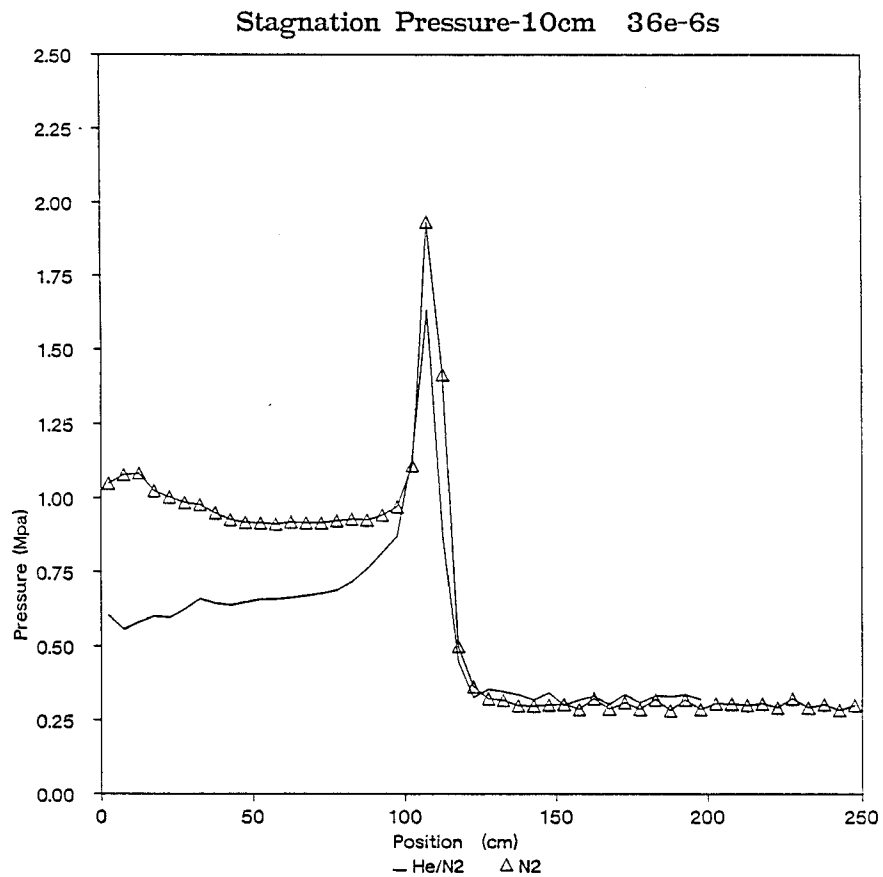


Fig. 13 Comparison between the Stagnation Pressure and Total Energy Density from the vented 10 cm and pure N_2 cases (target at 0 cm)

3. The MF-FIRE initialization for the 800 MJ case used a finer mesh near the target center to better resolve this high gradient region. One might expect a stronger venting effect for this case because of the much higher temperatures.

2.2.1 20 cm.

Figure 15 shows the initial axial gas temperature distribution for this case. The effects of the He region are clearly shown by the sudden drop in temperature at 220 cm; here, the target location was at 200 cm. This is a result of the low opacity of helium. Figures 16 and 17 show the axial gas and radiation temperatures for four simulation times. The target location and the helium zone for the simulation are indicated. One will note that the gas temperature remained at a high value for at least 1 microsecond. This is unlike the 200 MJ cases, shown in fig 11, where the gas temperature rapidly dropped as the core gas radiated; the gas and radiation temperatures converged for the 200 MJ yield. Comparison of the gas and radiation temperatures for the 800 MJ simulation in figures 16 and 17 show that the radiation temperature did not drastically increase. This is because the 800 MJ target fully ionized the nitrogen gas; the opacity became very small so the gas and radiation became weakly coupled.

Figure 16 also shows the expanding thermal fronts, both in the nitrogen and the helium regions. A thermal wave is evident in the nitrogen, where thermal radiation from the center of the fireball is absorbed and is re-emitted from successive layers of gas. This process occurs because of the high opacity of the nitrogen and is therefore not present in the helium, where the opacity is very low. Also shown is that the radiation temperature at the helium-nitrogen interface remained low; thus, fireball energy loss from radiation "leakage" to the helium region was low. This finding was the same as for the 200 MJ simulations.

The increased energy deposition of the 800 MJ target over the 200 MJ simulation resulted in a very different hydrodynamic behavior at the fireball core. Figures 18 and 19 show the initial and three subsequent axial density and velocity profiles. The very high gas temperatures resulted in a large pressure gradient which lead to rapid hydromotion of the gas out of the core. This is shown by the very low core density in figure 18 and the large, early time, outward velocities in figure 19. When the core gas temperature was reduced to a point where the nitrogen opacity became significant, little mass

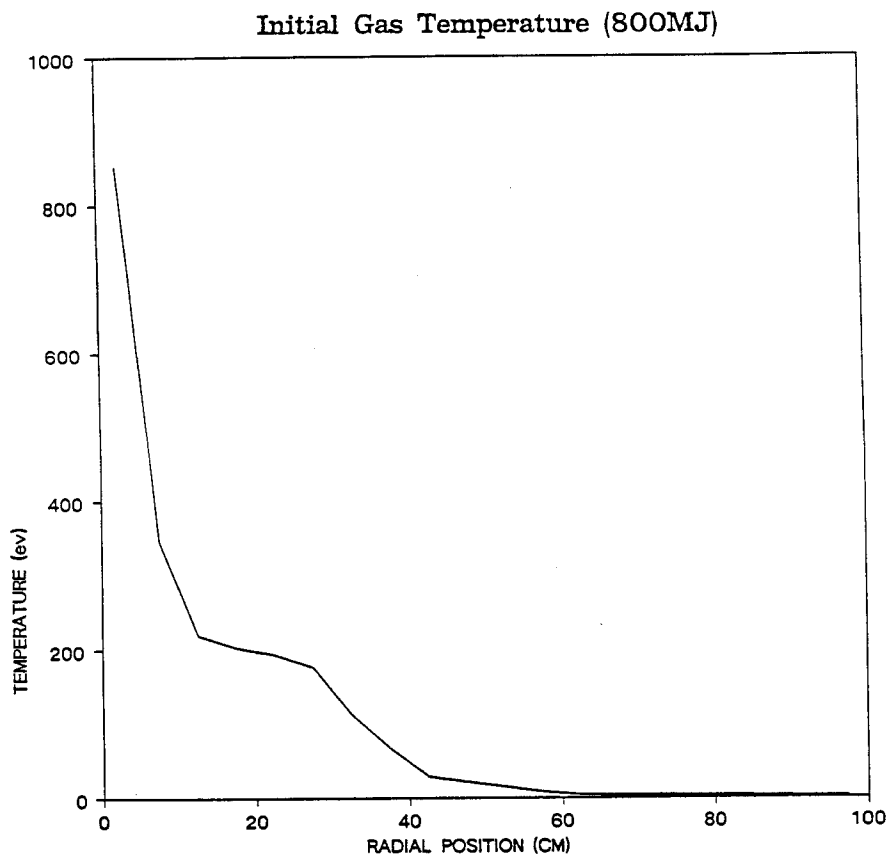


Fig. 14 Initial Radial Gas Temperature for 800 MJ Target in N_2 .

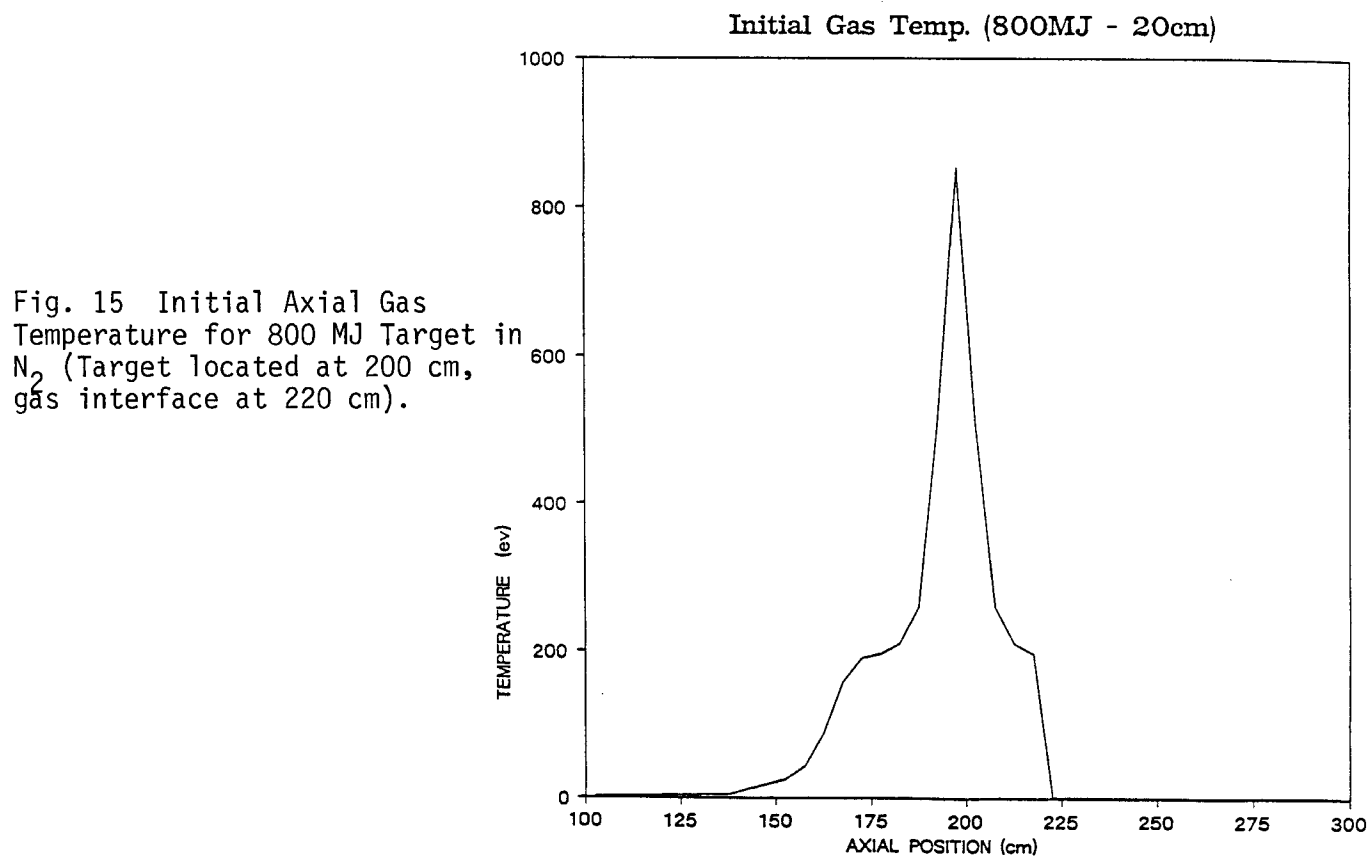


Fig. 15 Initial Axial Gas Temperature for 800 MJ Target in N_2 (Target located at 200 cm, gas interface at 220 cm).

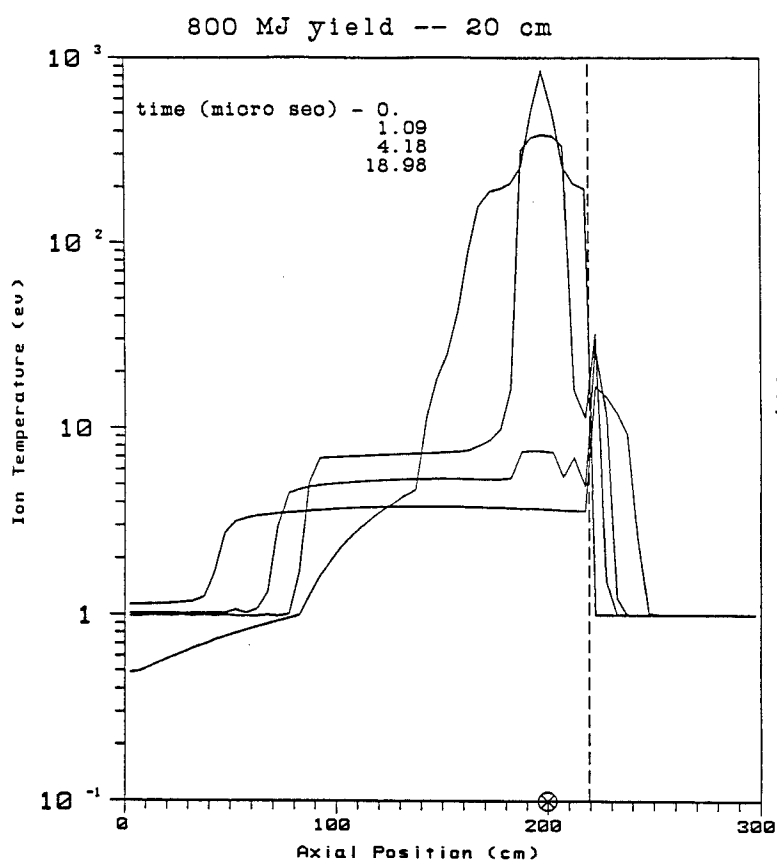


Fig. 16 Axial Gas Temperature for Target in N_2 region.

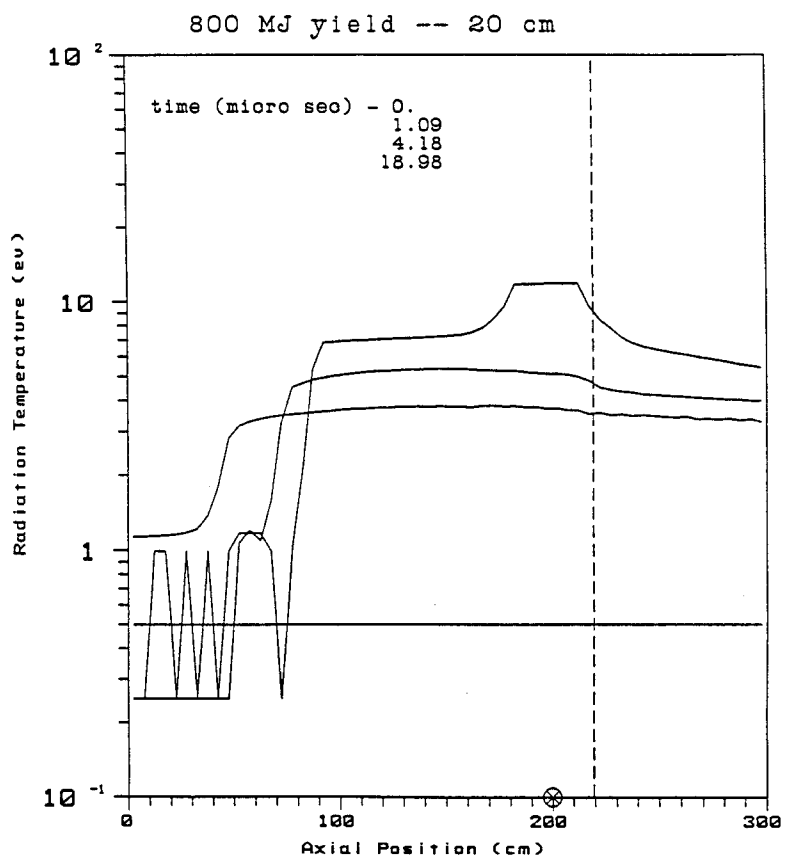


Fig. 17 Axial Radiation Temp. for 800 MJ Target in N_2 region.

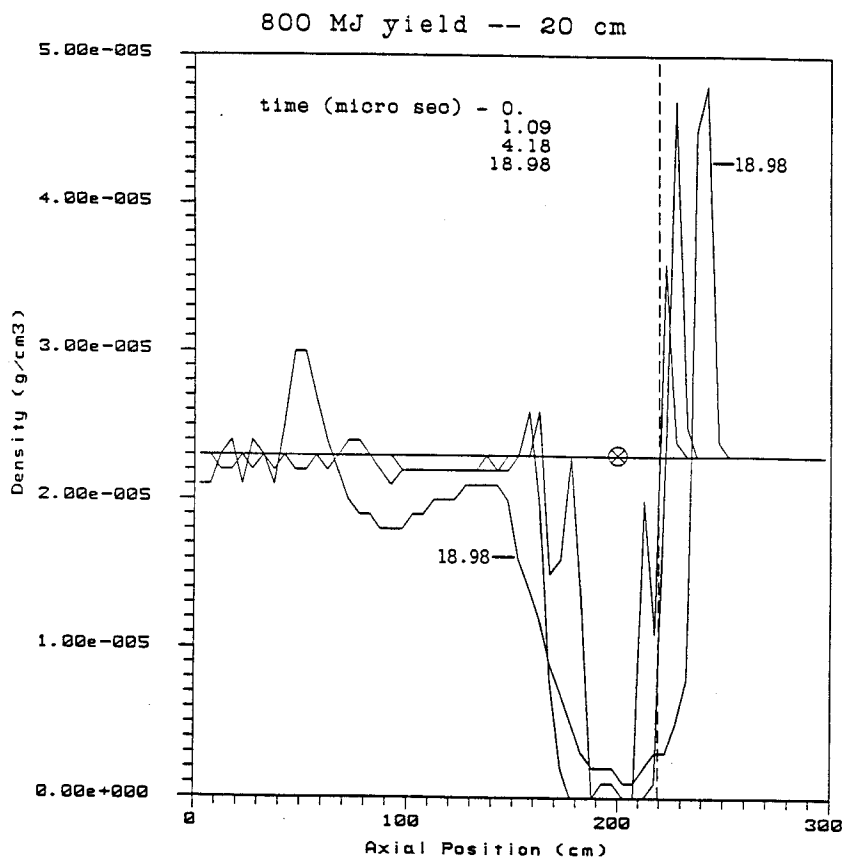
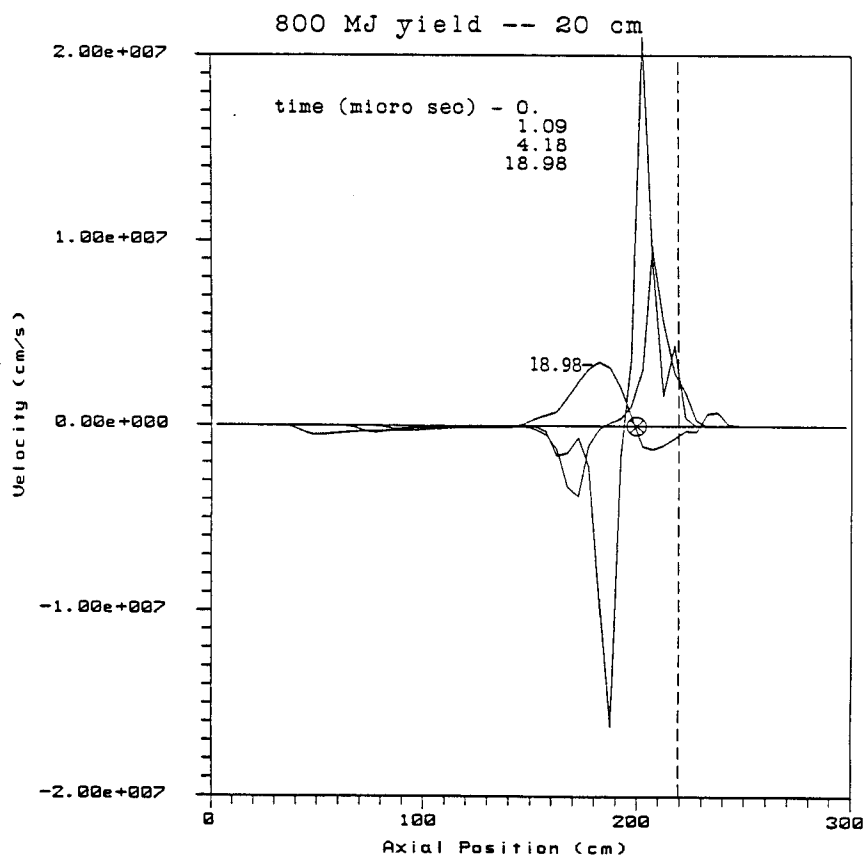


Fig. 18 Axial Fluid Density for 800 MJ Target in N₂ region.

Fig. 19 Axial Fluid Velocity for 800 MJ Target in N₂.



remained in the core. At this point in time, the gas temperature quickly dropped, as is shown in fig. 15, which resulted in an adverse pressure gradient. Therefore the hydromotion in the core was reversed and the core compressed as mass moved back into it. Figure 18 shows the increased density in the core at the last plotted time and figure 19, the change in sign of the velocity front. However, this effect is not important to the overall propagation of the fireball since only a small amount of mass is involved. The majority of the fireball's mass was located at its perimeter, as shown in figure 18. The high density helium region located at the gas interface was due to the same intense pressure gradient as discussed earlier for the 200 MJ case, that is, the result of a conduction and not radiation driven thermal wave in the helium region.

Figures 20 and 21 compare the stratified gas and pure nitrogen calculations where the gas temperature and pressure are shown. The spatial axis has been modified so that the target is at position 0 cm for both conditions. There are no significant differences between the two simulations at the edge of the fireball. The differences in the pressure at the core at 15 microseconds was that the radiation 'venting' allowed the flow reversal to occur earlier than for the pure nitrogen case. Essentially the core gas temperature was reduced faster through the radiation loss. Figure 22 shows pressure profiles for the pure nitrogen case. We can see that at 4.22 microseconds the flow reversal has not occurred, but at 50 microseconds it has.

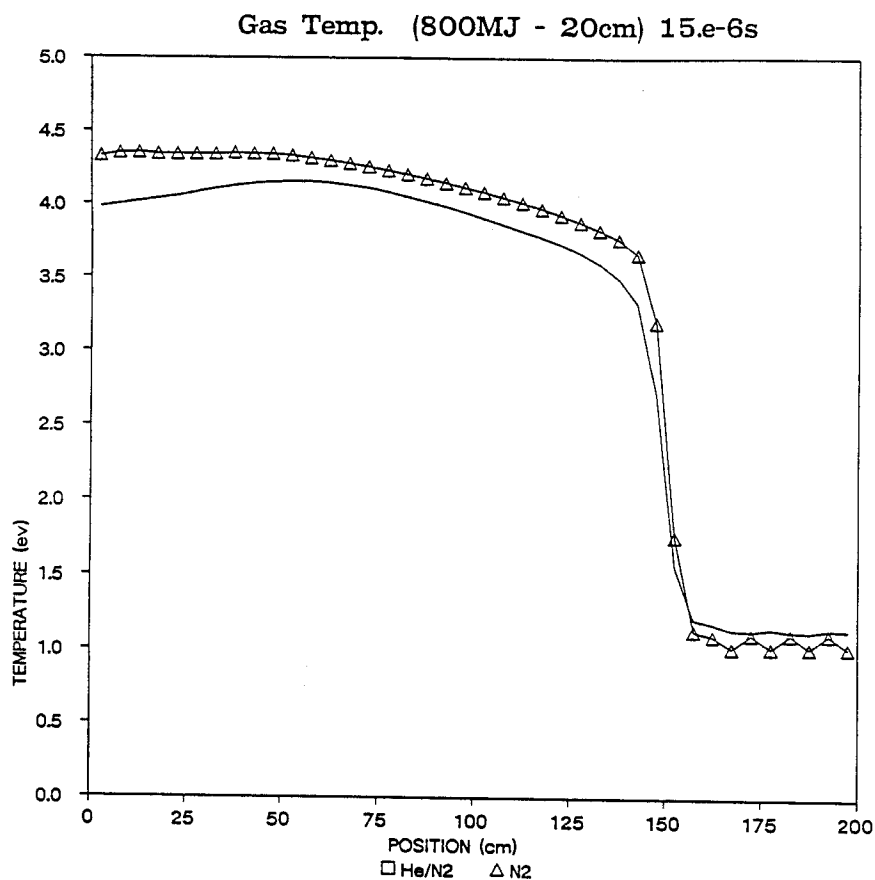
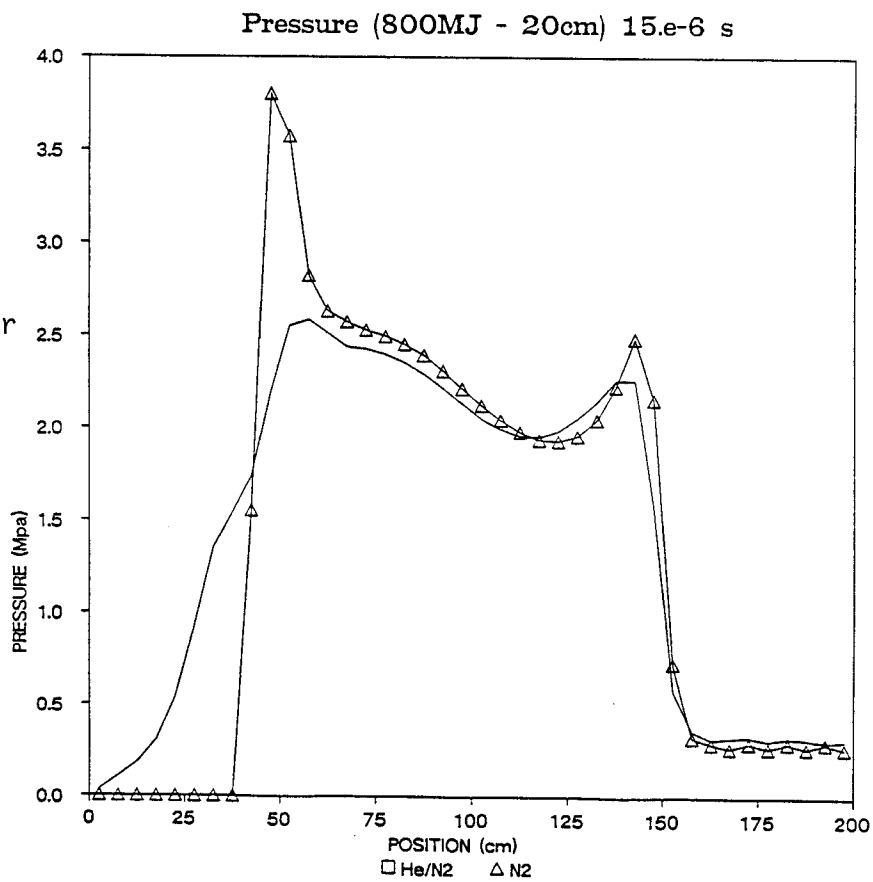


Fig. 20 Local Gas Temperatures for vented and pure N₂ case (target located at 0 cm).

Fig. 21 Local Gas Pressure for vented and pure N₂ case. (target located at 0 cm).



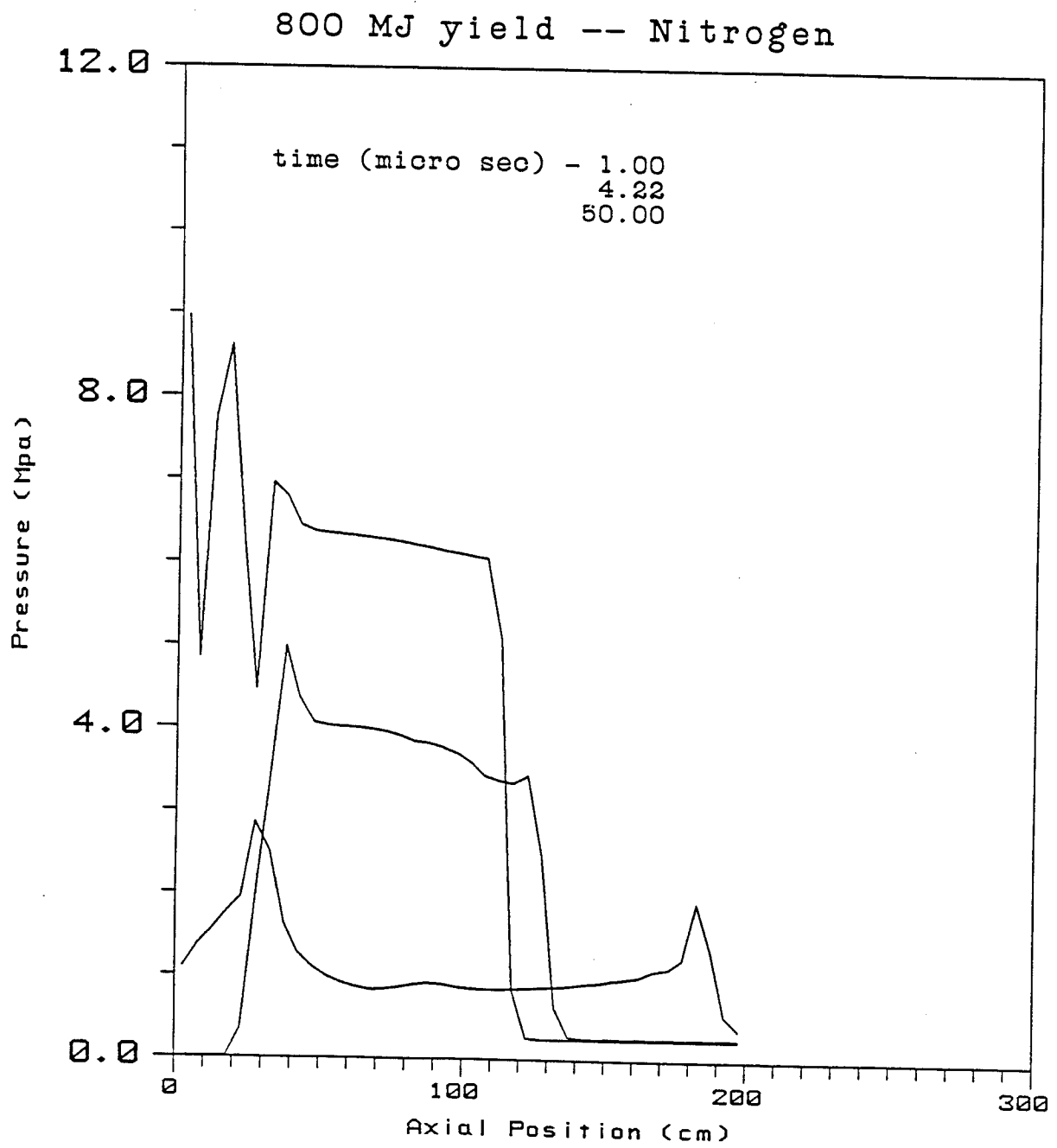


Fig. 22 Local Gas Pressure for Pure N_2 case.

3. Target in He Region

A series of one dimensional calculations were performed when the target was located in the helium region and the instrument package located in the nitrogen. The initial cavity density was taken as that which would have a pressure at 0° C of 15 torr, the same as the earlier calculations. Two target yields were simulated: 400 and 800 MJ. And as before, the distance from the target to the gas interface was varied to determine spatial effects. The distance from the target to the 'wall' was kept a constant for all cases: 300 cm.

MF-FIRE⁸ was used to simulate this series of calculations. This code has the X-ray deposition model and multi-material capability which were required. This code is only one-dimensional; a spherical coordinate system was chosen for the present investigation. In essence the geometry simulated was one of concentric spheres: the inner one was composed of helium and the outer spherical shell was nitrogen. A spherical system was used as opposed to a cartesian system to account for the $1/r^2$ nature of the X-ray deposition.

Recall that figures 1 and 2 show two cavity configurations for the case where the target is in the helium. From the prior discussion, it is evident that the present investigation identically models the geometry in fig. 2. However, the results can still be used to predict the initial pressure and heat flux loads on the instrument package for the cavity in fig. 1. Since the one dimensional simulation does not simulate the radiation losses or fluid motion to the upper region, only the initial wall responses can be used. The long term pressure impulse and surface heat flux history must be obtained from a full two dimensional simulation.

3.1 400 MJ Target Yield

Four calculations were performed with a target yield of 400 MJ: a target-to-interface distance of 25 and 50 cm and the target in either pure helium or nitrogen.

Figure 23 shows the initial gas temperatures for the 25 and 50 cm simulations. The temperatures are of course identical from 0 to 25 cm in the helium region. The much higher X-ray stopping power of the nitrogen gas caused the gas temperature in the 25 cm case to be very high at the interface; this effect is also seen for the 50 cm case. The pressure distribution

would be very similar to the temperature distribution. Thus, a sharp pressure gradient was created at the gas interface region. The fireball had become essentially a plane pressure source at the interface and could expand in either direction: into the helium or the nitrogen. One would thus expect the stagnation pressure on the wall to be reduced by a factor of 2.

Figure 24 shows the stagnation pressure on the wall, located 300 cm from the explosion, for the four 400 MJ simulations. The peak pressure for the pure nitrogen case is approximately 3 MPa while the peak pressures for either target in helium case is only 1.5 MPa; the maximum pressure point for a pure helium simulation is illustrated for comparison. Essentially the use of two gases with different opacities and X-ray stopping powers changes the fireball expansion from having kinetic energy in one direction to having it in two; the maximum pressures are reduced by 50% simply by momentum and energy conservation arguments.

The limiting case of target to interface distance, the pure helium simulation, had a maximum pressure of approximately 20% of the pure nitrogen case. This helium peak pressure would correspond to a target yield of 200 MJ in a pure nitrogen cavity. The reason for this effect will be described next.

A drawback to using the helium gas, either in conjunction with nitrogen with the geometry of figure 1 or as a single cavity gas, is the resulting increase in surface heat flux. This is simply due to the reduced opacity and X-ray stopping power of the helium. Table 1 shows the maximum surface heat fluxes for the 400 MJ and 800 MJ simulations. One can note the drastic reduction in surface heat loading by using an absorbing gas as opposed to a transparent gas, the helium. Since energy must be conserved, the ratio of pressure loading to surface heat flux can be varied, depending on the particular system limitations. The TDF cavity under consideration is an experimental facility which will explode targets only about 10 times a day; a commercial reactor is expected to have an operation cycle on the order of a fraction of a second. Therefore, the heat flux question is much more important for the reactor, because of wall ablation, than it is for a test facility.

Figure 25 shows velocity profiles for the 25 and 50 cm calculations for the times where the velocity pulse reached the wall. Several features can be observed. First, the pulse arrived at the wall at essentially the same time for both calculations and the peak velocities were also equivalent. The difference

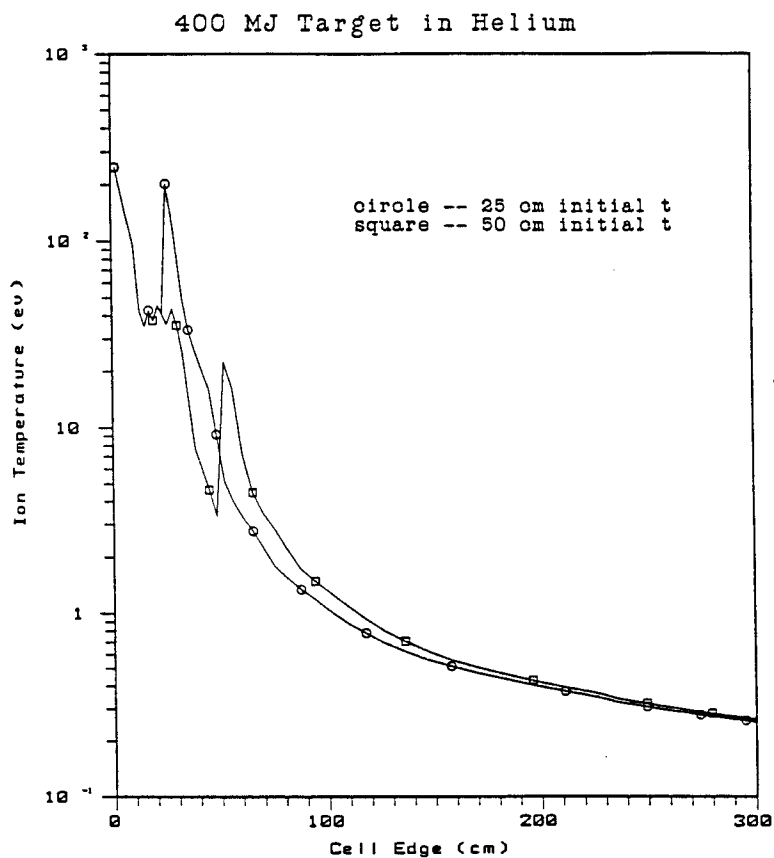
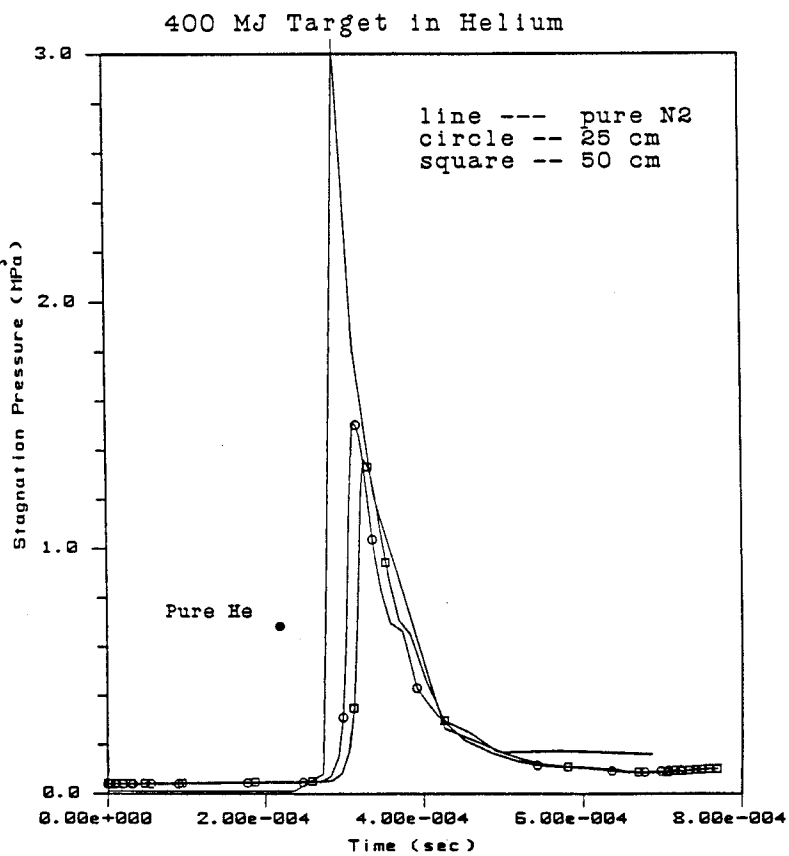


Fig. 23 Initial Gas Temperature for 400 MJ Target in He region.

Fig. 24 Stagnation Pressure for 400 MJ Target in He region and pure N₂ case (only max. value for pure He case shown).



in the helium region thickness was not enough change the initial wall loading by the blast wave. Now recall that these calculations were done in a spherical coordinate system. One will note that the fluid in the 25 cm case has reflected from the center and was propagating toward the gas interface; the helium fluid for the 50 cm calculation was still reversing toward the center. An important finding is that the magnitude of the velocity peak in the helium for either calculation is much smaller than the peak in the nitrogen; therefore, wall loading effects from this second pulse would not be important.

TABLE 1

<u>Maximum Surface Stagnation Pressure and Heat Flux</u>		
Case	Stagnation Pressure (MPa)	Heat Flux (MW/cm ²)

200 MJ pure Nitrogen	.62	
400 MJ pure Nitrogen	3.06	.03
400 MJ 25 cm	1.51	.18
400 MJ 50 cm	1.36	.13
400 MJ pure He	.68	5.75
800 MJ pure Nitrogen	6.32	.10
800 MJ 25 cm	3.19	.72

3.2 800 MJ Target Yield

A simulation with a single separation distance, 25 cm, was performed for the high yield target case. Figure 26 shows the wall stagnation pressure for both this case and one for a pure nitrogen cavity gas. Again, as was the situation for the 400 MJ targets, the peak pressure has been reduced by 50% with the use of a gas interface region. The maximum surface heat fluxes are given in Table 1. The heat flux follows the same inverse trend with the peak pressure as the 400 MJ simulations.

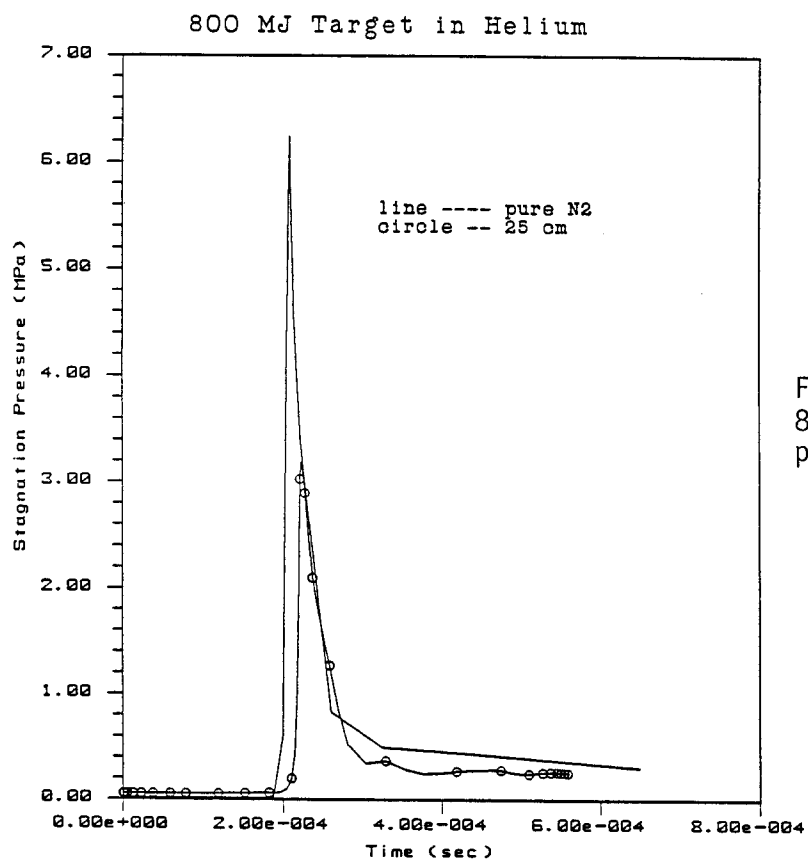


Fig. 25 Stagnation Pressure for 800 MJ Target in He region and pure N₂ case.

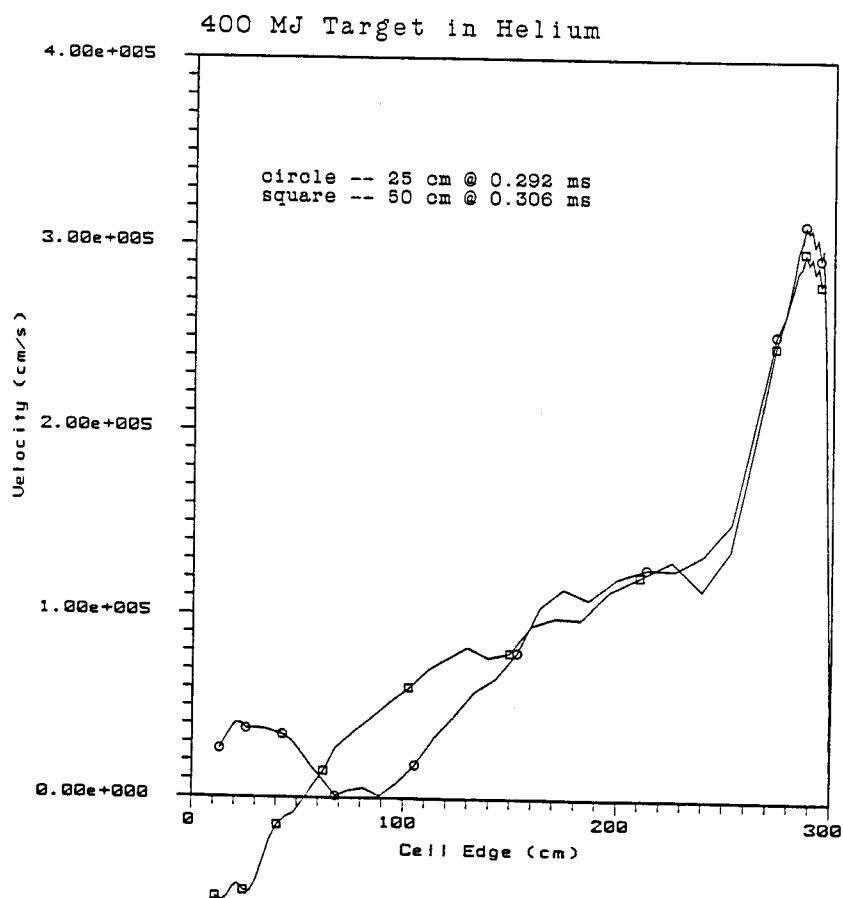


Fig. 26 Velocity Profiles for 400 MJ Target in He. (target at 0 cm).

4. Analysis

4.1 Target in N₂ Region

Figure 27 clearly shows the effects of the venting for the 200 MJ simulations. Here the energy in a pseudo-uniform fireball whose radial profile is taken as the vented case is scaled to the pure nitrogen case where no venting occurs. One can see that the 100 cm separation distance resulted in only a minimal effect while the 10 cm case achieved a reduction of approximately 20%. Since the radial position of the fireball, determined from the locations of the peak velocity, is similar for both the vented and non-vented cases, it is easy to determine the overpressure reduction one would expect. Strong shock theory^{3,4} states that the peak stagnation pressure is proportional to the total blast energy and inversely proportional to the radius cubed. Thus for the same radius, the impulse ratio between the vented and non-vented cases simply reduces to the ratio of the fireball energies; therefore, figure 27 gives the pressure reduction directly. An asymptotic value of a 20% pressure reduction was predicted for the 200 MJ simulations.

Figure 28 shows the temporal interface radiation temperature behavior for the three 200 MJ cases; it is equivalently the vented energy flux. This figure helps to interpret the results of the preceding figure. We can see that the temperatures for the 10 and 40 cm cases are essentially the same. Thus the differences between the energy ratios in figure 27 were due to the increased vent area for the 10 cm case. The 100 cm interface was too far from the target and thus its vented energy density was too low to significantly affect the fireball evolution.

4.2 Target in He Region

A significant reduction in the peak wall pressure was calculated for the case where the target is in the helium region. This was due to the conversion of the spherical fireball pressure expansion to a surface source; conservation of momentum and energy lead to a 50% reduction in wall pressure loading. A cavity with a single gas, helium, had an even further stagnation pressure reduction when compared with the case of a pure nitrogen cavity. The penalty for this pressure reduction is the increased surface heat flux as shown in table 1. The use of nitrogen in either a stratified gas mode or as a single cavity gas drastically reduced the wall heat loading. This is just a

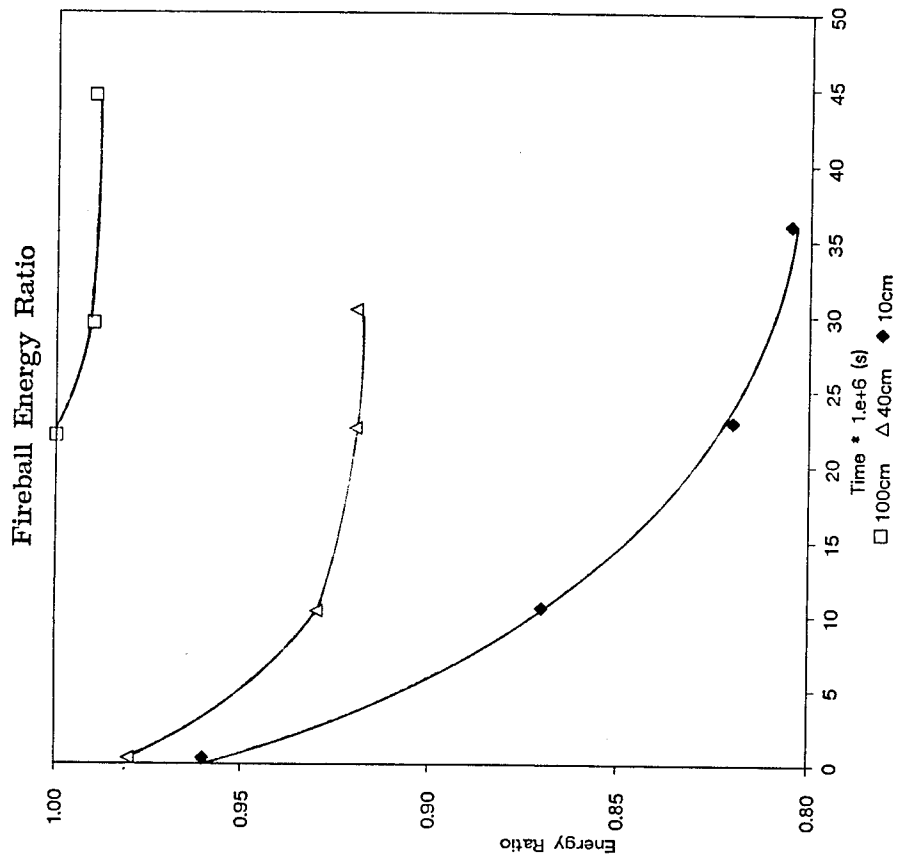


Fig. 27 Ratio of Fireball Total Energy for vented and pure N_2 case (200 MJ)

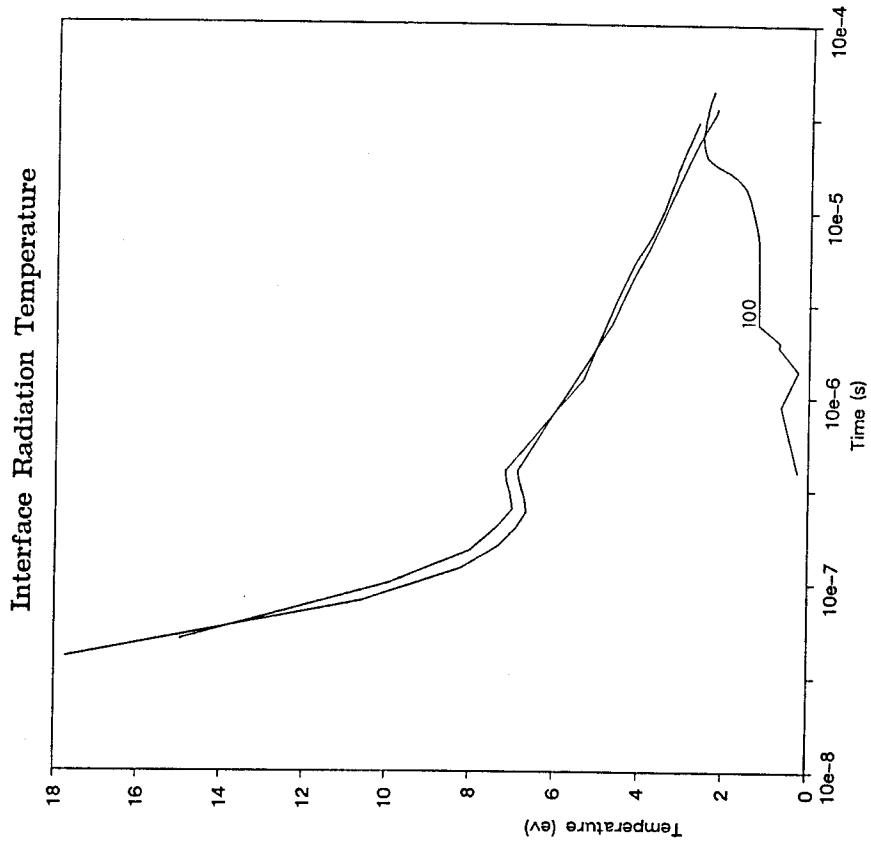


Fig. 28 Radiation Temperature at the gas interface along the z-axis for the 10, 40 and 100 cm cases (200 MJ)

statement about the conservation of energy.

The reduction in surface heat flux from 25 to the 50 cm case for 400 MJ target explosions is an interesting result. Recall that a 1-D simulation in spherical coordinates was used for these simulations. Thus the actual geometry is a sphere of helium in a larger sphere of nitrogen. The reason for the reduction in surface heat flux when the helium sphere was increased from 25 to 50 cm was that due to the low opacity of the He, the ion temperature reached an almost uniform value shortly after X-ray deposition. Now, from figure 23, it is easy to see that this equilibrium value for the 50 cm case will be much lower than for the 25 cm case because roughly the same energy is spread over 8 times the volume. The lower temperature of the 50 cm case simply means a lower source term for the surface heat flux; the initial maximum temperature in the nitrogen region is much lower for the 50 cm than for the 25 cm case. The net result from both of these effects is a reduced heat flux loading on the wall.

5. Conclusions

"Venting" the radiation energy from a target explosion in nitrogen to a helium region, shown in fig. 1, to reduce the surface pressure loading had only a minor effect for the 200 MJ target yields; the 800 MJ targets had little effect. The fireball inertia prevents this loss mechanism to be of significant benefit. The pressure shock is formed at very early times, before any appreciable energy loss can occur. The interesting core flow reversal of the 800 MJ target cases was not seen in the 200 MJ simulations. This could be simply attributed to the finer zoning used to determine the 800 MJ initial gas temperature profile, the X-ray deposition. The core temperature for the 800 MJ case was much higher than the 200 MJ one.

The geometries with the target in the helium region lead to a 50% peak pressure reduction on the instrumentation package due to the conversion of a spherical expansion to a surface source. However, the surface heat flux for this case was higher than for the pure nitrogen cavity. Table 1 summarizes these results for several calculations.

Exploding the target in the helium region will reduce the pressure on the instrumentation package; unfortunately, the diodes will experience a very high heat flux if the geometry of figure 1 is used. The use of a central cell of helium, for example a gas bag as shown in figure 2, might be a compromise between pressure reduction and wall heat flux loading for a test facility. Future calculations will investigate increasing the helium region to determine the minimum nitrogen region required. As the helium region is increased, the pressure loading will be reduced by simple geometric considerations. The target X-rays will expand in a spherical nature; thus when they are stopped in the nitrogen and a surface pressure source created, the energy per unit area will be lower. The surface heat flux will also be reduced by increasing the volume of the helium region which will result in a lower mixed-mean temperature as a radiation source.

ACKNOWLEDGEMENTS

This work has been supported by Sandia National Laboratory and USDOE under contract # DE-AS08-83DP40189.

6. References

1. Moses, G.A., R.R. Peterson, et al., "Preconceptual Design of the Light Ion Beam Fusion Target Development Facility", UWFD-664, November 1985.
2. Badger, B., et al., "Light Ion Beam Fusion Target Development Facility Studies: Progress Report for the Period Oct. 1, 1984 to Sept. 30, 1985", UWFD-652, 30 September 1985.
3. Zek'dovich, Y.B., Y.P. Raizer, Physics of Shock Waves and High-Temperature Hydrodynamic Phenomena, Academic Press, 1966.
4. Bethe, H.A., et al., "Blast Wave", LA-2000, August 1947.
5. Moses, G.A., R. Spencer, "Compact-Electron-Beam or Light-Ion-Beam Fusion Reactor Cavity Design Using Non-Spherical Blast Waves", Nuclear Fusion, Vol. 19, No.10 (1979), pp 1386-1388.
6. Pomraning, G.C., "Radiation Hydrodynamics", LA-UR-82-2625.
7. Peterson, R.R., G.A. Moses, "MIXERG-An Equation of State and Opacity Computer Code", UWFD-464, March 1982.
8. Moses, G.A., T.J. McCarville, R.R. Peterson, "Documentation for MF-FIRE, A Multifrequency Radiative Transfer Version of FIRE", UWFD-458, March 1982.
9. Uesaka, M., G.A. Moses, "Parametric Survey of Microfireball Calculations for the Light Ion Fusion Target Development Facility Design", UWFD-533, August 1983.
10. Cloutman, L.D., C.W. Hirt, N.C. Romero, "SOLA-ICE: A Numerical Solution Algorithm for Transient Compressible Fluid Flows", LA-6236, July 1976.
11. Spitzer, L., Physics of Fully Ionized Gases, Interscience, 1962.
12. Collatz, L. The Numerical Treatment of Differential Equations, Springer, 1966.
13. Schlichting, H., Boundary-Layer Theory, McGraw-Hill, 1968.

7. Appendix A

7.1 GAS2DRFD Overview

GAS2DRFD is a 2-D Eulerian radiation fluid dynamics computer code. It can simulate problems in spherical (R), cartesian (X-Y), or cylindrical (R-Z) coordinate systems. The code comprises about 2200 lines of standard Fortran (about 30% comments). It is written in a simple modular fashion which allows easy modification. The code is also highly vectorized; although it is a 2-D code, the arrays are simple vectors. Thus, the typical problem under discussion would have DO loop indices from 1 to 5000 rather than nested loops of from 1 to 70. This allowed the full vector potential of the Cray computer to be realized. The code will be briefly described here; only special, non-standard features will be discussed.

The SOLAICE¹⁰ algorithm was used to solve the standard compressible Navier-Stokes equations. A staggered mesh was used with cell edge velocities. Essentially, first upwind differencing was used on the convective terms and centered differencing on the diffusion terms. The SOLAICE technique is first order accurate in time. The convective terms vary from explicit to implicit based on the local pressure change during the time step; a simple point SOR method was used to iteratively solve the continuity equation and reduced momentum and energy equations. The fluid diffusion terms and convective energy transport were then updated in an explicit manner.

A single temperature diffusion approximation⁶ was used to simulate the radiation transport. Local thermodynamic equilibrium was assumed between the electrons and ions; a single temperature was used for the gas. A three parameter, both temperatures and fluid density, equation-of-state table was used to determine the Planck and Rosseland opacities. The coupling coefficients between the radiation and plasma fields are highly nonlinear; a simple explicit or Crank-Nicolson scheme for the diffusion terms would be inadequate. An iterative scheme to update these coefficients was used with an explicit differencing scheme to obtain the updated energy densities. A standard flux limiter model⁸ was used to limit the radiation field propagation speed.

7.2 Governing Equations

Let:

ρ -- fluid density
 u -- fluid velocity along X or R direction
 v -- fluid velocity along Y or Z direction
 ξ -- coordinate system controller
 0 -- cartesian
 1 -- cylindrical
 2 -- spherical
 E_m -- fluid specific internal energy
 E_r -- radiation energy density
 T_m -- material (gas) temperature
 T_r -- radiation temperature
 μ -- fluid viscosity
 k_m -- fluid thermal conductivity
 k_r -- effective radiation thermal conductivity
 (includes the flux limiter logic found in see ref. 8)
 g_x, g_y -- body accelerations (e.g. gravity)
 γ -- ratio of fluid specific heats
 ω_a -- radiation absorption coefficient (see ref. 6)
 ω_e -- radiation emission coefficient (see ref. 6)
 P -- total pressure (material + radiation)

note: - x direction is either X or R depending on ξ
- viscous dissipation terms, Φ , are neglected
 in the material energy equation
- Stokes Hypothesis¹³ used for viscous
 momentum terms

Continuity Equation:

$$\frac{\partial \rho}{\partial t} + \frac{\partial \rho u}{\partial x} + \frac{\partial \rho v}{\partial y} + \frac{\partial \rho u}{\partial x} = 0$$

Momentum Equations: (non-conservative form)

$$\begin{aligned} \rho \left(\frac{\partial u}{\partial t} + u \frac{\partial u}{\partial x} + v \frac{\partial u}{\partial y} \right) &= \rho g_x + - \frac{\partial P}{\partial x} + \\ &\mu \left(\frac{4}{3} \frac{\partial^2 u}{\partial x^2} + \frac{\partial^2 u}{\partial y^2} + \frac{1}{3} \frac{\partial^2 v}{\partial x \partial y} \right) + \frac{4}{3} \frac{\mu}{x} \left(\frac{\partial u}{\partial x} - \frac{u}{x} \right) \\ \rho \left(\frac{\partial v}{\partial t} + u \frac{\partial v}{\partial x} + v \frac{\partial v}{\partial y} \right) &= g_y + - \frac{\partial P}{\partial y} + \\ &\mu \left(\frac{4}{3} \frac{\partial^2 v}{\partial y^2} + \frac{\partial^2 v}{\partial x^2} + \frac{1}{3} \frac{\partial^2 u}{\partial x \partial y} \right) + \frac{\mu}{x} \left(\frac{\partial v}{\partial x} + \frac{1}{3} \frac{\partial u}{\partial x} \right) \end{aligned}$$

Energy Equations: (non-conservative form)

$$\begin{aligned} \rho \left(\frac{\partial E_m}{\partial t} + u \frac{\partial E_m}{\partial x} + v \frac{\partial E_m}{\partial y} \right) &= -p \left(\frac{\partial u}{\partial x} + \frac{\partial v}{\partial y} + \frac{\partial u}{\partial x} \right) + \\ &k_m \left(\frac{\partial^2 T_m}{\partial x^2} + \frac{\partial^2 T_m}{\partial y^2} + \frac{\partial}{\partial x} \frac{\partial T_m}{\partial x} \right) + \omega_a E_r - \omega_e T_m \\ \rho \left(\frac{\partial E_r}{\partial t} + u \frac{\partial E_r}{\partial x} + v \frac{\partial E_r}{\partial y} \right) &= -p \left(\frac{\partial u}{\partial x} + \frac{\partial v}{\partial y} + \frac{\partial u}{\partial x} \right) + \\ &k_r \left(\frac{\partial^2 T_r}{\partial x^2} + \frac{\partial^2 T_r}{\partial y^2} + \frac{\partial}{\partial x} \frac{\partial T_r}{\partial x} \right) - \omega_a E - \omega_e T_m \end{aligned}$$

One will note that since GAS2DRFD was based on a Navier-Stokes solver, the viscous momentum terms have been retained; these terms are not typically included in a radiation fluid dynamics code. For the problem under consideration, the fluid viscosity, μ , and the fluid thermal conductivity, k_m , were very small. The flow was essentially inviscid and the thermal transport dominated by the absorption and reemission of the radiation and fluid fields.

7.3 Equation-of-State

The present problem consisted of two different gases: nitrogen and helium. A three parameter EOS table⁷ was used to determine the nitrogen opacities: both Planck and Rosseland. The gas heat capacity, charge state, and specific energy density were also obtained from it. A standard Spitzer model¹¹ was used for the thermal conductivity. The Navier-Stokes gas dynamics code

was originally written assuming an ideal gas; that is, γ , the ratio of specific heats, was held constant. This limitation was removed by simply calculating a local time dependent γ for each grid point from the EOS tables. The actual gas behavior was then able to be modelled.

The helium region was treated differently. Since GAS2DRFD was used to model the case where the target and the diagnostic module were both in the nitrogen region, the helium region served only as a special boundary condition for the nitrogen field. Therefore its equation-of-state was greatly simplified. First, an ideal gas assumption was used: γ was held constant. Next, the helium was assumed to be optically transparent; the radiation flux propagated through the gas without being absorbed. Finally, the Spitzer thermal conductivity¹¹ was also used for the helium gas.

7.4 Special Features

The numeric techniques used to solve the hydrodynamic motion and the radiative transport are quite standard. However, several special features were incorporated into GAS2DRFD to better simulate the present problem. These include procedures for the initial conditions, time step control, and special diffusion stencils for the radiation transport.

7.4.1 Ion Deposition.

An X-ray deposition model was not included in GAS2DRFD. Therefore, the following procedure was utilized to obtain the initial energy profile in the cavity. First, the MFFIRE code⁸ was used to determine a 1-D (spherical) initial X-ray deposition profile with the target in nitrogen. All of the energy deposition was assumed to be absorbed in the gas; the radiation energy density remained at its initial state. No deposition was assumed in the helium region; it was modelled as optically transparent. After this initial time zero profile was established, the GAS2DRFD code was used to obtain the temporal solution; no further X-ray deposition modelling was used.

7.4.2 Time Step.

This problem has two vastly different time constants: the hydrodynamic motion and the energy exchange between the radiation and gas energy fields. The differences were further amplified by the use of a 2-T radiation transport model; the resulting highly nonlinear coupling coefficients made the equations very stiff. Therefore, for computational expediency, two different time steps were used in GAS2DRFD. The fluid motion was held constant during the

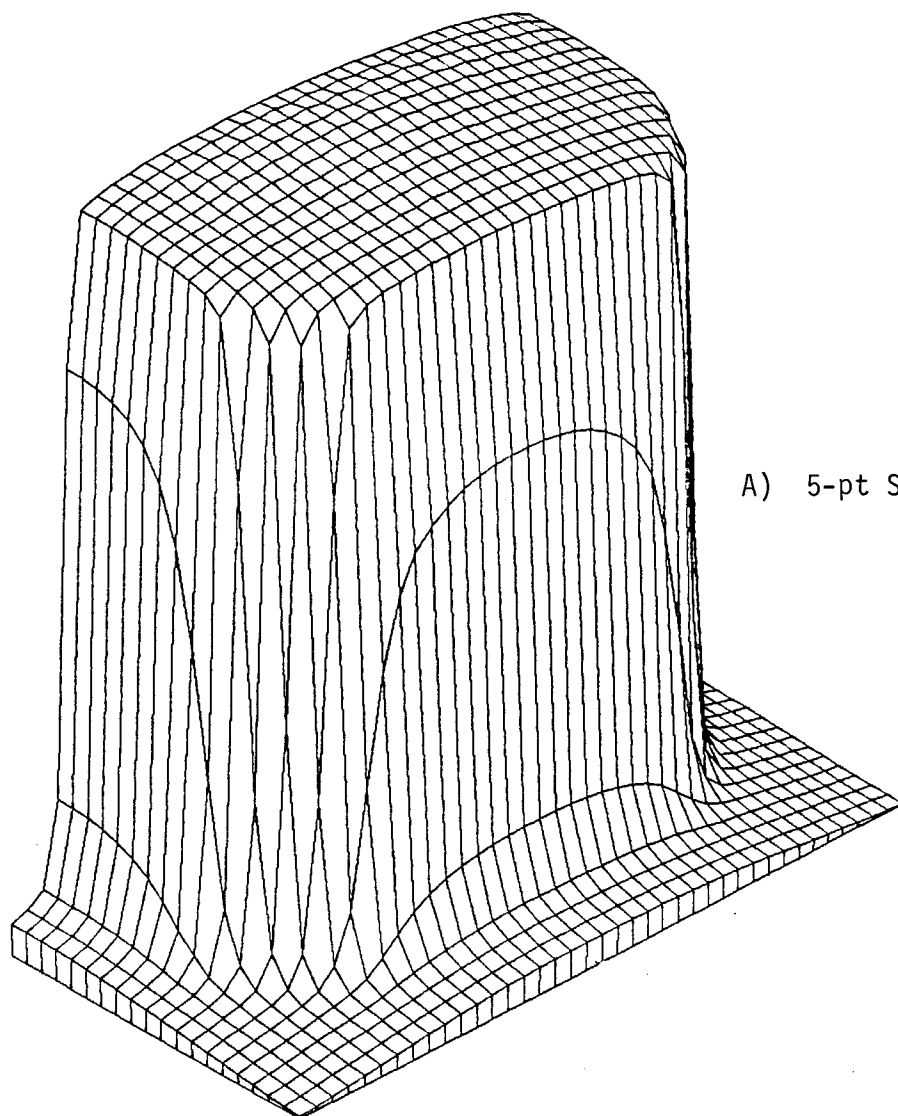
radiation time step; only the pressure work term was updated. At the end of a given number of radiation time steps, the hydrodynamic equations were solved. The radiation time step was typically from 1,000 to 10,000 times smaller than the hydrodynamic time step; the CFL limit for the radiative field was approximately 10^{-11} sec (based on the speed of light and a 5 cm mesh).

7.4.3 Radiation Diffusion Stencil

A second order centered difference scheme typically uses a 5-point symmetric stencil on a finite difference mesh. This creates a diffusion flux bias in the orthogonal directions (major mesh axes). A cylindrical coordinate system was used for the problem under consideration; the spherical expansion of the fireball caused the dominant fluxes to be along the diagonals of the computational cells. Initial calculations with the 5-pt stencil resulted in a definite cylindrical bias for the spherical expansion along the major mesh axes. Figure 29a shows a typical result for this stencil; the rectangular bias is clearly shown. A 9-pt stencil was developed which used the additional four nearest points, along the cell diagonals. The 8 perimeter points were essentially evenly weighted (adjusted for different physical lengths). This is unlike the 9-pt higher ordered methods of Collatz¹² which just increased the number of points along the major axes; these methods simply more accurately resolved the cylindrical bias. The new 9-pt stencil greatly reduced this bias and resulted in a near-spherical expansion. One can compare fig. 29a for the 5-pt stencil and fig. 29b for the new 9-pt stencil; the improvement is obvious.

An explicit solution scheme was used to advance the solution in time because it could be fully vectorized. There are no advantages to implicit schemes for calculating time accurate solutions. For the present problem, the numerical, flux limited⁸ diffusion propagation speed from an explicit scheme was more time accurate than either Crank-Nicolson or fully implicit, with an infinite diffusion speed, methods.

Figure 30 compares the radial velocity and ion temperature for a calculation performed in both a 1-D spherical and 2-D cylindrical coordinate system. The difference equations in GAS2DRFD were analytically manipulated to split them into a cartesian and radial portion; a simple multiplier was then used to indicate the coordinate system. The comparisons are quite good although the equations were not in conservative form.



A) 5-pt Stencil

B) 9-pt Stencil

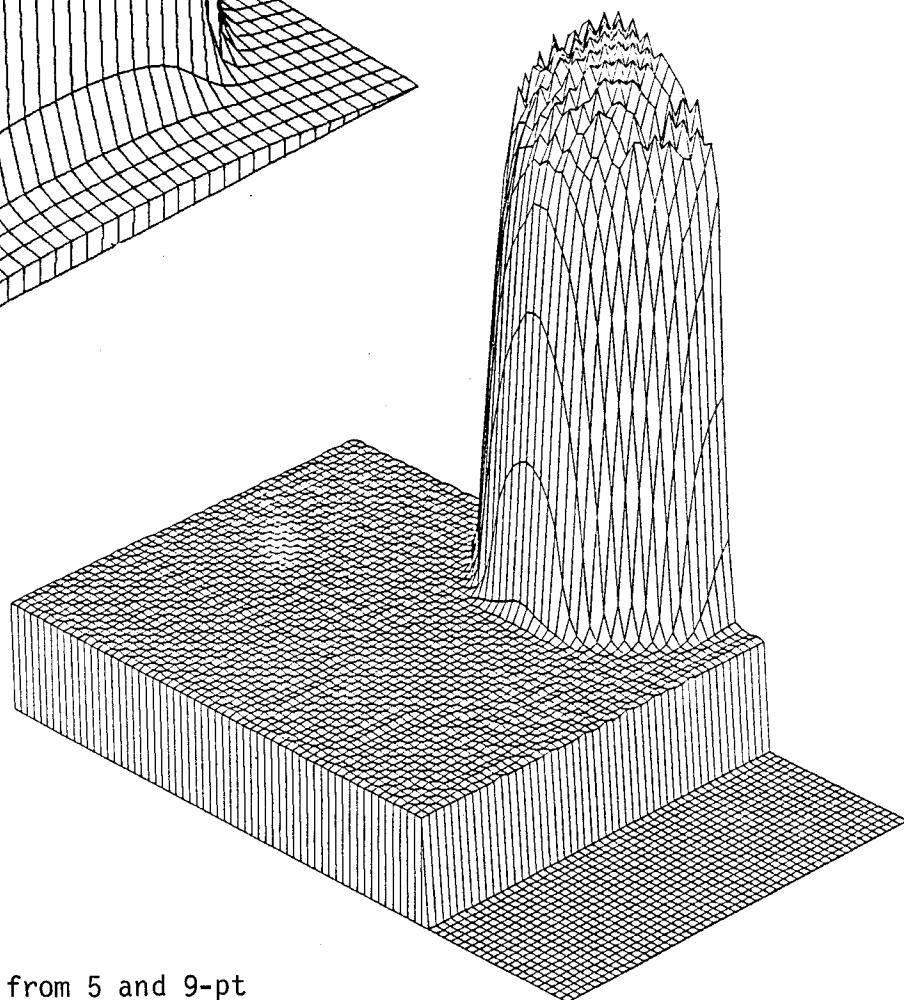


Fig. 29 Typical Results from 5 and 9-pt
mesh stencils.

Plasma Temperature $t = 2 \text{ e-}06 \text{ s}$

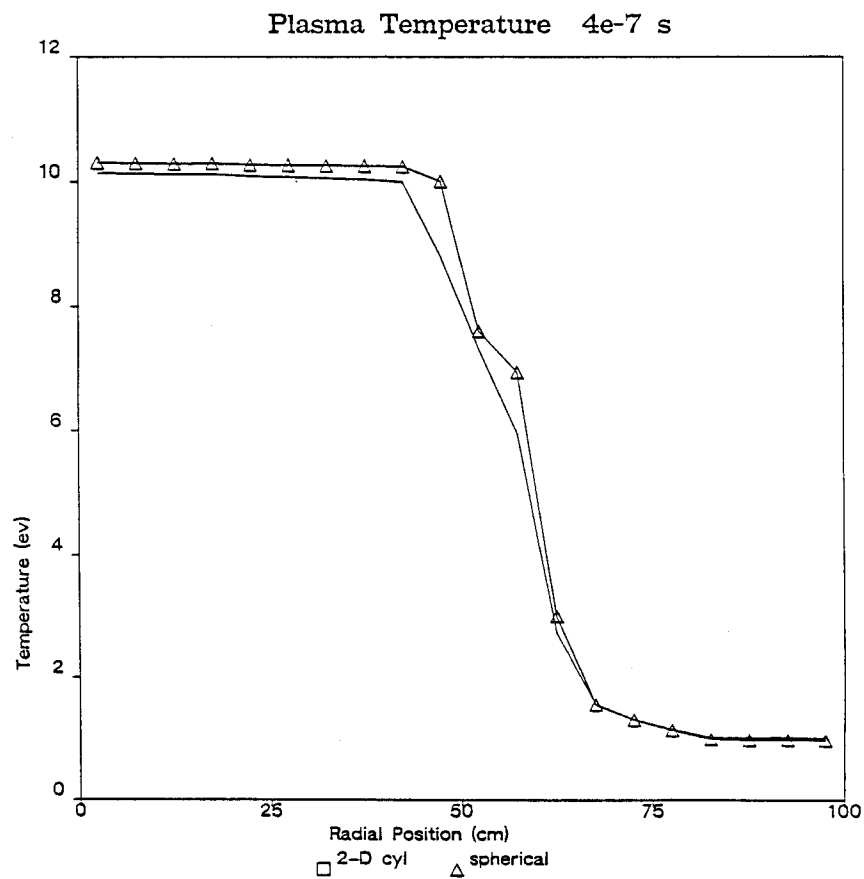
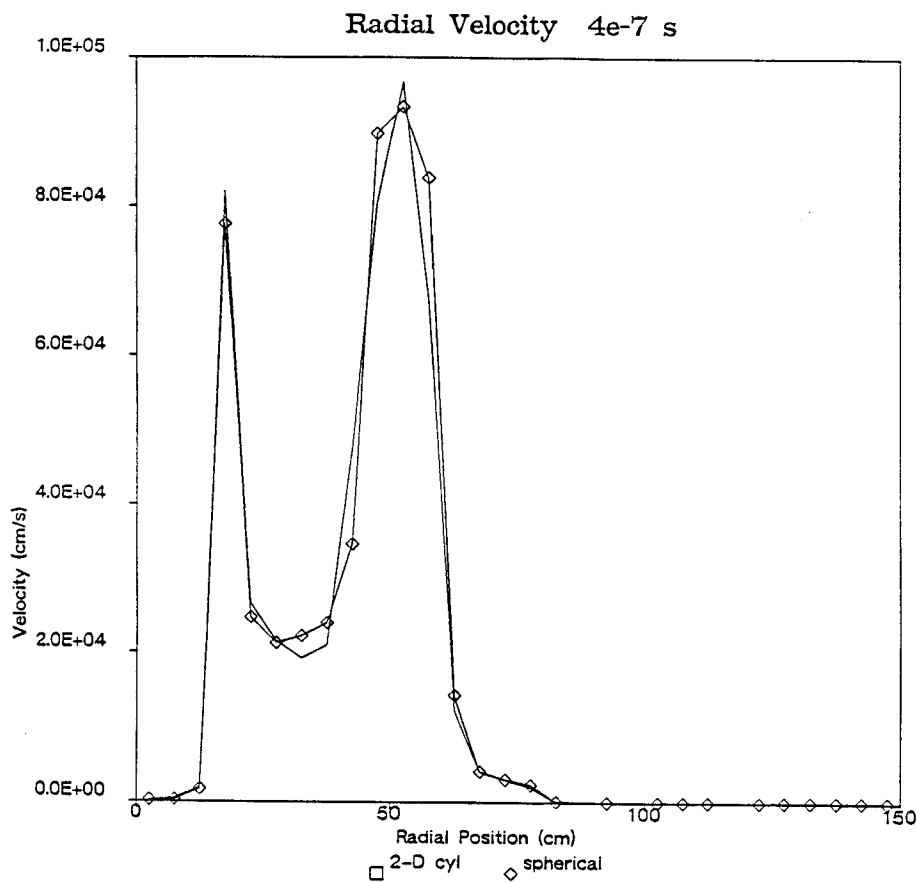


Fig. 30 Comparisons between 1-D spherical and 2-D cylindrical.


```

1      program gas2d
2      c version 4.9 rfd
3      c
4      c      this is a special version of gas2d--modified with radiation hydro.
5      c      2T approx made (single equation for radiation energy density).
6      c      an equation of state package is also integrated into the code.
7      c      the plasma ideal gas equation has been modified by using a mesh
8      c      varying ratio of specific heats .
9      c
10     c      caution:  nine pt diffusion stencil currently requires uniform mesh
11     c      with aspect ratio of unity
12     c
13     c      special modifications for the 2 gas layer blast problem
14     c      let----- gamma- ratio of specific heats for 'upper' region
15     c      xkap2- thermal conductivity for 'upper region'
16     c      bvar1- left hand boundary efor fit A
17     c      ivar2- location centre of energy deposition
18     c      bvar3- offset for the B fit
19     c      bvar4- plasma temperature at centerline (ev)
20     c      bvar5- epsilon energy for Er diffusion model
21     c      bvar6- exponential attenuation factor for B (1/cm)
22     c      bvar7- exponential attenuation factor for A (1/cm)
23     c      bvar8- right hand boundary of fit A
24     c      dmpcd- number of time steps for dump c/d
25     c      er1 - initial radiation temp for 'upper' region (ev)
26     c      ilоче-j location of the He 'upper region'
27     c      core - radius of initial energy core (cm)
28     c      delt - overall problem time step (control hydro and output)
29     c      dtrad- lagrangian radiation energy transfer time step only
30     c      note: dt2 << dt1
31     c      weight-weight factor for 9 pt diffusion stencil
32     c      for 'normal' axes (rotated axes is 1.-weight)
33     c      con(23)--relative error in tp (subroutine e2t)
34     c      con(24)--relative temp difference in RMFP
35     c      con(25)--floor tp in input
36     c      con(26)--floor value for Er (in ev)
37     c
38     c      assume He to be the 'upper' gas.  Let He be treated as
39     c      transparent. (see variable wtmol2)
40     c
41     c      units--- er      J/cm3 (radiation density)
42     c      x,y      cm
43     c      P,Pr      Mpa or J/cm3 (output only)
44     c      dyne/cm2 (erg/cm3) -- internal use
45     c      rho      gm/cm3
46     c      tp,tr      ev
47     c      e      J/gm (plasma specific energy density)
48     c
49     c*****
50     c
51     c      this is a one phase 2-d compressible code for the full navier-stokes
52     c      equations (e.g. includes an energy equation)
53     c      the present convective transport formulation is first order accurate
54     c
55     c      the solution procedure is sola-ice ref la-6236 (1976)

```

```

56 c          modified for variable mesh
57 c          pressure iteration modification
58 c
59 c      vectorized version---single vector instead of 2-d matrix
60 c      note: k      = i,j
61 c             k+1    = i+1,j
62 c             k-1    = i-1,j
63 c             k+imx  = i,j+1
64 c             k-imx  = i,j-1
65 c
66 c             imx = length of i subscript (x or r dimension)
67 c             jmx = length of j subscript (y or z dimension)
68 c
69 c             kpta = (2,2)
70 c             kptb = (imx-1, jmx-1)
71 c             kptc = (imx, jreg1p1)
72 c             kptd = (imx, jmx)
73 c             kpte = (imx, jmx-1)
74 c             kptf = (imx, jmx-2)
75 c      recall---boundary conditions meshes around physical mesh---imx=imesh+2
76 c
77 c      note---cdir$ ivdep forces do loop vectorization
78 c
79 c      input values:
80 c
81 c          tinit---initial problem start time
82 c          tend---problem end time
83 c          iterlmt---maximum # pressure iterations
84 c          rstrt---0 = no    1 = yes
85 c          xmu-----absolute viscosity (constant)
86 c          cyl----- 0 for cartesian and 1 for cylindrical
87 c          espi-----pressure iteration convergence criterion
88 c          xkap-----thermal conductivity
89 c          gx-----body acceleration in the positive x-direction
90 c          gy-----body acceleration in the positive y-direction
91 c          ui-----initial x velocity
92 c          vi-----initial y velocity
93 c          omega---sor relaxation factor for pressure iteration
94 c          alpha---controls the amount of donor cell fluxing
95 c             1.0---full donor cell
96 c             0.0---centered differencing
97 c          wl-----boundary condition-left side
98 c          wr-----boundary condition-right side
99 c          wt-----boundary condition-top side
100 c          wb-----boundary condition-bottom
101 c             1---rigid, free-slip wall
102 c             2---rigid, no-slip wall
103 c             3---continuative outflow wall
104 c             4---periodic (needs symmetric bc)
105 c             5---user defined
106 c          gamma---ratio of specific heats
107 c          asq-----square of sound speed used in the stiffened gas eos
108 c                   not currently implemented
109 c          rhoi-----reference density
110 c          eamb-----ambient temperature for i.c. and/or b.c.

```

```

111 c      edrive---temperature of right boundary for thermally driven
112 c      cavity problem
113 c      wtmol---molecular weight in amu
114 c      rgas---gas constant (8.3143e7 in cgs)
115 c      ireg1,2,3---number of real x (r) meshes in region
116 c      dx1,2,3---width of mesh in corresponding region
117 c      jreg1,2,3---number of real y (z) meshes in region
118 c      dy1,2,3---width of mesh in corresponding region
119 c      grid system such that ireg1 and jreg1 are low numbered
120 c      mesh points
121 c      cnrst---number of time steps per restart dump
122 c      cndmpa---number of time steps per dump type a
123 c      pressure iter, mesh ke, total energy, mass
124 c      cndmpb-----number of time steps per dump type b
125 c      icntrl-----control for type b dump fields
126 c      format field = 87654321 (0=no dmp, 1=dmp data)
127 c      1---u velocity
128 c      2---v velocity
129 c      3---pressure
130 c      4---density
131 c      5---specific internal energy
132 c      6---temperature
133 c      7---radiation energy density
134 c      8---gamma-1 in ideal gas eos
135 c      dt1-----time step 1
136 c      ndt1-----number of time steps of dt1
137 c      dt2,ndt2---time step 2 control
138 c      bvar1-----boundary condition 1
139 c      bvar2
140 c      bvar3
141 c      bvar4
142 c      bvar5
143 c      bvar6
144 c      bvar7
145 c      bvar8
146 c
147 c
148 c      stiffened gas eos   p = asq *(rho-rhoi) + (gamma-1)*rho*i
149 c      ref fluid dynamics la-4700
150 c
151 c      note---restart option used to define velocity, pressure, energy
152 c      and density fields. cycle 0 calculation is required to
153 c      determine beta for first 'real' time step
154 c
155 c
156 c      output file descriptions:
157 c
158 c      gswrst---echo input data and contains array dumps for
159 c      printing or editing for restart
160 c      also contains job timing info in last few lines
161 c      gsdmpa---global mesh data for conservation checks
162 c      gsdmpb---particular time and spatial data for post process plottin
163 c
164 c      integer cycle, wl, wr, wt, wb
165 c      real ke

```

```

166      integer*4 itemp, icntrl, ndt1, ndt2
167      integer rstrt
168      dimension xput(61), mask(9), value(8)
169      c
170      character*80 header
171      character*80 scratch
172      character*3 depen(8)
173      character*8 gasinp
174      character*8 gsdmpa
175      character*8 gsdmpb
176      character*8 gsdmpc
177      character*8 gsdmpd
178      character*8 gswrst
179      character*8 gsinrst
180      character*8 eostab
181      common /mesh/ xc(9999) , yc(9999) , dx(9999) , dy(9999) ,
182      1          rdx(9999) , rdy(9999) ,
183      2          rdx(9999), rdy(9999), rxc(9999), r2dx(9999),
184      3          r2dy(9999)
185      common /wrk/ un(9999) , vn(9999) , rhon(9999), en(9999) ,
186      1          pr(9999) , work(9999,7)
187      common /np1/ u(9999) , v(9999) , rho(9999) , e(9999) ,
188      1          er(9999) , p(9999) , tp(9999)
189      common /prop/ gam1(9999), rosmfp(9999), rmfp1t(9999),
190      1          rmfp2t(9999), rcsbv(9999), xkap(9999)
191      common /a/ beta(9999) , xmask(9999), con(30)
192      common /e/ cycle, wl, wr, wt, wb, iter, imx, jmx, delt, xmu,
193      1          im1, jm1, im2, jm2, iterlmt, cyl, epsi, gaminit,
194      2          gx, gy, ui, vi, cnrst, cndmp, omega, alpha, t, am1,
195      3          gamma, asq, rhoi, eamb, dtrd, otd, ftd, xkap2,
196      4          kpta, kptb, kptc, kptd, kpte, kptf, eamb2, rcsbv,
197      5          bvar1, ivar2, bvar3, bvar4, bvar5, bvar6, bvar7, bvar8
198      data length /9999/
199      data pi , ixero /3.1415927, 0/
200      data nimp /61/
201      6data wtmol2 / 14. /
202      data depen /'U ','V ','Pr ','Rho','Ep ','Tp ','Tr ','gm1'/
203      c
204      c      set file definitions
205      c
206      data ir,iwrst,ireos,idmpa,idmpb,irst/ 5,6,4,1,3,2/
207      data idmpc, idmpd /7,8/
208      data gsdmpa, gsdmpb, gasinp, gswrst, gsinrst
209      1      /'gsdmpa', 'gsdmpb', 'gasinp', 'gswrst', 'gsinrst'/
210      data eostab / 'eostab'/
211      data gsdmpc, gsdmpd /'gsdmpc', 'gsdmpd'/
212      c
213      c      ir--input problem file
214      c      iwrst--output restart file
215      c      irw--console
216      c      idmpa--plot save file a
217      c      idmpb--plot save file b
218      c      irst--initial condition or restart file
219      c
220      call dropfile (0)

```

```

221      c
222      c          define i/o files
223      c
224      open (1, file=gsdmpa ,status='new')
225      open (3, file=gsdmpb ,status='new')
226      open (5, file=gasinp ,status='old')
227      open (6, file=gswrst ,status='new')
228      open (4, file=eostab ,status='old')
229      open (7, file=gsdmpc ,status='new')
230      open (8, file=gsdmpd ,status='new')
231      c
232      c          input problem parameters
233      c
234      read(ir,10) header
235      read(ir,11) (xput(i),i=1,nimp)
236      10  format(a)
237      11  format(e10.0)
238      tinit= xput(1)
239      tend = xput(2)
240      iterlmt=xput(3) + .001
241      rstrt= xput(4) + .001
242      xmu  = xput(5)
243      cyl  = xput(6)
244      epsi = xput(7)
245      xkap2= xput(8)
246      gx   = xput(9)
247      gy   = xput(10)
248      ui   = xput(11)
249      vi   = xput(12)
250      omega= xput(13)
251      alpha= xput(14)
252      wl   = xput(15) + .001
253      wr   = xput(16) + .001
254      wt   = xput(17) + .001
255      wb   = xput(18) + .001
256      gamma= xput(19)
257      asq  = xput(20)
258      rhoi = xput(21)
259      eamb = xput(22)
260      edrive=xput(23)
261      wtmol= xput(24)
262      rgas = xput(25)
263      ireg1= xput(26) + .001
264      dx1  = xput(27)
265      ireg2= xput(28) + .001
266      dx2  = xput(29)
267      ireg3= xput(30) + .001
268      dx3  = xput(31)
269      jreg1= xput(32) + .001
270      dy1  = xput(33)
271      jreg2= xput(34) + .001
272      dy2  = xput(35)
273      jreg3= xput(36) + .001
274      dy3  = xput(37)
275      er1  = xput(38)

```

```

276          cnrst= xput(39)
277          cndmpa=xput(40)
278          cndmpb=xput(41)
279          icntrl=xput(42) + .001
280          delt = xput(43)
281          ndt1 = xput(44) + .001
282          dtradr= xput(45)
283          weight=xput(46)
284          bvar1= xput(47)
285          ivar2= xput(48) + .001
286          bvar3= xput(49)
287          bvar4= xput(50)
288          bvar5= xput(51)
289          bvar6= xput(52)
290          bvar7= xput(53)
291          bvar8= xput(54)
292          dmpcd= xput(55)
293          iloche=xput(56) + .001
294          core = xput(57)
295          con(24)=xput(58)
296          con(23)=xput(59)
297          con(25)=xput(60)
298          con(21) = xput(61)
299      c
300      c          echo print input file
301      c
302          rewind ir
303          read(ir,10) scratch
304          write(iwrst,101) scratch
305          do 91 i=1,nimp
306              read(ir,10) scratch
307              write(iwrst,102) i,xput(i),scratch
308          102      format(1x,i2,1x,e12.5,5x,a80)
309          101      format(1x,a80)
310          91      continue
311      c*****
312      c
313      c          compute constant terms
314      c
315      c*****
316          ibar = ireg1 + ireg2 + ireg3
317          jbar = jreg1 + jreg2 + jreg3
318          imx  = ibar + 2
319          jmx  = jbar + 2
320          im1  = imx - 1
321          jm1  = jmx - 1
322          im2  = imx - 2
323          jm2  = jmx - 2
324          ileft= ivar2*imx + 1
325          iright=ileft + im1
326          kpta = imx + 2
327          kptb = imx * jm1 - 1
328          kptc = imx * (iloche+1) - 1
329          kptd = imx * jmx
330          kpte = imx * jm1

```

```

331      kptf = imx * (jmx-2)
332      if (kptd.gt.length) go to 990
333      c
334      j1 = 1
335      j2 = kptc + 1
336      c
337      otd = 1./3.
338      ftd = 4./3.
339      am1 = 1. - alpha
340      c
341      c
342      c      con array initialization
343      c
344      con(1) = 7.6387e-22
345      con(2) = 0.7500e+10
346      con(3) = 2.2916e-11
347      con(4) = 3.0000e+10
348      con(5) = 1./ con(1)
349      con(6) = 6.0230e+23 / wtmol
350      con(8) = 1.2175e+02
351      con(9) = 1.6020e-19
352      con(11) = wtmol / rgas
353      con(12) = 1./11605.
354      con(13) = 11605.
355      con(14) = er1
356      con(15) = 0.001
357      con(16) = 1.e+07
358      con(17) = 1.e-07
359      con(18) = core
360      con(19) = (1.41421 * dx1)
361      con(10) = 1./con(19)
362      con(7) = 0.5*dx1
363      con(20) = weight
364      c
365      c      convert from K to ev
366      c
367      con(1) = con(1) * (con(13))**4
368      con(3) = con(3) * (con(13))**4
369      con(5) = 1./con(1)
370      con(11) = con(11) * con(12)
371      xkap2 = xkap2 * con(13)
372      rgas = rgas * con(13)
373      con(26) = con(1) * 0.25**4
374      con(22) = con(26)
375      6con(29) = .00001 * rhoi
376      6con(30) = 1.0
377      c
378      gaminit = gamma - 1.
379      rcsubin = wtmol * gaminit / rgas
380      rcsub2 = wtmol2 * gaminit / rgas
381      tpinit = eamb
382      con(27) = 0.1 / rcsubin
383      c
384      c*****
385      c

```

```

386 c      initialize mesh stuff for variable width option
387 c      do x mesh first, then y mesh
388 c
389 c*****
390      dx(1) = dx1
391      rdx(1) = 1./dx1
392      xc(1) = -0.5 * dx1
393      rxc(1) = 1. / xc(1)
394 c
395      do 15 i=2,im1
396          dxa = dx3
397          if (i. le. (ireg1+ireg2+1) ) dxa = dx2
398          if (i. le. (ireg1 + 1) )      dxa = dx1
399          dx(i) = dxa
400          rdx(i) = 1./dxa
401          xc(i) = xc(i-1) + 0.5*( dx(i-1) + dx(i) )
402          rxc(i) = 1./xc(i)
403      15 continue
404      dx(imx) = dx(im1)
405      rdx(imx) = 1./dx(imx)
406      xc(imx) = xc(im1) + 0.5*( dx(im1)+dx(imx))
407      rxc(imx) = 1. / xc(imx)
408 c
409      do 16 i=1,im1
410          rdxc(i) = 1./(dx(i) + dx(i+1))
411      16 continue
412      rdxc(imx)= 0.5/dx(imx)
413 c
414 c      now fill entire matrix
415 c
416 ctim
417      do 17 i=1,imx
418          do 17 j=1,jm1
419              k = i + imx*j
420              dx(k) = dx(i)
421              rdx(k) = rdx(i)
422              xc(k) = xc(i)
423              rxc(k) = rxc(i)
424              rdxc(k)= rdxc(i)
425      17 continue
426 c
427 c
428 c      now the y mesh variables
429 c
430 c
431      dy(1) = dy1
432      rdy(1) = 1./dy1
433      yc(1) = -0.5 * dy1
434      do 20 j=2,jm1
435          dya = dy3
436          if ( j. le. (jreg1+jreg2+1) ) dya = dy2
437          if ( j. le. (jreg1+1) )      dya = dy1
438          kpt = (j-1) * imx + 1
439          dy(kpt) = dya
440          rdy(kpt) = 1./dya

```



```

441         yc(kpt) = yc(kpt-imx) + 0.5*( dy(kpt-imx) + dy(kpt) )
442     20 continue
443         kpt      = kpte + 1
444         dy(kpt)  = dy(kpt-imx)
445         rdy(kpt) = 1./dy(kpt-imx)
446         yc(kpt)  = yc(kpt-imx) + 0.5*( dy(kpt-imx)+dy(kpt))
447         do 21 k=1,kpte,imx
448             rdy(k) = 1./(dy(k) + dy(k+imx))
449     21 continue
450         rdy(kpt) = 0.5/dy(kpt)
451     c
452     c         fill up entire mesh
453     c
454     ctim
455         do 22 kj=1,kptd,imx
456             do 22 i=1,im1
457                 k      = kj + i
458                 dy(k)   = dy(kj)
459                 rdy(k)  = rdy(kj)
460                 yc(k)   = yc(kj)
461                 rdy(k)  = rdy(kj)
462     22 continue
463     c
464     c         compute 2nd order diffusion delx, dely
465     c
466         do 18 k=kpta,kptb
467             r2dx(k) = 1. / ( dx(k-1) + 2.*dx(k) + dx(k+1) )
468             r2dy(k) = 1. / ( dy(k-imx) + 2.*dy(k) + dy(k+imx) )
469     18 continue
470 c*****
471 c
472 c         initialize mask vector---1.0 interior mesh, 0.0 bc mesh
473 c
474 c*****
475 c
476         do 23 k=kpta,kptb
477             xmask(k)      = 1.
478     23 continue
479     c
480     cdir$ ivdep
481         do 24 k=1,imx
482             xmask(k)      = 0.0
483             xmask(k+kpte) = 0.0
484     24 continue
485     c
486     cdir$ ivdep
487         do 25 k=1,kptd,imx
488             xmask(k)      = 0.0
489             xmask(k+im1)  = 0.0
490     25 continue
491 c*****
492 c
493 c         initialize counters
494 c
495 c*****

```

```

496      t      = tinit
497      iter   = 0
498      cycle  = 0
499      trst   = tinit
500      tdmpa  = tinit
501      tdmpb  = tinit
502      tdmpcd = tinit
503      c*****
504      c
505      c      initialize dependent variables
506      c      call subroutine init2 to input eos tables
507      c
508      c      check for standard/restart option
509      c
510      c*****
511      c
512      c      call init2 (ireos)
513      c
514      c      if (rstrt.eq.1) then
515      c          open (2, file=gsinrst, status='old')
516      c          call restart (irst,iwrst)
517      c          call eos (j1,j2)
518      c          go to 58
519      c      endif
520      c
521      c      do 56 kk=1,2
522      c
523      c          note: eamb is temperature on input
524      c
525      c          if (kk.eq.1) then
526      c              rhoinit = rhoi
527      c              einit   = eamb / rsubin
528      c              pinit   = gaminit * rhoinit * einit * con(16)
529      c              erinit  = con(1) * con(14)**4
530      c              ka      = 1
531      c              kb      = kptc + 1
532      c          else
533      c              rhoinit = rhoi * wtmol2 / wtmol
534      c              eamb2   = eamb / rsub2
535      c              einit   = eamb2
536      c              pinit   = gaminit * rhoinit * einit * con(16)
537      c              erinit  = con(1) * con(14)**4
538      c              ka      = kptc + 2
539      c              kb      = kptd
540      c          endif
541      c      do 56 k=ka,kb
542      c          u(k)      = ui
543      c          v(k)      = vi
544      c          e(k)      = einit
545      c          rho(k)     = rhoinit
546      c          p(k)      = pinit
547      c          rhon(k)    = rhoinit
548      c          en(k)      = einit
549      c          er(k)      = erinit
550      c          tp(k)     = tpinit

```

```

551          pr(k)      = pinit + otd * erinit
552      56      continue
553      c
554      c*****
555      c
556      c          initial energy ball profile
557      c
558      c*****
559      c
560      c          call epinit
561      c
562      58      continue
563      c
564      c          set properties for He region -- constant
565      c
566      c          do 57 k=kptc+2,kptd
567      c              xkap(k)      = xkap2
568      c              rosmfp(k)     = 1.e-6
569      c              rmfp1t(k)     = 1.e-6
570      c              rmfp2t(k)     = 1.e-6
571      c              rcsbv(k)      = rcsbv2
572      c              gam1(k)       = gaminit
573      57      continue
574      c*****
575      c
576      c          unscrunch icntrl
577      c
578      c*****
579      c          ndepb = 0
580      c          do 30 i=1,8
581      c              itemp = 0.1 * icntrl
582      c              itemp = icntrl - 10 * itemp
583      c              icntrl = 0.1 * icntrl
584      c              if (itemp.eq.0) go to 30
585      c                  ndepb = ndepb + 1
586      c                  mask(ndepb) = i
587      30      continue
588      c*****
589      c
590      c          initialize dump files
591      c
592      c*****
593      c
594      c          ndmpb = 0
595      c          ndmpcd = 0
596      c          nrst = 0
597      c          write(idmpa,810) header
598      810      format(a80)
599      c
600      c          write(idmpb,810) header
601      c          write(idmpb,811) ndepb
602      811      format(1x,i2)
603      c          write(idmpb,812) ibar,jbar,(depen(mask(i)),i=1,ndepb)
604      812      format(1x,'time (sec)',i3,i3,8a3)
605      c          do 813 k=2,im1

```

```

606          write(idmpb,814) xc(k)
607      814      format(1x,e12.5)
608      813      continue
609          do 816 k=kpta,kpte,imx
610              write(idmpb,814) yc(k)
611      816      continue
612      c
613          write(idmpc,810) header
614          write(idmpc,811) ndepb
615          write(idmpc,815) (depen(mask(i)),i=1,ndepb)
616      815      format(' time (sec)          ',' cell centre (cm)    ',8a3)
617      c
618          write(idmpd,810) header
619          write(idmpd,811) ndepb
620          write(idmpd,815) (depen(mask(i)),i=1,ndepb)
621      c
622      c*****
623      c*****
624      c
625      c          call subroutine solaice for each time step
626      c          note: time step 0 skips hydro and just sets up
627      c          beta array and properties
628      c
629      c          add time splitting lagrangian energy calculation e2t here
630      c          note: jump around this subroutine for cycle 0
631      c
632      c          computational loop begins now
633      c
634      c*****
635      c*****
636      c
637      100      continue
638          if (cycle.eq.0) go to 111
639      c
640      c          2T energy equation solver section
641      c          solve for e-tilde, p-tilde, and er-tilde
642      c          note---split time step solution technique used for speed
643      c          perform lagrangian radiation energy transport and
644      c          exchange only using time step dtradi
645      c          grad (velocity) assumed constant for this loop
646      c
647      c          sub eosset iterates on Tp to satisfy Ep from EOS tables
648      c
649      c
650          ja = 1
651          jb = kptc + 1
652          call eosset (ja,jb)
653          call e2t
654      c
655      c
656      c          set time n vectors
657      c
658      111      continue
659          do 650 k=1,kptd
660              vn(k) = v(k)

```

```

661          un(k) = u(k)
662          rhon(k) = rho(k)
663          pr(k) = p(k) + otd * er(k) * con(16)
664      650 continue
665      c
666      c      update He thermal conductivity (Spitzer Conductivity)
667      c      k = J/cm-s-ev      t--ev
668      c
669      do 651 k=kptc+2,kptd
670          xkap(k) = 274. * tp(k)**2.5
671      651 continue
672      c
673      c
674      call solaice
675      c
676      c
677      c*****
678      c
679      c      check for output options
680      c
681      c      check for dmp file a output
682      c
683      110 if (t.lt.tdmpa.and.(t+delt).lt.tend) go to 799
684          tdmpa = tdmpa + cndmpa*delt
685      c
686      c      calculate grid ke, mass, and internal energy
687      c
688      ke = 0.
689      energy = 0.
690      xmass = 0.
691      do 701 k=kpta,kptb
692          vol = (1. - cyl + 2.*pi*xc(k)*cyl) * dx(k) * dy(k)
693          vol = vol * xmask(k)
694          uave = u(k-1) + u(k)
695          vave = v(k) + v(k-imx)
696          ke = ke + rho(k) * vol * (uave*uave + vave*vave)
697          xmass = xmass + rho(k) * vol
698          energy = energy + e(k) * vol * rho(k)
699      701 continue
700          ke = 0.125 * ke * con(17)
701          write(idmpa,800) t,iter,ke,xmass,energy
702      800 format(2x,e12.5,2x,i3,'.',2x,3(e12.5,2x))
703      c
704      c      check restart file control
705      c
706      799 if (t.lt.trst.and.(t+delt).lt.tend) go to 580
707          trst = trst + cnrst*delt
708          write(iwrst,880) t
709      880 format('1      time = ',e12.5)
710          write(iwrst,801)
711      801 format('      k',10x,'u',12x,'v',12x,'p',11x,'rho',11x,
712          1      'e',11x,'Tp ',11x,'Er')
713          do 575 k=1,kptd
714              write(iwrst,802)k,u(k),v(k),p(k),rho(k),e(k),tp(k),er(k)
715      575 continue

```

```

716      802      format(1x,i5,3x,7(1x,e12.5))
717          nrst = nrst + 1
718          write(idmpa,777) nrst,t
719      777      format(23x,'wrst file -- ',i3,' time = ',e12.5)
720      c
721      c          check dump file b control
722      c
723      580      if (t.lt.tdmpb.and.(t+delt).lt.tend) go to 590
724          tdmpb = tdmpb + cndmpb*delt
725          write(idmpb,804) t,ibar,jbar
726      804      format(1x,e12.5,2x,i3,2x,i3)
727          do 585 k=1,kptd
728              value(1) = u(k)
729              value(2) = v(k)
730              value(3) = pr(k) * con(17)
731              value(4) = rho(k)
732              value(5) = e(k)
733              value(6) = tp(k)
734              value(7) = (con(5)*er(k))**0.25
735              value(8) = gam1(k)
736              write(idmpb,805)(value(mask(kk)),kk=1,ndepb)
737      585      continue
738      805      format(1x,9(e12.5,1x))
739          ndmpb = ndmpb + 1
740          write(idmpa,778) ndmpb,t
741      778      format(23x,'dmpb file -- ',i3,' time = ',e12.5)
742      590      continue
743      c
744      c          check for dump file c/d control
745      c
746          if (t.lt.tdmpcd.and.(t+delt).lt.tend) go to 599
747          tdmpcd = tdmpcd + dmpcd*delt
748          write(idmpc,804) t,imx
749          do 592 k=ileft,iright
750              value(1) = u(k)
751              value(2) = v(k)
752              value(3) = pr(k) * con(17)
753              value(4) = rho(k)
754              value(5) = e(k)
755              value(6) = tp(k)
756              value(7) = (con(5)*er(k))**0.25
757              value(8) = gam1(k)
758              write(idmpc,805) xc(k),(value(mask(kk)),kk=1,ndepb)
759      592      continue
760          write(idmpd,804) t,jmx
761          do 593 k=2,kptd,imx
762              value(1) = u(k)
763              value(2) = v(k)
764              value(3) = pr(k) * con(17)
765              value(4) = rho(k)
766              value(5) = e(k)
767              value(6) = tp(k)
768              value(7) = (con(5)*er(k))**0.25
769              value(8) = gam1(k)
770          write(idmpd,805) yc(k),(value(mask(kk)),kk=1,ndepb)

```

```

771      593      continue
772              ndmpcd = ndmpcd + 1
773              write(idmpa,779) ndmpcd,t
774      779      format(23x,'dmpcd file -- ',i3,' time = ',e12.5)
775      599      continue
776      c
777      c          advance time  t = t + delt
778      c
779              t = t + delt
780              if (t.gt.tend) go to 999
781              call timeleft (isec)
782              if (isec.lt.40) then
783                  tend = 0.
784                  go to 110
785              endif
786              cycle = cycle + 1
787              go to 100
788      990      continue
789      c
790      c*****
791      c
792              write(iwrst,991)
793      991      format(' input error')
794      999      continue
795      c
796      c          housekeeping and file closing
797      c
798              t = t - delt
799              write(idmpa,776) t,cycle
800      776      format(' last dump time = ',e12.5,' cycle = ',i5)
801              call timeused (icpu,iio,isys,imem)
802              tcpu = icpu* 1.e-6
803              tio  = iio * 1.e-6
804              tsys = isys* 1.e-6
805              tmem = imem*1.e-12
806              write(idmpa,775)tcpu,tio,tsys,tmem
807      775      format(2x,'cpu(s) = ',e12.5,' i/o(s) = ',e12.5,' sys(s) = ',
808      a          e12.5,' mem(s) = ',e12.5)
809      c
810              close (1)
811              close (3)
812              close (6)
813              close (7)
814              close (8)
815      c
816      c          save dropfile for possible restart
817      c
818              call exit (1)
819      c
820      end

```

```

821      SUBROUTINE EOS (j1,j2)
822      C
823      eos calculates equation of state quantities by table look-up
824      output---
825      c          xkap --- thermal conductivity
826      c          gam1 --- (gamma-1) for ideal gas eos
827      c          rcsbv - reciprocal of Cv
828      c          rmfp --- radiation mfp
829      c          ross2t - rosseland mfp for 2 temperatures
830      c          rosmfp - rosseland mfp for 1 temperature
831      c      input--
832      c          ja, jb limits on input array
833      c
834      c          this eos package is constructed around those in MF-FIRE FDM-458
835      c
836      c          note: an effort was made to conserve arrays here
837      c          several arrays perform double duty here
838      c          en, rhon, un, and vn are fair game here
839      c
840      c      con array:
841      c          5 --- c/(4.*sigma)
842      c          6 --- number density / mass density
843      c          9 --- pressure conversion constant (from MF-FIRE)
844      c          11 --- mol wt / rgas (constant)
845      c          22 --- eos floor value energy density (j/cm3)
846      c
847      common/eos1/ ad, bd, at, bt, nmat, nfg, ja, jb,
848      1      rad, rdb, rat, rbt
849      common/eostab/ ztab(20,10,2), entab(20,10,2),
850      1      rostab(20,20,10,2), rmftab(20,20,10,2)
851      common/wrk / work(9999,12)
852      common/eoswrk/ trl(9999), tpl(9999), rho1(9999),
853      1      meos(9999), leos(9999), keos(9999)
854      common /np1/ u(9999) , v(9999) , rho(9999) , e(9999) ,
855      1      er(9999) , p(9999) , tp(9999)
856      common /prop/ gam1(9999), rosmfp(9999), rmfp1t(9999),
857      1      rmfp2t(9999), rcsbv(9999), xkap(9999)
858      common /a/ beta(9999) , xmask(9999), con(30)
859      common /e/ cycle, wl, wr, wt, wb, iter, imx, jmx, delt, xmu,
860      1      im1, jm1, im2, jm2, iterlmt, cyl, epsi, gaminit,
861      2      gx, gy, ui, vi, cnrst, cndmp, omega, alpha, t, am1,
862      3      gamma, asq, rhoi, eamb, dtrd, otd, ftd, xkap2,
863      4      kpta, kptb, kptc, kptd, kpte, kptf, eamb2, rcsbin,
864      5      bvar1, ivar2, bvar3, bvar4, bvar5, bvar6, bvar7, bvar8
865      c
866      dimension z(9999), ee(9999), dummy(9999), dedt(9999)
867      dimension xflg(9999)
868      c
869      equivalence (ee(1), work(1,11)) , (z(1), work(1,12)),
870      1      (dummy(1),work(1,10)), (dedt(1), work(1,9))
871      c
872      ja = j1
873      jb = j2
874      C
875      C COMPUTE THE LOGARITHMS OF THE TEMPERATURES AND DENSITY FOR USE IN

```



```

876 C THE TABLE LOOK-UP ROUTINES
877 c
878 DO 10 J = ja,jb
879     erad    = er(j)
880     erad    = cvmgn ( erad , con(22) , (erad-con(22)) )
881     tfluid  = tp(j)
882     trl(j)  = 0.25 * alog10( con(5)*erad )
883     tpl(j)  = alog10( tfluid )
884     rho1(j) = alog10( rho(j)*con(6) )
885 10 continue
886 c
887 C FIRST FIND THE (K,L) POINTS THAT CORRESPOND TO THE TEMPERATURE AND
888 C DENSITY IN EACH ZONE
889 c
890 CALL POINT
891 c
892 C NOW FIND THE VALUES IN THE CHARGE STATE TABLE
893 c
894 CALL TABLE2 (ZTAB,Z,dummy,tp)
895 c
896 C NEXT FIND THE VALUES IN THE SPECIFIC ENERGY TABLE
897 c
898 CALL TABLE2 (ENTAB,EE,dedt,tp)
899 c
900 c      calculate xkap (from subroutine kappa)
901 c      gam1 and rcubv from Z and EE
902 c
903 call kappa (Z, ja, jb)
904 c
905 c      note: p = gam1 * rho * e = c9 * c6 * rho * tp * (1 + z)
906 c      check for values below table (leos=0) use initial values then
907 c
908 do 40 j = ja,jb
909     xgam1    = con(9)*con(6) * tp(j) * (1.+z(j)) / e(j)
910 ceos      gam1(j) = cvmgn ( xgam1, gaminit, float(leos(j)) )
911 ceos      rsubv(j) = cvmgn ( 1./dedt(j), rsubin, float(leos(j)) )
912     gam1(j) = xgam1
913     rsubv(j) = 1./dedt(j)
914 40 continue
915 c
916 C FIND THE VALUES IN THE RADIATION MFP TABLE
917 c
918 CALL TABLE3 (RMFTAB,RMFP2T)
919 c
920 C FIND THE VALUES IN THE ROSSELAND MFP TABLE
921 c
922 CALL TABLE3 (ROSTAB,ROSMFP)
923 c
924 C FIND THE VALUES WHEN TR = TP
925 c
926 do 60 j= ja,jb
927     KEOS(J) = LEOS(J)
928     trl(j)  = tpl(j)
929 60 CONTINUE
930 c

```

```
931      CALL TABLE3 (rmftab,rmfp1t)
932      c
933      return
934      END
```

```

935      SUBROUTINE EOSSET (j1,j2)
936      C
937      c      eosset iterates on tp to satisfy e with the EOS tables
938      c
939      c      input--
940      c          ja, jb - limits on input array
941      c          con(21) - relative error on Tp iteration
942      c
943      c
944      common/eos1/  ad, bd, at, bt, nmat, nfg, ja, jb,
945      1             rad, rdb, rat, rbt
946      common/eostab/ ztab(20,10,2),      entab(20,10,2),
947      1             rostab(20,20,10,2), rmftab(20,20,10,2)
948      common/wrk    / work(9999,12)
949      common/eoswrk/ trl(9999),  tpl(9999), rho1(9999),
950      1             meos(9999), leos(9999), keos(9999)
951      common /np1/  u(9999) , v(9999) , rho(9999) , e(9999) ,
952      1             er(9999) , p(9999) , tp(9999)
953      common /prop/ gam1(9999), rosmfp(9999), rmfp1t(9999),
954      1             rmfp2t(9999), rcsbv(9999), xkap(9999)
955      common /a/    beta(9999) , xmask(9999), con(30)
956      common /e/    cycle, wl, wr, wt, wb, iter, imx, jmx, delt, xmu,
957      1             im1, jm1, im2, jm2, iterlmt, cyl, epsi, gaminit,
958      2             gx, gy, ui, vi, cnrst, cndmp, omega, alpha, t, am1,
959      3             gamma, asq, rhoi, eamb, dtrd, otd, ftd, xkap2,
960      4             kpta, kptb, kptc, kptd, kpte, kptf, eamb2, rcsbin,
961      5             bvar1, ivar2, bvar3, bvar4, bvar5, bvar6, bvar7, bvar8
962      c
963      dimension z(9999), ee(9999), dummy(9999), dedt(9999)
964      dimension xflg(9999)
965      data limit / 25/
966      c
967      equivalence (ee(1), work(1,11)) , (z(1), work(1,12)),
968      1             (dummy(1),work(1,10)), (dedt(1), work(1,9))
969      c
970      ja = j1
971      jb = j2
972      nloop = 0
973      C
974      C COMPUTE THE LOGARITHMS OF THE TEMPERATURES AND DENSITY FOR USE IN
975      C THE TABLE LOOK-UP ROUTINES
976      c
977      DO 10 J = ja,jb
978          erad = er(j)
979          erad = cvmgrp ( erad , con(22) , (erad-con(22)) )
980      9tfluid = cvmgrp (tp(j), 0.25, (tp(j) - 0.25))
981          trl(j) = 0.25 * alog10( con(5)*erad )
982          tpl(j) = alog10( tfluid )
983          rho1(j) = alog10( rho(j)*con(6) )
984      10 continue
985      C
986      C FIRST FIND THE (K,L) POINTS THAT CORRESPOND TO THE TEMPERATURE AND
987      C DENSITY IN EACH ZONE
988      c
989      50 continue

```

```

990      CALL POINT
991      C
992      C NEXT FIND THE VALUES IN THE SPECIFIC ENERGY TABLE
993      C
994      CALL TABLE2 (ENTAB,EE,dedt,tp)
995      C
996      C      now iterate on Tp until the convergence criterion is achieved
997      C
998      xflag = 1.0
999      nloop = nloop + 1
1000     do 20 j = ja,jb
1001         tnew = tp(j) + (e(j) - ee(j)) / dedt(j)
1002         relt = abs (tnew-tp(j)) / tp(j)
1003         xflag = xflag * cvmgrp ( 0.0, 1.0, (relt-con(21)) )
1004     9tp(j) = cvmgrp (tnew, 0.25, (tnew - 0.25))
1005         tpi(j)= alog10 (tp(j))
1006     20 continue
1007     C
1008         if (xflag.gt.0.01) go to 999
1009         if (nloop.lt.limit) go to 50
1010     C
1011     999 continue
1012     return
1013     END

```

```

1014      SUBROUTINE EOSINIT (j1,j2)
1015      C
1016      c      eosinit initializes energy density and pressure for epinit
1017      c
1018      c      input--
1019      c          ja, jb - limits on input array
1020      c
1021      c
1022      common/eos1/  ad, bd, at, bt, nmat, nfg, ja, jb,
1023      1             rad, rdb, rat, rbt
1024      common/eostab/ ztab(20,10,2),      entab(20,10,2),
1025      1             rostab(20,20,10,2), rmftab(20,20,10,2)
1026      common/wrk   / work(9999,12)
1027      common/eoswrk/ trl(9999),  tpl(9999), rho1(9999),
1028      1             meos(9999), leos(9999), keos(9999)
1029      common /np1/  u(9999)   , v(9999)   , rho(9999) , e(9999)   ,
1030      1             er(9999) , p(9999)   , tp(9999)
1031      common /prop/ gam1(9999), rosmfp(9999), rmfp1t(9999),
1032      1             rmfp2t(9999), rcsbv(9999),  xkap(9999)
1033      common /a/    beta(9999) , xmask(9999), con(30)
1034      common /e/    cycle, wl, wr, wt, wb, iter, imx, jmx, delt, xmu,
1035      1             im1, jm1, im2, jm2, iterlmt, cyl, epsi, gaminit,
1036      2             gx, gy, ui, vi, cnrst, cndmp, omega, alpha, t, am1,
1037      3             gamma, asq, rhoi, eamb, dtrd, otd, ftd, xkap2,
1038      4             kpta, kptb, kptc, kptd, kpte, kptf, eamb2, rcsbv,
1039      5             bvar1, ivar2, bvar3, bvar4, bvar5, bvar6, bvar7, bvar8
1040      c
1041      dimension z(9999), ee(9999), dummy(9999), dedt(9999)
1042      dimension xflg(9999)
1043      c
1044      equivalence (ee(1), work(1,11)) , (z(1), work(1,12)),
1045      1             (dummy(1),work(1,10)), (dedt(1), work(1,9))
1046      c
1047      ja = j1
1048      jb = j2
1049      C
1050      C COMPUTE THE LOGARITHMS OF THE TEMPERATURES AND DENSITY FOR USE IN
1051      C THE TABLE LOOK-UP ROUTINES
1052      c
1053      DO 10 J = ja,jb
1054          erad = er(j)
1055          erad = cvmgs ( erad , con(22) , (erad-con(22)) )
1056          tfluid = tp(j)
1057          trl(j) = 0.25 * alog10( con(5)*erad )
1058          tpl(j) = alog10( tfluid )
1059          rho1(j) = alog10( rho(j)*con(6) )
1060      10 continue
1061      C
1062      C FIRST FIND THE (K,L) POINTS THAT CORRESPOND TO THE TEMPERATURE AND
1063      C DENSITY IN EACH ZONE
1064      c
1065      CALL POINT
1066      C
1067      C NEXT FIND THE VALUES IN THE SPECIFIC ENERGY TABLE
1068      c

```

```
1069      CALL TABLE2 (ENTAB,EE,dedt,tp)
1070      c
1071      call table2 (ztab,z,dummy,tp)
1072      c
1073      do 40 j = ja,jb
1074          xgam1      = con(9)*con(6) * tp(j) * (1.+z(j)) / ee(j)
1075      ceos      gam1(j) = cvmgn (xgam1, gaminit, float(leos(j)) )
1076      ceos      rcsbv(j) = cvmgn (1./dedt(j), rcsbin, float(leos(j)) )
1077          gam1(j) = xgam1
1078          rcsbv(j) = 1./dedt(j)
1079          e(j)      = ee(j)
1080      40      continue
1081      return
1082      END
```

```

1083      subroutine epinit
1084      c
1085      c      this subroutine determines the initial plasma specific energy
1086      c      density (En) and initial radiation density (Er) for a fireball.
1087      c      It uses a linear fit for the initial plasma temperature.
1088      c
1089      c
1090      integer cycle, wl, wr, wt, wb
1091      common /mesh/ xc(9999) , yc(9999) , dx(9999) , dy(9999) ,
1092      1      rdx(9999) , rdy(9999) ,
1093      2      rdx(9999), rdy(9999), rxc(9999), r2dx(9999),
1094      3      r2dy(9999)
1095      common /wrk/ un(9999) , vn(9999) , rhon(9999), en(9999) ,
1096      1      pr(9999) , work(9999,7)
1097      common /np1/ u(9999) , v(9999) , rho(9999) , e(9999) ,
1098      1      er(9999) , p(9999) , tp(9999)
1099      common /prop/ gam1(9999), rosmfp(9999), rmfp1t(9999),
1100      1      rmfp2t(9999), rcsbv(9999), xkap(9999)
1101      common /a/ beta(9999) , xmask(9999), con(30)
1102      common /e/ cycle, wl, wr, wt, wb, iter, imx, jmx, delt, xmu,
1103      1      im1, jm1, im2, jm2, iterlmt, cyl, epsi, gaminit,
1104      2      gx, gy, ui, vi, cnrst, cndmp, omega, alpha, t, am1,
1105      3      gamma, asq, rhoi, eamb, dtrd, otd, ftd, xkap2,
1106      4      kpta, kptb, kptc, kptd, kpte, kptf, eamb2, rcsbv,
1107      5      bvar1, ivar2, bvar3, bvar4, bvar5, bvar6, bvar7, bvar8
1108      dimension xr(16),tr(16)
1109      data xr /1.0, 2.5, 6.12, 8.0, 11.5, 12.3, 18.3, 21., 25.4, 30.0,
1110      1      32.6,41.5,60.0 ,114., 189., 250. /
1111      6data tr / 1226., 853., 450., 310., 235., 220., 200., 195., 190.,
1112      1      160., 110., 30., 4.7, 1.0, 0.5, 0.37 /
1113      c
1114      c      find limits first
1115      c
1116      kcenter= ivar2*imx + 2
1117      ycent = yc(kcenter)
1118      xcent = xc(kcenter) - 0.5 * dx(kcenter)
1119      k1 = 1
1120      k2 = kptc + 1
1121      ntab = 16
1122      c
1123      c      profile initialization
1124      c      set Tr profile using linear fits
1125      c      determine Ep from EOS tables
1126      c
1127      c
1128      do 100 k=k1,k2
1129      d = sqrt( (xcent-xc(k))**2 + (ycent-yc(k))**2 )
1130      do 90 i=2,ntab
1131      if (xr(i).lt.d) go to 90
1132      tp(k) = tr(i) + (tr(i-1)-tr(i))*(d-xr(i))/(xr(i-1)-xr(i))
1133      ?go to 91
1134      90 continue
1135      917continue
1136      if (tp(k).lt.con(25).or.d.ge.xr(ntab)) tp(k) = con(25)
1137      100 continue

```

```

1138 c
1139       call eosinit (k1,k2)
1140 c
1141       set pressure profile with eos properties
1142 c
1143       do 110 k=k1,k2
1144           p(k) = gam1(k) * rho(k) * e(k) * con(16)
1145           en(k) = e(k)
1146           pr(k) = p(k) + otd*er(k)*con(16)
1147       110 continue
1148 c
1149       return
1150     end
1151 6subroutine e2t
1152 c
1153 c*****
1154 c
1155 c       2T energy equation solver section
1156 c       use implicit technique to solve for e-tilde and er-tilde
1157 c       also calculate p-tilde
1158 c       note---use centered differencing on Er diffusion term
1159 c
1160 c       special update---use split time step to solve lagrangian
1161 c       portion only in this subroutine:
1162 c           diffusion + radiation exchange + pdv work term
1163 c
1164 c       new update---incorporate quickie nine pt diffusion stencil
1165 c           assume uniform mesh weight controlled by
1166 c           variable con(20)
1167 c
1168 c       set properties to n+1 with 2 loop iteration
1169 c
1170 c*****
1171 c
1172       integer cycle, wl, wr, wt, wb
1173       common /mesh/ xc(9999) , yc(9999) , dx(9999) , dy(9999) ,
1174       1          rdx(9999) , rdy(9999) ,
1175       2          rdx(9999), rdy(9999), rxc(9999), r2dx(9999),
1176       3          r2dy(9999)
1177       common /wrk/ un(9999) , vn(9999) , rhon(9999), en(9999) ,
1178       1          pr(9999) , work(9999,7)
1179       common /np1/ u(9999) , v(9999) , rho(9999) , e(9999) ,
1180       1          er(9999) , p(9999) , tp(9999)
1181       common /prop/ gam1(9999), rosmfp(9999), rmfp1t(9999),
1182       1          rmfp2t(9999), rcsbv(9999), xkap(9999)
1183       common /a/ beta(9999) , xmask(9999), con(30)
1184       common /e/ cycle, wl, wr, wt, wb, iter, imx, jmx, delt, xmu,
1185       1          im1, jm1, im2, jm2, iterlmt, cyl, epsi, gaminit,
1186       2          gx, gy, ui, vi, cnrst, cndmp, omega, alpha, t, am1,
1187       3          gamma, asq, rhoi, eamb, dtrd, otd, ftd, xkap2,
1188       4          kpta, kptb, kptc, kptd, kpte, kptf, eamb2, rcsbin,
1189       5          bvar1, ivar2, bvar3, bvar4, bvar5, bvar6, bvar7,bvar8
1190 c
1191       dimension fluxx(9999), fluxy(9999), fluxxy(9999), fluxyx(9999),
1192       1          etrans(9999), gradv(9999), ern(9999)

```



```

1193 c
1194     equivalence (fluxx(1),work(1,1)), (fluxy(1),work(1,2)),
1195     1          (fluxxy(1),work(1,3)), (fluxyx(1),work(1,4)),
1196     2          (etrans(1),work(1,5)),
1197     3          (ern(1),work(1,7))
1198     equivalence (tt, con(20)), (delxy, con(19)), (rdelxy, con(10)),
1199     1          (rerror, con(23)), (halfdx, con(7)), (dtemp, con(24))
1200     data looplmt / 10/
1201 c
1202 c          first calculate number of lagrangian loops to perform
1203 c
1204     nloop = delt / dtrad
1205     j1    = 1
1206     j2    = kptc + 1
1207     xtt   = 1. - tt
1208 c
1209 c          now calculate velocity gradient — constant for all loops
1210 c
1211     do 5 k=kpta,kptd
1212         gradv(k) =( rdx(k) * ( un(k) - un(k-1) ) +
1213     1             rdy(k) * ( vn(k) - vn(k-imx) ) +
1214     2             cyl      * ( un(k) + un(k-1) ) * 0.5*rx(c(k) )
1215     5     continue
1216 c*****
1217 c
1218 c          the lagranian loop begins now
1219 c
1220 c*****
1221 c
1222     do 100 loop=1,nloop
1223 c
1224 c
1225 c          call eos routine for opacities, conductivity, gam1
1226 c          determine tp from constant volume process
1227     call eos (j1, j2)
1228 c
1229 c          set n level plasma and radiation energy densities
1230 c          also put fix in for RMFP2T
1231 c
1232     do 51 k=kpta,kptd
1233         en(k) = e(k)
1234         ern(k)= er(k)
1235         trad = (con(5)*er(k))**0.25
1236         temp = abs(trad-tp(k))/tp(k)
1237         rmfp2t(k) = cvmgrp( rmfp2t(k), rmfp1t(k), (temp-dtemp) )
1238     9rmfp2t(k) =cvmgrp(rmfp2t(k),rmfp1t(k),(tp(k)-con(30)))
1239     51     continue
1240 c
1241 c          point-jacobi iteration loop
1242 c
1243     349     iter = 0
1244     350     flag = 1.
1245 c
1246 c          set lefthand b.c. (zero gradient)
1247 c

```

```

1248 cdir$ ivdep
1249   do 52 k=1,kptd,imx
1250       er(k) = er(k+1)
1251       tp(k) = tp(k+1)
1252   52 continue
1253 c
1254 c       set top and bottom bc
1255 c
1256 cdir$ ivdep
1257   do 53 k=1,imx
1258       er(k)      = er(k+imx)
1259       er(k+kpte) = er(k+kpte-imx)
1260       tp(k)      = tp(k+imx)
1261       tp(k+kpte) = tp(k+kpte-imx)
1262   53 continue
1263 c
1264 c       first determine misc intermediate quantities for Er
1265 c
1266   do 10 k=kpta,kptd
1267       delxeb = er(k-1) - er(k)
1268 cupwind ebxstar = cvmgp( er(k-1), er(k), delxeb)
1269       ebxstar = 0.5 * ( er(k-1) + er(k) )
1270       fluxx(k) = con(2) * ebxstar * delxeb /
1271   1          (.375*ebxstar*( rho(k-1)*rosmfp(k-1)*dx(k-1) +
1272   2          rho(k) *rosmfp(k) *dx(k) ) +
1273   3          abs(delxeb) + bvar5 )
1274   10 continue
1275   do 11 k=kpta,kptd
1276       delyeb = er(k-imx) - er(k)
1277       ebystar = 0.5 * ( er(k-imx) + er(k) )
1278       fluxy(k) = con(2)*ebystar * delyeb /
1279   1          (.375*ebystar*(rho(k-imx)*rosmfp(k-imx)*dy(k-imx)+
1280   2          rho(k) *rosmfp(k) *dy(k) )+
1281   3          abs(delyeb) + bvar5 )
1282   11 continue
1283   do 12 k=kpta,kptd
1284       delxye = er(k-imx-1)- er(k)
1285       ebxystr = 0.5 * ( er(k-imx-1) + er(k) )
1286       fluxxy(k)= con(2) * ebxystr * delxye /
1287   1          (.375*ebxystr*delxy*(rho(k-imx-1)*rosmfp(k-imx-1)+
1288   2          rho(k) *rosmfp(k) )+
1289   3          abs(delxye) + bvar5 )
1290   12 continue
1291   do 13 k=kpta,kptd
1292       delyxe = er(k-imx+1)- er(k)
1293       ebyxstr = 0.5 * ( er(k-imx+1) + er(k) )
1294       fluxyx(k)= con(2) * ebyxstr * delyxe /
1295   1          (.375*ebyxstr*delxy*(rho(k-imx+1)*rosmfp(k-imx+1)+
1296   2          rho(k) *rosmfp(k) )+
1297   3          abs(delyxe) + bvar5 )
1298   13 continue
1299 c
1300 c       calculate energy transfer by emission and absorption
1301 c       ( assume positive for Er )
1302 c

```

```

1303      do 15 k=kpta,kptd
1304          etrans(k)= rho(k) * ( con(3)*rmfp1t(k)*tp(k)**4 -
1305      1          con(4)*rmfp2t(k)*er(k) )
1306      15  continue
1307      c
1308      c      now for the solution of er-tilde
1309      c
1310      do 25 k=kpta,kptb
1311          r1      = xc(k) - halfdx
1312          r2      = xc(k) + halfdx
1313          r3      = xc(k)
1314      c
1315          ebx     = rdx(k)*( fluxx(k) - fluxx(k+1) )
1316          eby     = rdy(k)*( fluxy(k) - fluxy(k+imx) )
1317          ebc     = 0.5*cyl*rx(k)*( fluxx(k) + fluxx(k+1))
1318          ebxy    = rdelxy*(fluxxy(k)*r1-fluxxy(k+imx+1)*r2)/r3
1319          ebyx    = rdelxy*(fluxyx(k)*r2-fluxyx(k+imx-1)*r1)/r3
1320          erwork  = -otd * er(k) * gradv(k)
1321          ediff   = tt * (ebx+eby-ebc) + xtt * (ebxy+ebyx)
1322      c
1323          deler   = dtrd * xmask(k) * ( ediff + etrans(k) + erwork )
1324          ernp1   = ern(k) + deler
1325          er(k)   = ernp1
1326          er(k)   = cvmgs ( er(k), con(26), (er(k)-con(26)) )
1327      25  continue
1328      c
1329      c      determine intermediate quantities for E
1330      c
1331      do 20 k=kpta,kptd
1332          fluxx(k)= 2.* (tp(k-1)-tp(k)) * (xkap(k-1)*xkap(k)) /
1333      1          ( dx(k-1)*xkap(k) + dx(k)*xkap(k-1) )
1334      20  continue
1335      do 21 k=kpta,kptd
1336          fluxy(k)= 2.* (tp(k-imx)-tp(k)) * (xkap(k-imx)*xkap(k)) /
1337      1          ( dy(k-imx)*xkap(k) + dy(k)*xkap(k-imx) )
1338      21  continue
1339      do 22 k=kpta,kptd
1340          fluxxy(k)=2. * rdelxy *
1341      1          (tp(k-imx-1) - tp(k)) * (xkap(k-imx-1)*xkap(k))/
1342      2          ( xkap(k-imx-1) + xkap(k) )
1343      22  continue
1344      do 23 k=kpta,kptb
1345          fluxyx(k)=2. * rdelxy *
1346      1          (tp(k-imx+1) - tp(k)) * (xkap(k-imx+1)*xkap(k))/
1347      2          ( xkap(k-imx+1) + xkap(k) )
1348      23  continue
1349      c
1350      c      the solution for e-tilde
1351      c
1352      do 30 k=kpta,kptb
1353          r1      = xc(k) - halfdx
1354          r2      = xc(k) + halfdx
1355          r3      = xc(k)
1356      c
1357          ex      = rdx(k)*( fluxx(k) - fluxx(k+1) )

```

```

1358      ey      = rdy(k)*( fluxy(k) - fluxy(k+imx) )
1359      ec      = 0.5*cyl*rxk(k)* (fluxx(k) + fluxx(k+1))
1360      exy     = rdelxy*(fluxxy(k)*r1-fluxxy(k+imx+1)*r2)/r3
1361      eyx     = rdelxy*(fluxyx(k)*r2-fluxyx(k+imx-1)*r1 )/r3
1362      epwork  = -p(k) * con(17) * gradv(k)
1363      ediff   = tt * (ex+ey-ec) + xtt * (exy+eyx)
1364      c
1365      dele    = dtrd * xmask(k) * (ediff -etrans(k) +epwork) /rho(k)
1366      enp1    = en(k) + dele
1367      enp1    = cvmgrp( enp1, con(27), (enp1-con(27)))
1368      temp    = abs(enp1-e(k)) - e(k) * rerror
1369      flag    = flag * cvmgrp ( 0.0, 1.0, temp )
1370      c
1371      p(k)    = gam1(k) * rho(k) * enp1 * con(16)
1372      tp(k)   = tp(k) + rcsbv(k) * (enp1 -e(k))
1373      e(k)    = enp1
1374      30      continue
1375      c
1376      iter = iter + 1
1377      if (flag.gt.0.01) go to 360
1378      if (iter.lt.looplmt) go to 350
1379      write(1,700) cycle,loop
1380      700      format(' iteration e2t exceeded ',i6,2x,i4)
1381      ctim     close (1)
1382      ctim     close (3)
1383      ctim     close (6)
1384      ctim     close (7)
1385      ctim     close (8)
1386      ctimn    stop 1
1387      360      continue
1388      c
1389      c      update time value of e for later plasma temp calculations
1390      c
1391      do 40 k=kpta,kptb
1392          en(k) = e(k)
1393      40      continue
1394      c
1395      100      continue
1396      return
1397      end

```

```

1398      SUBROUTINE INIT2 (ireos)
1399      C
1400      C  INIT2 reads in opacity tables
1401      c      taken from MF-FIRE    ref. UWFD-458
1402      C
1403      common/eos1/  ad, bd, at, bt, nmat, nfg, ja, jb,
1404      1            rad, rdb, rat, rbt
1405      common/eostab/ ztab(20,10,2),      entab(20,10,2),
1406      1            rostab(20,20,10,2), rmftab(20,20,10,2)
1407      character*40 headr1, headr2
1408      dimension hnu1(1),hnu11(1),hnu12(1),rrtab(20,20,10,2),
1409      1            rptab(20,20,10,2)
1410      equivalence (rostab(1,1,1,1), rrtab(1,1,1,1))
1411      equivalence (rmftab(1,1,1,1), rptab(1,1,1,1))
1412      C
1413      nmat = 1
1414      nfg = 0
1415      C
1416      C  READ IN EOS DATA FROM ireos FOR MATERIAL 1 &
1417      c      FROM ireos2 FOR MATERIAL 2
1418      READ(ireos,1002) HEADR1
1419      READ(ireos,1001) AD1, BD1, AT1, BT1, NFG1
1420      IF (NMAT .EQ. 2) then
1421          read(ireos2,1002) headr2
1422          READ(ireos2,1001) AD2, BD2, AT2, BT2, NFG2
1423      endif
1424      5  AD = AD1
1425      BD = BD1
1426      AT = AT1
1427      BT = BT1
1428      rad= 1./ad
1429      rbd= 1./bd
1430      rat= 1./at
1431      rbt= 1./bt
1432      c
1433      READ(ireos,1000) ((ZTAB(L,M,1), L=1,20), M=1,10)
1434      READ(ireos,1000) ((ENTAB(L,M,1), L=1,20), M=1,10)
1435      READ(ireos,1000) (((ROSTAB(K,L,M,1), K=1,20), L=1,20), M=1,10)
1436      READ(ireos,1000) (((RMFTAB(K,L,M,1), K=1,20), L=1,20), M=1,10)
1437      IF (NMAT .EQ. 1) GOTO 15
1438      READ(ireos2,1000) ((ZTAB(L,M,2), L=1,20), M=1,10)
1439      READ(ireos2,1000) ((ENTAB(L,M,2), L=1,20), M=1,10)
1440      READ(ireos2,1000) (((ROSTAB(K,L,M,2), K=1,20), L=1,20), M=1,10)
1441      READ(ireos2,1000) (((RMFTAB(K,L,M,2), K=1,20), L=1,20), M=1,10)
1442      15  CONTINUE
1443      1000 FORMAT(4(1x,E12.6))
1444      1001 FORMAT(4(1x,E12.6),I12)
1445      1002 FORMAT(40A1)
1446      20 DO 50 M = 1,10
1447          DO 50 L = 1,20
1448              DO 50 KMAT = 1, nmat
1449                  IF(ZTAB(L,M,KMAT) .NE. 0.0) ZTAB(L,M,KMAT) =
1450      1                      ALOG10(ZTAB(L,M,KMAT))
1451                  IF(ENTAB(L,M,KMAT) .NE. 0.0) ENTAB(L,M,KMAT) =
1452      1                      ALOG10(ENTAB(L,M,KMAT))

```

```
1453          DO 50 K = 1,20
1454             IF(RMFTAB(K,L,M,KMAT).NE.0.0) RMFTAB(K,L,M,KMAT) =
1455                1          ALOG10(RMFTAB(K,L,M,KMAT))
1456             IF(ROSTAB(K,L,M,KMAT).NE.0.0) ROSTAB(K,L,M,KMAT) =
1457                1          ALOG10(ROSTAB(K,L,M,KMAT))
1458          50 CONTINUE
1459  c
1460          RETURN
1461          END
```

```

1462      subroutine kappa (z,ja,jb)
1463      c
1464      c      this subroutine computes the plasma thermal conductivity
1465      c      it uses a curve fit to loglamda
1466      c      see subs. llam and pcond in MF-FIRE   FDM-458
1467      c      vectorized
1468      c
1469      common/wrk / work(9999,12)
1470      common /np1/ u(9999) , v(9999) , rho(9999) , e(9999) ,
1471      1      er(9999) , p(9999) , tp(9999)
1472      common /prop/ gam1(9999), rosmfp(9999), rmfp1t(9999),
1473      1      rmfp2t(9999), rcsbv(9999), xkap(9999)
1474      common /a/ beta(9999) , xmask(9999), con(30)
1475      c
1476      real lnx(10), lny(14)
1477      dimension xt(10), yt(14), rxt(10), ryt(14), z(*)
1478      dimension x(9999), dens(9999), xisx(9999), xisy(9999),
1479      1      xloglm(9999), sqtp(9999)
1480      c
1481      equivalence (x(1) , work(1,1)), (dens(1), work(1,2)),
1482      1      (xisx(1) , work(1,3)), (xisy(1), work(1,4)),
1483      2      (xloglm(1), work(1,5)), (sqtp(1), work(1,6))
1484      c
1485      data xt / 1.e3, 100., 10., 1., .1, .01, .001, .0001, 1.e-5, 1.e-6/
1486      data rxt/ .001, .01, .1, 1., 10., 100., 1000., 1.e4, 1.e+5, 1.e+6/
1487      data yt / 1.e28, 1.e27, 1.e26, 1.e25, 1.e24, 1.e23, 1.e22, 1.e21,
1488      1      1.e20, 1.e19, 1.e18, 1.e17, 1.e16, 1.e15 /
1489      data ryt/ 1.e-28, 1.e-27, 1.e-26, 1.e-25, 1.e-24, 1.e-23, 1.e-22,
1490      1      1.e-21, 1.e-20, 1.e-19, 1.e-18, 1.e-17, 1.e-16, 1.e-15 /
1491      data lnx / 6.91, 4.60, 2.30, 0.0, -2.30, -4.60, -6.91, -9.21,
1492      1      -11.51,-13.81 /
1493      data lny / 64.47, 62.17, 59.87, 57.56, 55.26, 52.96, 50.66,
1494      1      48.35, 46.05, 43.75, 41.45, 39.14, 36.84, 34.54 /
1495      c
1496      c      define misc goodies here
1497      c
1498      do 150 j=ja,jb
1499      sqtp(j) = sqrt( tp(j) )
1500      x(j) = 3.1623e-5 * tp(j) * sqtp(j) / z(j)
1501      dens(j) = con(6) * rho(j)
1502      xisx(j) = 1.0
1503      xisy(j) = 1.0
1504      150 continue
1505      c
1506      c      search for limits on x
1507      c      switch order of loops for efficiency
1508      c
1509      do 155 i=1,9
1510      do 155 j=ja,jb
1511      xtemp = float(i) + 1.
1512      delx = x(j) - xt(i)
1513      xisx(j) = cvmcp ( xisx(j), xtemp, delx )
1514      155 continue
1515      c
1516      c      now search for limits on density

```

```

1517 c
1518     do 160 i=1,13
1519         do 160 j=ja,jb
1520             xtemp = float(i) + 1.
1521             delrho = dens(j) - yt(i)
1522             xisy(j) = cvmgrp ( xisy(j), xtemp, delrho )
1523         160 continue
1524 c
1525 c         determine loglamdas in a scalar loop
1526 c
1527     do 170 j=ja,jb
1528         isx = int( xisx(j) )
1529         isy = int( xisy(j) )
1530         xlog = 33.825 + lnxb(isx) + .26 * x(j) * rxt(isx) -
1531     1         0.5 * ( lnyb(isy) + .26*dens(j) * ryt(isy) )
1532         xloglm(j) = cvmgrp ( xlog, 1.0, (xlog-1.0) )
1533     170 continue
1534 c
1535 c         now put all this stuff together to get kappa
1536 c
1537     do 180 j=ja,jb
1538         xkap(j) = con(8) * tp(j) * tp(j) * sqtp(j) /
1539     1         ( xloglm(j) * (4. + z(j) ) )
1540     180 continue
1541 c
1542     return
1543 end

```



```

1544      SUBROUTINE POINT
1545      C
1546      C POINT COMPUTES THE (K,L,M) INDEX IN THE EOS TABLES THAT CORRESPOND
1547      C TO (R-TEMP,P-TEMP,DENSITY) IN EACH ZONE OF THE PLASMA
1548      c      modified for cray vectorization
1549      C
1550      common/eos1/  ad, bd, at, bt, nmat, nfg, ja, jb,
1551      1      rad, rdb, rat, rbt
1552      common/eoswrk/ trl(9999), tpl(9999), rhol(9999),
1553      1      meos(9999), leos(9999), keos(9999)
1554      C
1555      C FIND THE INDEX FOR THE DENSITY
1556      c
1557      DO 100 J = ja,jb
1558      temp      = (rhol(j) - bd) * rad + 1.
1559      x          = cvmgp( temp, 0., temp-1.)
1560      9x7= cvmgp(4x, 9.,39.-x )
1561      MEOS(J) = ifix(x)
1562      100 CONTINUE
1563      C
1564      C FIND THE INDEX FOR radiation TEMPERATURE
1565      c
1566      DO 200 J = ja,jb
1567      temp      = (trl(j) - bt ) * rat + 1
1568      x          = cvmgp( temp, 0.0, temp-1.)
1569      9x7= cvmgp(4x, 19., 19.-x )
1570      keos(J) = ifix(x)
1571      200 CONTINUE
1572      C
1573      C FIND THE INDEX FOR plasma TEMPERATURE
1574      c
1575      DO 300 J = ja,jb
1576      temp      = (tpl(j) - bt ) * rat + 1
1577      x          = cvmgp( temp, 0.0, temp-1.)
1578      9x7= cvmgp(4x, 19., 19.-x )
1579      leos(J) = ifix(x)
1580      300 CONTINUE
1581      c
1582      return
1583      END

```

```

1584      subroutine restart (irst,iwrst)
1585      integer cycle, wl, wr, wt, wb
1586      common /wrk/  un(9999)  , vn(9999)  , rhon(9999), en(9999)  ,
1587      1      pr(9999)  , work(9999,7)
1588      common /np1/  u(9999)  , v(9999)  , rho(9999) , e(9999)  ,
1589      1      er(9999)  , p(9999)  , tp(9999)
1590      common /a/    beta(9999)  , xmask(9999), con(30)
1591      common /e/    cycle, wl, wr, wt, wb, iter, imx, jmx, delt, xmu,
1592      1      im1, jm1, im2, jm2, iterlmt, cyl, epsi, gaminit,
1593      2      gx, gy, ui, vi, cnrst, cndmp, omega, alpha, t, am1,
1594      3      gamma, asq, rhoi, eamb, dtrd, otd, ftd, xkap2,
1595      4      kpta, kptb, kptc, kptd, kpte, kptf, eamb2, rcsubin,
1596      5      bvar1, ivar2, bvar3, bvar4, bvar5, bvar6, bvar7,bvar8
1597      character*80 header
1598      c
1599      read(irst,1) ir,jr,header
1600      1      format(i3,i3,a80)
1601      write(iwrst,2) header
1602      2      format(a80)
1603      do 20 k=1,kptd
1604          read(irst,*) ipt,u(k),v(k),p(k),rho(k),e(k),tp(k),er(k)
1605          rhon(k) = rho(k)
1606          en(k)   = e(k)
1607          pr(k)   = p(k) + otd*er(k)*con(16)
1608      20      continue
1609      return
1610      end

```

```

1611      subroutine solabc (iflag)
1612      c
1613      c          boundary condition subroutine
1614      c          bc flags (wl, wr, wt, wb) +
1615      c          1--rigid, free slip wall
1616      c          2--rigid, no-slip wall
1617      c          3--continuative outflow wall
1618      c          4--periodic (symmetric bc)
1619      c          5--user defined
1620      c
1621      c          note: since explicit routines used for e, er, and rho
1622      c          only n+1 bc values needed--called at end of time step
1623      c
1624      integer cycle, wl, wr, wt, wb
1625      common /mesh/ xc(9999) , yc(9999) , dx(9999) , dy(9999) ,
1626      1          rdx(9999) , rdy(9999) ,
1627      2          rdx(9999), rdy(9999), rxc(9999), r2dx(9999),
1628      3          r2dy(9999)
1629      common /wrk/ un(9999) , vn(9999) , rhon(9999), en(9999) ,
1630      1          pr(9999) , work(9999,7)
1631      common /np1/ u(9999) , v(9999) , rho(9999) , e(9999) ,
1632      1          er(9999) , p(9999) , tp(9999)
1633      common /prop/ gam1(9999), rosmfp(9999), rmfp1t(9999),
1634      1          rmfp2t(9999), rcsbv(9999), xkap(9999)
1635      common /a/ beta(9999) , xmask(9999), con(30)
1636      common /e/ cycle, wl, wr, wt, wb, iter, imx, jmx, delt, xmu,
1637      1          im1, jm1, im2, jm2, iterlmt, cyl, epsi, gaminit,
1638      2          gx, gy, ui, vi, cnrst, cndmp, omega, alpha, t, am1,
1639      3          gamma, asq, rhoi, eamb, dtrd, otd, ftd, xkap2,
1640      4          kpta, kptb, kptc, kptd, kpte, kptf, eamb2, rcsbv,
1641      5          bvar1, ivar2, bvar3, bvar4, bvar5, bvar6, bvar7, bvar8
1642      c
1643      do 140 k=1,kptb+2,imx
1644      rho(k) = rho(k+1)
1645      e(k) = e(k+1)
1646      en(k) = en(k+1)
1647      er(k) = er(k+1)
1648      gam1(k) = gam1(k+1)
1649      rcsbv(k)= rcsbv(k+1)
1650      xkap(k) = xkap(k+1)
1651      tp(k) = tp(k+1)
1652      ctim rho(k+im1) = rho(k+im2)
1653      ctim e(k+im1) = e(k+im2)
1654      ctim en(k+im1) = en(k+im2)
1655      ctim er(k+im1) = er(k+im2)
1656      c
1657      c          left bc
1658      c
1659      go to (102, 104, 106, 108, 110) wl
1660      102          u(k) = 0.0
1661          v(k) = v(k+1)
1662          go to 111
1663      104          u(k) = 0.0
1664          v(k) = -v(k+1)
1665          go to 111

```

```

1666      106      e(k)      = e(k+1)
1667      er(k)     = er(k+1)
1668      if(iflag.gt.0) go to 111
1669      u(k)       = u(k+1)
1670      v(k)       = v(k+1)
1671      go to 111
1672      108      u(k)       = u(k+im2)
1673      v(k)       = v(k+im2)
1674      rho(k)     = rho(k+im2)
1675      e(k)       = e(k+im2)
1676      en(k)      = en(k+im2)
1677      er(k)      = er(k+im2)
1678      go to 111
1679      110      continue
1680      u(k)       = 0.0
1681      v(k)       = v(k+1)
1682      c
1683      c      right bc
1684      c
1685      111      go to (122, 124, 126, 128, 130) wr
1686      122      u(k+im2) = 0.0
1687      v(k+im1) = v(k+im2)
1688      go to 140
1689      124      u(k+im2) = 0.0
1690      v(k+im1) = -v(k+im2)
1691      go to 140
1692      126      if(iflag.gt.0) go to 140
1693      u(k+im2) = u(k+im2-1)
1694      v(k+im1) = v(k+im2)
1695      go to 140
1696      128      u(k+im1) = u(k+1)
1697      v(k+im1) = v(k+1)
1698      rho(k+im1) = rho(k+1)
1699      e(k+im1) = e(k+1)
1700      er(k+im1) = er(k+1)
1701      go to 140
1702      130      continue
1703      c
1704      c
1705      140      continue
1706      do 190 k=2,im1
1707      rho(k)    = rho(k+imx)
1708      e(k)      = e(k+imx)
1709      en(k)     = en(k+imx)
1710      en(k+kpte) = en(k+kptf)
1711      rho(k+kpte) = rho(k+kptf)
1712      e(k+kpte) = e(k+kptf)
1713      er(k)     = er(k+imx)
1714      er(k+kpte) = er(k+kptf)
1715      tp(k)     = tp(k+imx)
1716      tp(k+kpte) = tp(k+kptf)
1717      c
1718      c      top bc
1719      c
1720      go to (152, 154, 156, 158, 160) wt

```

```

1721      152      v(k+kptf) = 0.0
1722              u(k+kpte) = u(k+kptf)
1723              go to 161
1724      154      v(k+kptf) = 0.0
1725              u(k+kpte) = -u(k+kptf)
1726              go to 161
1727      156      if(iflag.gt.0) go to 161
1728              v(k+kptf) = v(k+kptf-imx)
1729              u(k+kpte) = u(k+kptf)
1730              go to 161
1731      158      v(k+kpte) = v(k+imx)
1732              u(k+kpte) = u(k+imx)
1733              rho(k+kpte) = rho(k+imx)
1734              e(k+kpte) = e(k+imx)
1735              er(k+kpte) = er(k+imx)
1736              go to 161
1737      160      continue
1738      c
1739      c      bottom bc
1740      c
1741      161      go to (172, 174, 176, 178, 180) wb
1742      172      v(k) = 0.0
1743              u(k) = u(k+imx)
1744              go to 190
1745      174      v(k) = 0.0
1746              u(k) = -u(k+imx)
1747              go to 190
1748      176      if(iflag.gt.0) go to 190
1749              v(k) = v(k+imx)
1750              u(k) = u(k+imx)
1751              go to 190
1752      178      v(k) = v(k+kptf)
1753              u(k) = u(k+kptf)
1754              rho(k) = rho(k+kptf)
1755              e(k) = e(k+kptf)
1756              er(k) = er(k+kptf)
1757              go to 190
1758      180      continue
1759      190      continue
1760              return
1761              end

```

```

1762      subroutine solaice
1763      c
1764      c      this subroutine solves a single time step of a 2-d
1765      c      compressible flow problem (with energy equation)
1766      c      using the sola-ice technique
1767      c      modified for
1768      c      vectorized loops
1769      c      pressure iteration
1770      c      note:  k  ----- i,j
1771      c              k-1 ----- i-1,j
1772      c              k+1 ----- i+1,j
1773      c              k-imx ---- i,j-1
1774      c              k+imx ---- i,j+1
1775      c
1776      integer cycle, wl, wr, wt, wb
1777      common /mesh/ xc(9999) , yc(9999) , dx(9999) , dy(9999) ,
1778      1      rdx(9999) , rdy(9999) ,
1779      2      rdx(9999), rdy(9999), rxc(9999), r2dx(9999),
1780      3      r2dy(9999)
1781      common /wrk/ un(9999) , vn(9999) , rhon(9999), en(9999) ,
1782      1      pr(9999) , work(9999,7)
1783      common /np1/ u(9999) , v(9999) , rho(9999) , e(9999) ,
1784      1      er(9999) , p(9999) , tp(9999)
1785      common /prop/ gam1(9999), rosmfp(9999), rmfp1t(9999),
1786      1      rmfp2t(9999), rcsbv(9999), xkap(9999)
1787      common /a/ beta(9999) , xmask(9999), con(30)
1788      common /e/ cycle, wl, wr, wt, wb, iter, imx, jmx, delt, xmu,
1789      1      im1, jm1, im2, jm2, iterlmt, cyl, epsi, gaminit,
1790      2      gx, gy, ui, vi, cnrst, cndmp, omega, alpha, t, am1,
1791      3      gamma, asq, rhoi, eamb, dtrd, otd, ftd, xkap2,
1792      4      kpta, kptb, kptc, kptd, kpte, kptf, eamb2, rcsbin,
1793      5      bvar1, ivar2, bvar3, bvar4, bvar5, bvar6, bvar7, bvar8
1794      c
1795      dimension enp1(9999), ernp1(9999)
1796      equivalence ( enp1(1), work(1,1) ), ( ernp1(1), work(1,2) )
1797      c
1798      c      start cycle
1799      c
1800      if (cycle.eq.0) go to 480
1801      c
1802      c*****
1803      c
1804      c      first compute u-tilde and v-tilde using explicit solver
1805      c
1806      c*****
1807      c      compute u tilde
1808      c
1809      do 60 k=kpta, kptb
1810      fux = am1*un(k)*rdxc(k)*(un(k+1)-un(k-1)) +
1811      1      0.5*alpha*(rdx(k+1)*(un(k+1)-un(k))*(un(k)-abs(un(k)))+
1812      2      rdx(k)*(un(k)-un(k-1))*(un(k)+abs(un(k)))) )
1813      vstar= 0.5*rdxc(k)*( dx(k)*(vn(k)+vn(k-imx)) +
1814      1      dx(k+1)*(vn(k+imx+1)+vn(k-imx+1)) )
1815      fuy = 2.*am1*vstar*( un(k+imx)-un(k-imx) ) * r2dy(k) +
1816      1      alpha*(rdyc(k)*(un(k+imx)-un(k))*(vstar-abs(vstar)) +

```

```

1817      2          rdy(k-imx)*(un(k)-un(k-imx))*(vstar-abs(vstar)))
1818      vk = 2.*xmu/(rhon(k)+rhon(k+1))
1819      visx = vk*( ftd * rdx(k) * ( rdx(k-1) * (un(k-1) - un(k)) -
1820      a          rdx(k) * (un(k) - un(k+1)) ) +
1821      1          rdy(k) * ( rdy(k-imx) * (un(k-imx) - un(k)) -
1822      a          rdy(k) * (un(k) - un(k+imx)) ) +
1823      2          (vn(k+1)-vn(k-imx+1)-vn(k)+vn(k-imx))*otd*rdy(k)*
1824      3          2.*rdxc(k) +
1825      4          ftd*cyl*( (un(k+1)-un(k-1)) * 2.*r2dx(k) -
1826      5          un(k)/(abs(xc(k))+.5*dx(k)) ) /
1827      6          ( abs(xc(k))+.5*dx(k) ) )
1828      dp = 2.*(pr(k)-pr(k+1)) / (dx(k)*rhon(k) + dx(k+1)*rhon(k+1))
1829      c
1830      c
1831      u(k) = un(k) + xmask(k) * delt*( dp + gx - fux - fuy + visx )
1832      60 continue
1833      c
1834      c      compute v tilde
1835      c
1836      do 61 k=kpta, kptb
1837      ustar= 0.5*rdyc(k)*( dy(k)*(un(k)+un(k-1)) +
1838      1          dy(k+imx)*(un(k+imx)+un(k+imx-1)) )
1839      fvx = 2.*am1*ustar*( vn(k+1) - vn(k-1) ) * r2dx(k) +
1840      1          alpha*(rdxc(k)*(vn(k+1)-vn(k))*(ustar - abs(ustar)) +
1841      2          rdx(k-1)*(vn(k)-vn(k))*(ustar - abs(ustar)) )
1842      fvy = am1*vn(k)*rdyc(k)*( vn(k+imx) - vn(k-imx) ) +
1843      1          .5*alpha*(rdy(k+imx)*(vn(k+imx)-vn(k))*(vn(k)-abs(vn(k)))+
1844      2          rdy(k)*(vn(k)-vn(k-1))*(vn(k)-abs(vn(k))) )
1845      vk = 2.*xmu/(rhon(k)+rhon(k+imx))
1846      visy= vk*( rdx(k-1) * ( rdx(k-1) * (vn(k-1) - vn(k)) -
1847      a          rdx(k) * (vn(k) - vn(k+1)) ) +
1848      1          ftd*rdy(k) * ( rdy(k-imx) * (vn(k-imx) - vn(k)) -
1849      b          rdy(k) * (vn(k) - vn(k+imx)) ) +
1850      2          (un(k+imx)-un(k)-un(k+imx-1)+un(k-1))*otd*rdx(k)*
1851      3          2.*rdyc(k) +
1852      4          cyl*rx(k)*( (vn(k+1)-vn(k-1))*2.*r2dx(k) +
1853      5          2.*otd*rdyc(k)*( un(k+imx)+un(k+imx-1)-
1854      6          un(k)-un(k-1)) ))
1855      dp =2.*(pr(k)-pr(k+imx))/(dy(k)*rhon(k)+dy(k+imx)*rhon(k+imx))
1856      c
1857      c
1858      v(k)= vn(k) + xmask(k)*delt*( dp + gy - fvx - fvy + visy )
1859      61 continue
1860      c*****
1861      c
1862      c      pressure solver sequence -- determine u,v,p (n+1)
1863      c      satisfy continuity and reduced momentum equations
1864      c      implicit technique
1865      c
1866      c*****
1867      iter = 0
1868      flg = 0.
1869      c
1870      c      now set boundary conditions
1871      c

```



```

1927      3      alpha*abs(v(k-imx))*( rhon(k-imx)-rhon(k)))
1928      f4      = -rxc(k)*( u(k)*( rhon(k)+ rhon(k+1) ) +
1929      1      alpha*abs(u(k))*( rhon(k) - rhon(k+1) )
1930      2      + u(k-1)*( rhon(k-1)+ rhon(k) ) +
1931      3      alpha*abs(u(k-1))*( rhon(k-1)- rhon(k)) )
1932      rho(k)   = f1 + xmask(k) * delt * 0.5 * ( f2 + f3 + cyl*f4 )
1933 9rho(k)3= cvmgrp (rho(k), con(29), (rho(k) - con(29)) )
1934 450 continue
1935 c
1936 c      energy equation---convective portion only
1937 c      for both e and er energy densities
1938 c
1939      do 475 k=kpta, kptb
1940      f1 = e(k)
1941      f2 = am1*(u(k)+u(k-1))*( e(k+1) - e(k-1) ) * r2dx(k) +
1942      1      am1*(v(k)+v(k-imx))*( e(k+imx) - e(k-imx) ) * r2dy(k)+
1943      2      0.5*alpha*( rdx(k)*(u(k)+u(k-1) -abs(u(k)+u(k-1))) ) *
1944      3      ( e(k+1) - e(k) ) +
1945      4      rdx(k-1)*(u(k)+u(k-1)+abs(u(k)+u(k-1))) ) *
1946      5      ( e(k) - e(k-1) ) ) +
1947      6      0.5*alpha*(rdy(k)*(v(k)+v(k-imx)-abs(v(k)+v(k-imx)))*
1948      7      ( e(k+imx) - e(k) ) +
1949      8      rdy(k-imx)*(v(k)+v(k-imx)+abs(v(k)+v(k-imx)))*
1950      9      ( e(k) - e(k-imx) ) )
1951 c
1952      enp1(k)= f1 - xmask(k) * delt* f2
1953 475 continue
1954 c
1955      do 476 k=kpta, kptb
1956      f1 = er(k)
1957      f2 = am1*(u(k)+u(k-1))*( er(k+1) - er(k-1) ) * r2dx(k) +
1958      1      am1*(v(k)+v(k-imx))*( er(k+imx) - er(k-imx) ) * r2dy(k)+
1959      2      0.5*alpha*( rdx(k)*(u(k)+u(k-1) -abs(u(k)+u(k-1))) ) *
1960      3      ( er(k+1) - er(k) ) +
1961      4      rdx(k-1)*(u(k)+u(k-1)+abs(u(k)+u(k-1))) ) *
1962      5      ( er(k) - er(k-1) ) ) +
1963      6      0.5*alpha*(rdy(k)*(v(k)+v(k-imx)-abs(v(k)+v(k-imx)))*
1964      7      ( er(k+imx) - er(k) ) +
1965      8      rdy(k-imx)*(v(k)+v(k-imx)+abs(v(k)+v(k-imx)))*
1966      9      ( er(k) - er(k-imx) ) )
1967 c
1968      ernp1(k)= f1 - xmask(k) * delt* f2
1969 476 continue
1970 c
1971      do 477 k=kpta,kptb
1972      tp(k) = tp(k) + rcsbv(k) * (enp1(k) - e(k))
1973      e(k) = enp1(k)
1974      erad = ernp1(k)
1975      er(k) = cvmgrp ( erad, con(26), (erad-con(26)) )
1976 477 continue
1977 c
1978 c      now update the hydro pressure and total pressure
1979 c
1980      do 478 k=1,kptd
1981      p(k) = gam1(k) * rho(k) * e(k) * con(16)

```

```

1982          pr(k) = p(k) + otd * er(k) * con(16)
1983          en(k) = e(k)
1984      478  continue
1985      c
1986      c
1987      480  continue
1988      c
1989      c      call boundary conditons since loops go to im1, and jm1
1990      c
1991          iflag = 0
1992          call solabc (iflag)
1993      c*****
1994      c
1995      c      compute the relaxation factors--constant for time step
1996      c
1997      c*****
1998          do 490 k=kpta, kptb
1999              pto = gam1(k) * rho(k) * e(k) * con(16)
2000              delp = 1.e-4 * pto
2001              ur = 2.0*delt * rdx(k) * delp / (rho(k)+rho(k+1))
2002              ul = -2.0*delt * rdx(k) * delp / (rho(k-1)+rho(k))
2003              vt = 2.0*delt * rdy(k) * delp / (rho(k)+rho(k+imx))
2004              vb = -2.0*delt * rdy(k) * delp / (rho(k-imx)+rho(k))
2005              dt = delt * (rdx(k)*(ur-ul) + rdy(k)*(vt-vb)
2006                  1      + cyl*(ur+ul)*0.50*rxk(k))
2007              rot = rho(k)/(1.0 + dt)
2008              et = e(k) - p(k)/rho(k)*dt*con(17)
2009              pt = gam1(k)*rot*et*con(16)
2010              beta(k) = omega*delp/(delp-(pt-pt0))
2011      490  continue
2012      502  continue
2013          return
2014      end
2015      END

```

```

2016      SUBROUTINE TABLE2(A,AA,AADER,tp)
2017      C
2018      C  TABLE2 INTERPOLATES IN THE TWO-DIMENSIONAL EOS TABLES USING THE
2019      C  LEOS AND MEOS INDICES
2020      c      modified for cray vectorization
2021      c      cvmgz (=0, <>0, test)
2022      C
2023      C
2024      common/eos1 / ad, bd, at, bt, nmat, nfg, ja, jb,
2025      1          rad, rdb, rat, rbt
2026      common/wrk / work(9999,12)
2027      common/eoswrk/ trl(9999), tpl(9999), rho1(9999),
2028      1          meos(9999), leos(9999), keos(9999)
2029      c
2030      dimension A(*), AA(*), AADER(*), tp(*),
2031      1          dtp(9999), dden(9999), xpt(9999)
2032      c
2033      equivalence (work(1,5), dtp(1)), (work(1,6), dden(1)),
2034      1          (work(1,7), xpt(1))
2035      c
2036      data kmat, xtab, itab, xytabs /1, 20., 20, 200./
2037      c
2038      const = float(kmat-1) * xytabs
2039      C
2040      C  FIND THE EOS QUANTITIES
2041      c
2042      DO 100 J = ja,jb
2043      I      = LEOS(J)
2044      M      = MEOS(J)
2045      dtp(j) = tpl(J) - AT * (L-1) - BT
2046      dden(j) = rho1(J) - AD * (M-1) - BD
2047      C
2048      C  TEST FOR LOWER TABLE LIMIT
2049      c
2050      xl      = float(l)
2051      dtp(j) = cvmgz (0.0, dtp(j), xl)
2052      xl      = cvmgz (1.0, xl, xl)
2053      xm      = float(m)
2054      dden(j) = cvmgz (0.0, dden(j), xm)
2055      xm      = cvmgz (1.0, xm, xm)
2056      xpt(j) = (xm - 1.)*xtabs + xl + const
2057      100 continue
2058      C
2059      C  IF THE DENSITY BECOMES LOWER THAN THE MINIMUM IN THE TABLE, WE MUST
2060      C  EXTRAPOLATE TO GET Z2B AND EN2B USING Y=SLOPE*X + B FORMULA.
2061      C  EXTRAPOLATE THE DENSITY AT L.
2062      C      SLOPE1 = -(A(L,1,KMAT) - A(L,2,KMAT))/AD
2063      C      B1 = A(L,1) - SLOPE1 * BD
2064      C      ALMS = SLOPE1 * rho1(J) + B1
2065      C  EXTRAPOLATE THE DENSITY AT L + 1
2066      C      SLOPE2 = -(A(L+1,1,KMAT) - A(L+1,2,KMAT))/AD
2067      C      B2 = A(L+1,1,KMAT) - SLOPE2 * BD
2068      C      ALMSS = SLOPE2 * rho1(J) + B2
2069      C      GO TO 30
2070      C

```

```

2071      c
2072      c  set table values in a scalar loop
2073      c
2074          do 110 j=ja,jb
2075              ipt      = ifix(xpt(j))
2076              work(j,1) = a(ipt)
2077              work(j,2) = a(ipt+itab)
2078              work(j,3) = a(ipt+1)
2079              work(j,4) = a(ipt+itab+1)
2080          110 continue
2081      c
2082      c  now finish with a vectorized loop
2083      c
2084          do 150 j=ja,jb
2085              c
2086              C  INTERPOLATE THE DENSITY AT L and l+1
2087              c
2088                  ALMS = work(j,1) + (work(j,2) - work(j,1)) * rad * dden(j)
2089                  alms = work(j,3) + (work(j,4) - work(j,3)) * rad * dden(j)
2090              C
2091              C  COMPUTE THE PLASMA TEMPERATURE DERIVATIVE
2092              c
2093                  ADER = (ALMSS - ALMS) * rat
2094                  QUAN =  ALMS + ADER * DTP(j)
2095              C
2096              C  CONVERT FROM LOGARITHMIC BACK TO REAL UNITS
2097              c
2098                  AA(J)      = 10.**QUAN
2099                  AADER(J) = ADER * AA(J) / tp(j)
2100              C
2101          150 CONTINUE
2102          RETURN
2103          END

```

```

2104      SUBROUTINE TABLE3(B,AA)
2105      C
2106      C  TABLE3 INTERPOLATES IN THE THREE-DIMENSIONAL EOS TABLES USING THE
2107      C  KEOS, LEOS, AND MEOS INDICES
2108      c    modified for cray vectorization
2109      C
2110      common/eos1 / ad, bd, at, bt, nmat, nfg, ja, jb,
2111      1      rad, rdb, rat, rbt
2112      common/wrk / work(9999,12)
2113      common/eoswrk/ trl(9999), tpl(9999), rho1(9999),
2114      1      meos(9999), leos(9999), keos(9999)
2115      c
2116      dimension B(*), aa(*), xpt(9999), dden(9999),
2117      1      dtp(9999), dtr(9999)
2118      c
2119      equivalence (xpt(1), work(1,11)), (dden(1), work(1,9)),
2120      1      (dtp(1), work(1,12)), (dtr(1), work(1,10))
2121      c
2122      data kmat,xtab,xytab,itab,ijtab
2123      1 / 1, 20., 400., 20, 400/
2124      c
2125      DO 200 J = ja,jb
2126      xk      = float(KEOS(J))
2127      xl      = float(LEOS(J))
2128      xm      = float(MEOS(J))
2129      dden(j) = rho1(J) - AD * (xm-1.) - BD
2130      dtp(j)  = tpl(J) - AT * (xl-1.) - BT
2131      dtr(j)  = trl(J) - AT * (xk-1.) - BT
2132      C
2133      C  TEST FOR LOWER TABLE LIMIT
2134      c
2135      dtr(j) = cvmgn ( dtr(j), 0.0, xk)
2136      xk      = cvmgn ( xk, 1.0, xk)
2137      dtp(j) = cvmgn ( dtp(j), 0.0, xl)
2138      xl      = cvmgn ( xl, 1.0, xl)
2139      dden(j) = cvmgn ( dden(j), 0.0, xm)
2140      xm      = cvmgn ( xm, 1.0, xm)
2141      xpt(j) = (xm-1.)*xytab + (xl-1.)*xtab + xk
2142      200 continue
2143      c
2144      c  setup property arrays---scalar mode
2145      c
2146      do 250 j=ja,jb
2147      ipt      = ifix(xpt(j))
2148      work(j,1) = b(ipt)
2149      work(j,2) = b(ipt+itab)
2150      work(j,3) = b(ipt+1)
2151      work(j,4) = b(ipt+itab+1)
2152      work(j,5) = b(ipt+ijtab)
2153      work(j,6) = b(ipt+ijtab+itab)
2154      work(j,7) = b(ipt+ijtab+1)
2155      work(j,8) = b(ipt+ijtab+itab+1)
2156      250 continue
2157      c
2158      c  now finish the job with vectorized loop

```

```

2159      c
2160      do 300 j=ja,jb
2161      c
2162      c  INTERPOLATE THE PLASMA TEMPERATURE AT M and M+1
2163      c
2164          AMS = work(j,1) + (work(j,2) - work(j,1)) * rat * dtp(j)
2165          AMSS = work(j,3) + (work(j,4) - work(j,3)) * rat * dtp(j)
2166      c
2167          AM1S = work(j,5) + (work(j,6) - work(j,5)) * rat * dtp(j)
2168          AM1SS = work(j,7) + (work(j,8) - work(j,7)) * rat * dtp(j)
2169      c
2170      c  COMPUTE THE RADIATION TEMPERATURE DERIVATIVE AT M AND M+1
2171      c
2172          ADER = (AMSS - AMS) * rat
2173          ADER1 = (AM1SS - AM1S) * rat
2174      c
2175      c  INTERPOLATE THE RADIATION TEMPERATURE AT M AND M+1
2176      c
2177          QUAN = AMS + ADER * DTR(j)
2178          QUAN1 = AM1S + ADER1 * DTR(j)
2179      c
2180      c  INTERPOLATE THE DENSITY
2181      c
2182          QUAN = QUAN + (QUAN1-QUAN) * rad * dden(j)
2183      c
2184      c  CONVERT FROM LOGARITHMIC BACK TO REAL UNITS
2185      c
2186          AA(J) = 10.0**QUAN
2187      300 CONTINUE
2188          RETURN
2189      END

```